

We are committed to providing [accessible customer service](#).

If you need accessible formats or communications supports, please [contact us](#).

Nous tenons à améliorer [l'accessibilité des services à la clientèle](#).

Si vous avez besoin de formats accessibles ou d'aide à la communication, veuillez [nous contacter](#).

2021 Vertical Time-Domain Electromagnetic (“VTEM™” Plus) Airborne Geophysical Survey

Cannon Copper Property, Ontario, Canada

Kamichisitit Township

NTS 41J06 / 41J11

**TAYLOR MCPHERSON, G.I.T
MARTIN ST.-PIERRE, GEOPHYSICIST**

Contents

A.	Program Objectives & Summary.....	4
A.1	Cannon Copper.....	6
B.	Introduction	7
C.	Location and Access.....	11
D.	Claims and Land Status	12
E.	History.....	13
F.	Geological Setting.....	17
F.1	Cannon Copper Project Regional Geology.....	17
F.2	Cannon Copper - Property Geology	19
F.2.1	Gowganda Formation (Ritchie, 1968).....	19
F.2.2	Keweenawan Intrusives (Ritchie, 1968).....	20
F.3	Cannon Copper Property Showings/Deposits.....	20
F.3.1	Rita Lake Zone:.....	20
F.3.2	West Zone	22
F.3.3	J Zone	22
F.3.4	Mineral Occurrences.....	22
G.	Mineralization.....	22
G.1	Quartz-Sulphide Veins.....	23
G.1.1	Main Vein (Ritchie, 1968).	23
G.2	Diabase Contact Deposits	23
G.3	Bedded Deposits	24
H.	2020 Airborne Geophysical Survey Summary.....	25
H.1.1	Cannon Copper Versatile Time Domain Electromagnetic (VTEM TM Plus) and Horizontal Magnetic Gradiometer Geophysical Survey	25
H.1.2	Magnetics.....	25
I.	Summary and Recommendations.....	36
I.1	Cannon Copper Property.....	36
J.	References	1

FIGURES

Figure 1. Cannon Copper Project location map.....	5
Figure 2. Airborne Survey Area over Google Earth.....	7
Figure 3. VTEM™ Plus System Configuration	9
Figure 4. Cannon Copper Project access.....	10
Figure 5. 2021 Airborne Geophysical Survey, Flight Lines.....	11
Figure 6. Cannon Copper Claims.....	12
Figure 7. Example of Repositioned Historical Drill Hole Locations.....	16
Figure 8. Regional Geology, Cannon Copper Project.....	18
Figure 9. Historical Showings and Deposits, Cannon Copper Project.....	21
Figure 10. Total Magnetic Intensity.....	26
Figure 11. TMI Vertical Derivative.....	26
Figure 12. Powerline Monitor Parameter.....	27
Figure 13. Channel 5 with Historical DDH, Showings, and Hydrology.....	28
Figure 14. Channel 10 with Historical DDH, Showings, and Hydrology.....	29
Figure 15. Channel 11 with Historical DDH, Showings, and Hydrology	30
Figure 16. Channel 12 with Historical DDH, Showings, and Hydrology	31
Figure 17. Channel 13 with Historical DDH, Showings, and Hydrology	32
Figure 18. Channel 14 with Historical DDH, Showings, and Hydrology	33
Figure 19. Channel 15 with Historical DDH, Showings, and Hydrology	34
Figure 20. VTEM Airborne Survey Interpretation Map.....	35

Tables

Table 1. Cannon Copper Airborne Geophysical Survey Statistics.....	6
Table 2. Survey Schedule	6

Appendices

APPENDIX 1: Claim Listing - Cannon Copper Property

APPENDIX 2: Geotech Ltd. – Report on a Helicopter-Borne Versatile Time Domain Electromagnetic (VTEM™ Plus) and Horizontal Magnetic Gradiometer Geophysical Survey, Project Number GL210096

APPENDIX 3: Cost Summary

APPENDIX 4: Certificate

A. PROGRAM OBJECTIVES & SUMMARY

This report describes the specifications and parameters of a helicopter-borne geophysical survey performed by Geotech Ltd. (“Geotech”) on behalf of ALX Resources Corp. (“ALX”) over the Cannon Copper Project near Elliot Lake, ON (Figure 1 and Figure 2).

The geophysical survey consisted of helicopter-borne electromagnetics (“EM”) using the versatile time-domain electromagnetic (VTEM™) Plus system with Full-Waveform processing. Measurements consisted of Vertical (Z) and In-line Horizontal (X) components of the EM fields using an induction coil and a horizontal magnetic gradiometer using two caesium magnetometers. A total of 203 line-km of geophysical data were acquired during the survey.

The crew was based out of Elliot Lake, ON (Figure 2) for the acquisition phase of the survey. The survey started on July 10, 2021 and was completed on August 5, 2021. The survey was flown using a Eurocopter Aerospatiale (A-Star) 350 B2 helicopter, registration C- GVMU. The helicopter is owned and operated by Geotech Aviation Ltd. Installation of the geophysical and ancillary equipment was carried out by a Geotech Ltd. crew.

Data quality control and quality assurance, and preliminary data processing were carried out on a daily basis during the acquisition phase of the project. Final data processing followed immediately after the end of the survey. Final reporting, data presentation and archiving were completed in October 2021.

Digital data collected include all electromagnetic and magnetic products, plus ancillary data including the waveform.

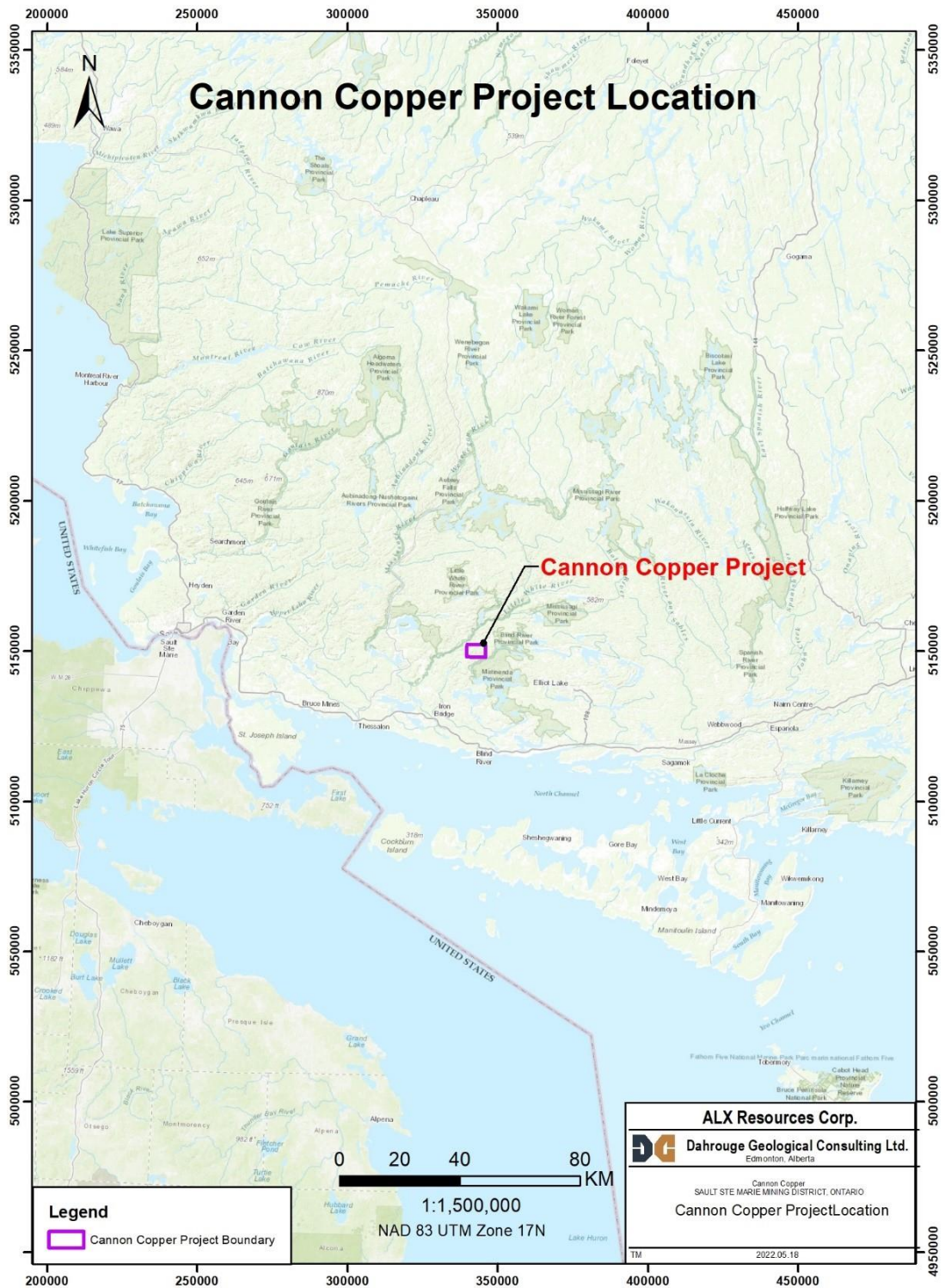


Figure 1: Project location

A.1 Cannon Copper

This report documents a geophysical survey program totaling 203 line-kilometres of helicopter-borne electromagnetic surveying at 150-metre spacing completed at the Cannon Copper Project. All work was recorded in UTM NAD83 coordinate system Zone 17N. The 2021 airborne survey was 100% funded by ALX.

Table 1: Survey Specifications

Survey block	Line spacing (m)	Area (km ²)	Planned ¹ Line-km	Actual Line-km	Flight direction	Line numbers
Cannon Copper	Traverse: 150	27	194	203	N 0° E / N 180° E	L1000 – L1410
	Tie: 1,500				N 90° E / N 270° E	T2000 – T2020
Total		27	194	203		

Table 2: Survey schedule

Date	Comments
10-July	Crew arrived Elliot Lake
11-July	System assembly
12-July	System assembly and base station setup
13-July	Helicopter arrival
14-July	System assembly
15-July	Helicopter installation completed
16-July	Geometry, altimeter and flight test completed
17-July	System calibration, radar altimeter and test flight completed
18-July	Test flight and system troubleshooting
19-July	Test flight with geometry adjustments
20-July	Standby due to poor weather
21-July	Standby due to poor weather and radar altimeter troubleshooting
22-July	Radar altimeter installation and testing
23-July	Test flights
24-July	Standby due to poor weather
25-July	System calibration
26-July	Production Flight – 62.5 km flown
27-July	Production Flight – 41.7 km flown
28-July	Production Flight – 47.94 km flown
29-July	Standby due to poor weather
30-July	System troubleshooting due to elevated noise level
31-July	Standby due to poor weather
01-August	Standby due to poor weather
02-August	System troubleshooting

03-August	Test flights
04-August	Production Flight – 38.0 km flown
05-August	Demobilization

¹ Note: Actual line kilometres represent the total line kilometres in the final database.

B. INTRODUCTION

The Cannon Copper Project (“Cannon Copper”, or the “Project”) is located in the Sault Ste. Marie Mining District, 33km northwest of Elliot Lake, ON. The Project is accessible by paved highway to secondary roads or trails and a powerline transects the southern part of the property. At the time of the 2021 airborne survey, Cannon Copper was comprised of 117 contiguous mineral dispositions totalling 2,600.09 ha., all of which are 100% owned by ALX.



Figure 2: Airborne survey area location map on Google Earth.

ALX commissioned the 2021 Geotech airborne EM survey at Cannon Copper to collect high-resolution geophysical data and imagery to be utilized in conjunction with surface exploration programs. The purpose

of a survey of this type is to collect high-resolution geophysical data that can be used to prospect directly for economic minerals that are characterized by anomalous magnetic and electromagnetic responses. Secondly, the geophysical patterns can be used indirectly for exploration by mapping the geology in detail, including rock types, faults, shear zones, folding, alteration zones and other structures. To obtain this data, the area was systematically traversed by a helicopter carrying geophysical equipment along parallel flight lines. The lines are oriented to intersect the geology and structure so as to provide optimum resolution of the geophysical data.

Local mineralization at the Project is predominantly chalcopyrite, with minor gold, lead and silver and is dominantly seen disseminated and in seams, in fractured zones in quartz and in brecciated zones or stockworks (Ritchie, 1968). Trace pyrrhotite mineralization is seen in vertically dipping diabase. The quartz and quartz breccia cuts across both the conglomerate-argillite beds and the quartzite, and it appears that the better mineralization is near the formational contact, which contact may have a controlling influence on the formation and attitude of copper concentrations within the mineralized zones (Szetu, 1965). The 2021 Geotech airborne EM survey was commissioned to potentially map and better identify such mineralized zones at a greater depth of investigation than was achieved by historical airborne surveys (Figure 3).

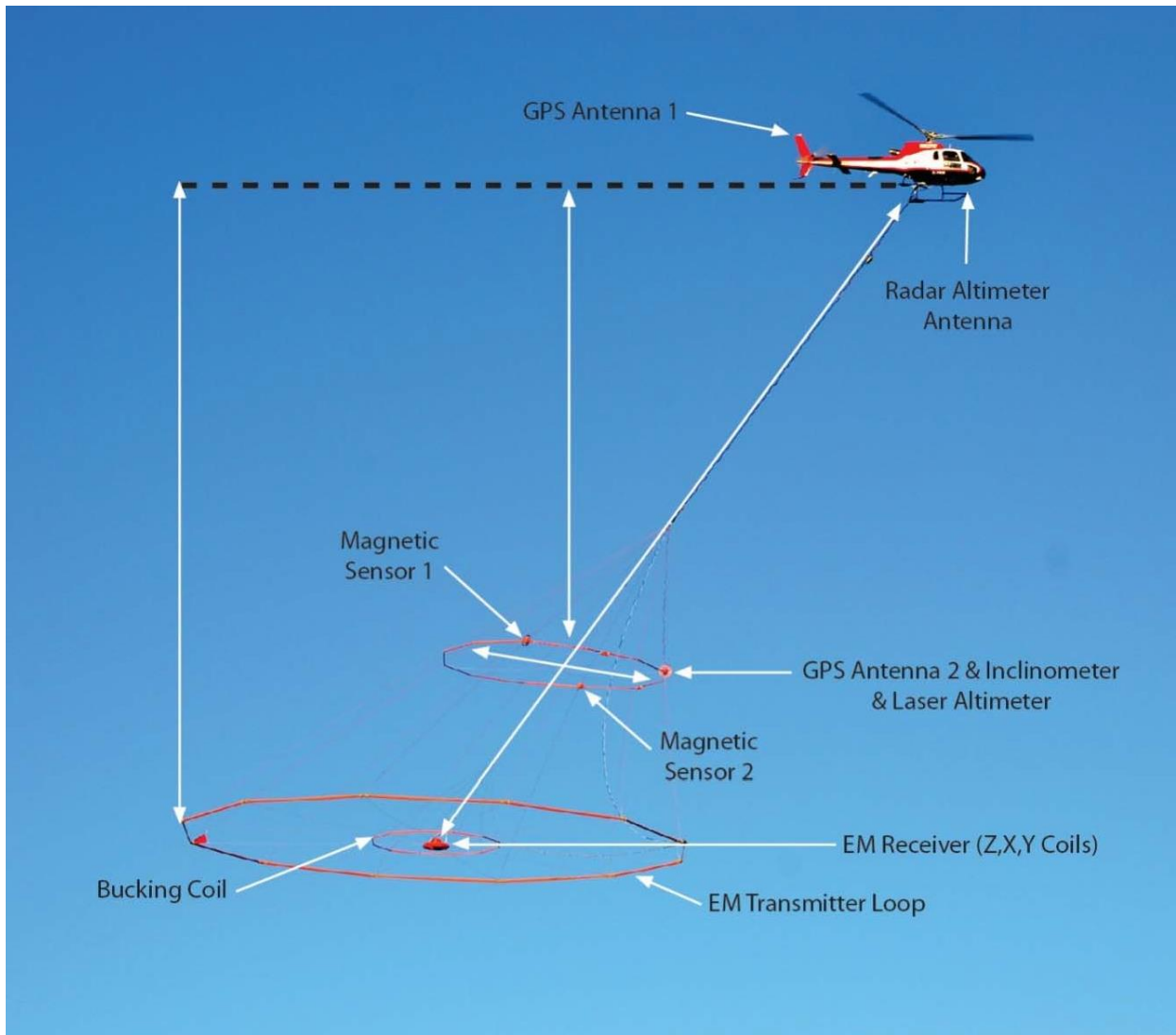


Figure 3: VTEM™ Plus System Configuration.

During the survey, the helicopter was maintained at a mean altitude of 115 metres above the ground with an average survey speed of 72 km/hour. This allowed for an actual average transmitter-receiver loop terrain clearance of 60 metres and a magnetic sensor clearance of 70 metres.

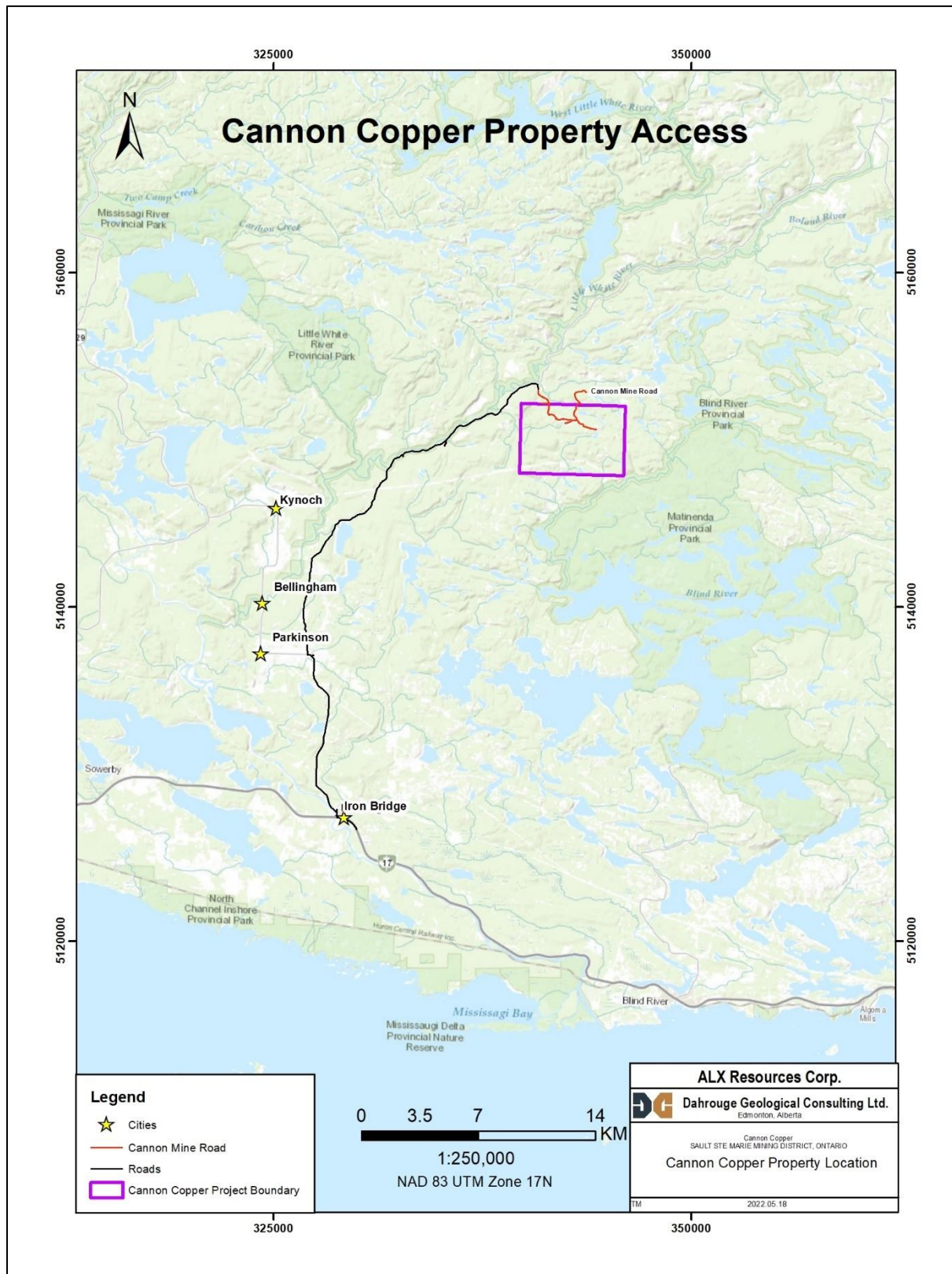


Figure 4. Cannon Copper Project access

C. LOCATION AND ACCESS

Cannon Copper is situated in Township 168 and is accessed from the village of Iron Bridge, Ontario 130km east of Sault Ste. Marie on Highway 17, by travelling north for 11km along Highway 554, then 25 km along Highway 546 to the Cannon (Crownbridge) Mine Road. The Cannon (Crownbridge) Mine Road provides access throughout the property (Figure 4).

The Cannon Copper airborne survey block was rectangular with four corners and measured approximately 6.25 kilometres east-west and 4.25 kilometres north-south. The centre of the survey block is approximately 515000N and 343000E (UTM NAD 83, Zone 17N). The 2021 survey slightly overflow neighbouring mineral properties and open ground in order to preserve the 3km minimum flightline length required for the VTEM™ survey system (Figure).

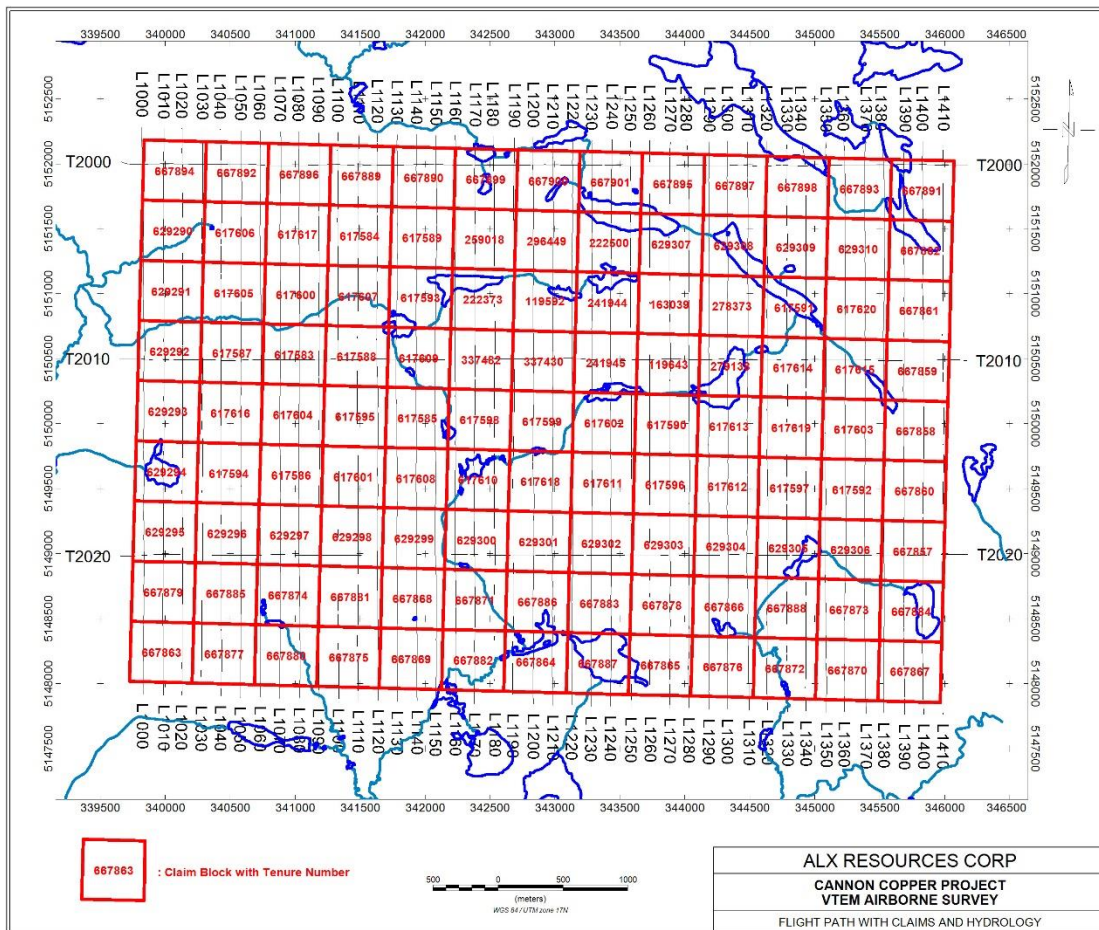


Figure 5: 2021 Airborne Geophysical Survey Flight Lines over Claims and Hydrology

D. Claims and Land Status

As of December 2021, Cannon Copper is comprised of 117 contiguous mineral claims, totalling 2,600.09 ha.

A map of the claims is portrayed in Figure 6 and a complete list of the claims is contained in Appendix 1.

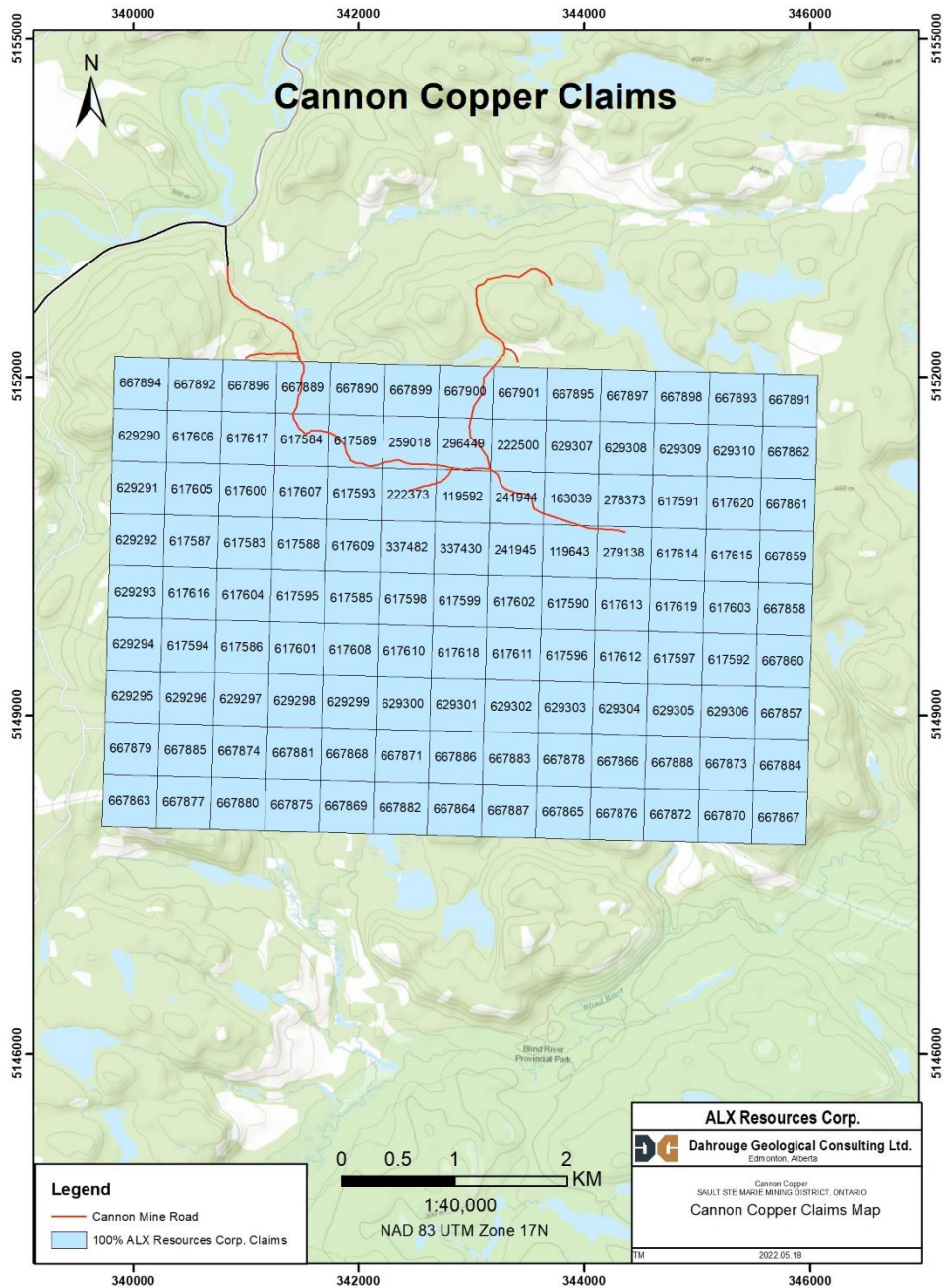


Figure 6: Cannon Copper Project Claims

E. HISTORY OF EXPLORATION

1942 - Erie Canadian Mines Limited

Report summarizes a prospecting program done in 1942. Eleven ore samples taken from trenches were assayed for copper and came back with eight samples over 1.0% Cu. The highest copper values were found in samples D-71153 @ 3.38% Cu and D-71154 @ 2.47% Cu. Length of samples is unknown.

1946 - Great Lakes Copper Mines Limited

Drilled five diamond drill holes, totalling 1,176 ft. (358.54m). Drill hole logging data is contained in report. No assay data was presented.

1958 to 1960 - Andover Mining and Exploration Limited

Andover Mining and Exploration Limited carried on a program of drilling between September 1958 and March 1960, comprising a total of 30,133 linear feet (9,186.89) in 75 drill holes. Twenty-five DDH totaling 12,168 ft. (3,709.76m) were drilled in the "J" Zone and 50 DDH totaling 17,965 ft. (5,477.13m) were drilled in the West Lens. The West Lens was calculated at 412,000 tons grading 2.1% Cu, and the "J" Zone was calculated at 135,000 tons averaging just under 2.0% Cu (Figure 9). Some notable assays:

- Hole 168-8: 78.5 to 96m grading approximately 2.7% over 14m;
- Hole 168-9: 62.5 to 68m at 2.10% Cu;
- Hole 168-10: 96.0 to 101m at 4.10% Cu;
- Hole 168-11: 64.5 to 70m at approximately 2.24% Cu;
- Hole 168-16: 97.0 to 101m at 1.23% Cu;
- Hole 168-17: 70 to 72.5 at 2.95% Cu;
- Hole 168-18: 110.0 to 113.5 at 4.0% Cu;
- 168-101: 192.6 to 220.5 at 3.88% Cu;
- 168-102: 175.0 to 184.0 at 3.66% Cu;
- 168-103: 201.6 to 205.5 at 3.78% Cu.

Chalcopyrite mineralization is found in quartz, and in a quartz brecciated zone alongside the quartz vein. This zone has been partially drilled off along a strike length of 1,000 feet, and to a depth of about 500 feet, which work has indicated a concentration of the chalcopyrite in the quartz vein, in the form of a pitching

deposit, with a pitch length of around 1,100 feet, and still open at depth, with an average horizontal width of 6.1 feet, and which the author estimated to contain 160,000 tons and predicted to average 2.03% copper (McKenzie, 1959).

1960 - Kennedy Agencies Limited

Carried out a three-hole diamond drill program in 1960's. Very limited data on report. No assays in report.

1963 to 1965 - Crownbridge Copper Mines Limited

Drilled 34 holes up to March 15, 1965, totaling 22,244.0 feet of drilling, making a grand total of 52,377.0 feet in 109 drill holes. The purpose for the holes were to fill in the known deposit parameters. As well, drill deep holes explored the ore zone at depth, and tested favourable structure zones for mineralization. There were also some holes targeted at the Rita Lake showings. Overall, chalcopyrite mineralization is found in quartz, and in a quartz brecciated zone alongside the quartz vein. The vein has been partially drilled off along a strike length of 4,100 feet, and to a depth of around 1,000 feet. This work has indicated concentration of chalcopyrite in the quartz vein zone. There was also a large compilation done on the previous historical data.

1964 to 1965 - Pathfinder Copper Limited

Carried out a small prospecting program in October 1964 and a copper showing was found in the SW corner of the claim (not on property). Mineralization is nearly all Cpy, with minor Py as seams and disseminated grains in quartz and quartz breccia. One chip sample on the vein, 3 feet in length, came back at 4.13% Cu and 0.01 oz./ton Au. Grab samples assayed at 3.06% Cu to 3.16% Cu.

1965 - J. W. G. Hunter

Carried out a one-hole diamond drill program in 1965, totalling 969 ft. The purpose was to better define the "J" zone (Figure 9). Very limited data on report. No assays in report.

1968 to 1969 - Cannon Mines Limited

A picket line system and geological mapping were carried out, and nine diamond drill holes were bored on the property, totalling 3,700.5 ft in total. The purpose was to investigate electromagnetic anomalies located on the property. Hole "D" came back with assay results of 2.0% over 5 feet, at 127 ft. depth. This anomalous value may suggest that the electromagnetic anomaly at the hole's location may be due to copper

mineralization, rather than conductive overburden. Cannon Mines Ltd. also completed line cutting and a magnetometer and electromagnetic survey, which produced two maps. From the electromagnetic survey, nine anomalies were detected, all striking east to south-east.

1968 - Fidelity Mining Investments Limited

A combined airborne Electromagnetic and Magnetic survey were flown over the property. The purpose of the survey, which was flown in March 1968, was to map near-surface magnetic or electromagnetic anomalous readings that might indicate a potential copper-bearing sulphide deposit, which have been previously reported in the area. The surveys may help indicate potential structures which continue to depth and could control deep-seated, uranium-bearing conglomerates. Only weak magnetic signatures were seen and no immediate ground follow-up was completed.

1969 - Subeo Limited

Combined airborne Magnetometer, Radiometric and Electromagnetic surveys were flown over the property. The purpose of the survey was to search for strong electrical conductors which may indicate potential massive sulphide deposits, concentration of uranium deposits and to map magnetic signatures to aid in ground exploration. The surveys produced no anomalous responses.

1979 - North American Nuclear Limited

A combined fixed-wing magnetometer and gamma ray spectrometer survey was conducted over the property in January 1979. Two flight lines were flown over the claim in the north-south direction, with an average flight line of 4km. The surveys produced six maps. There was little-to-no interpretative data represented in the reports.

During the integration of the 2021 VTEM™ Plus survey data with historical information, it was recognized that the historical drillhole locations contained in the digital OGS ODHD database appear to be in error, as the hole locations do not coincide properly with the historical mineral showings portrayed in various reports and other documents available to the authors. A thorough review was made to geo-register historical claim maps from the OGS archive to the mineral showings and historical drill hole location maps. The results of the review indicate that the ODHD digital drill hole archive is misregistered by approximately 400 metres to the southwest, as shown in Figure 7.

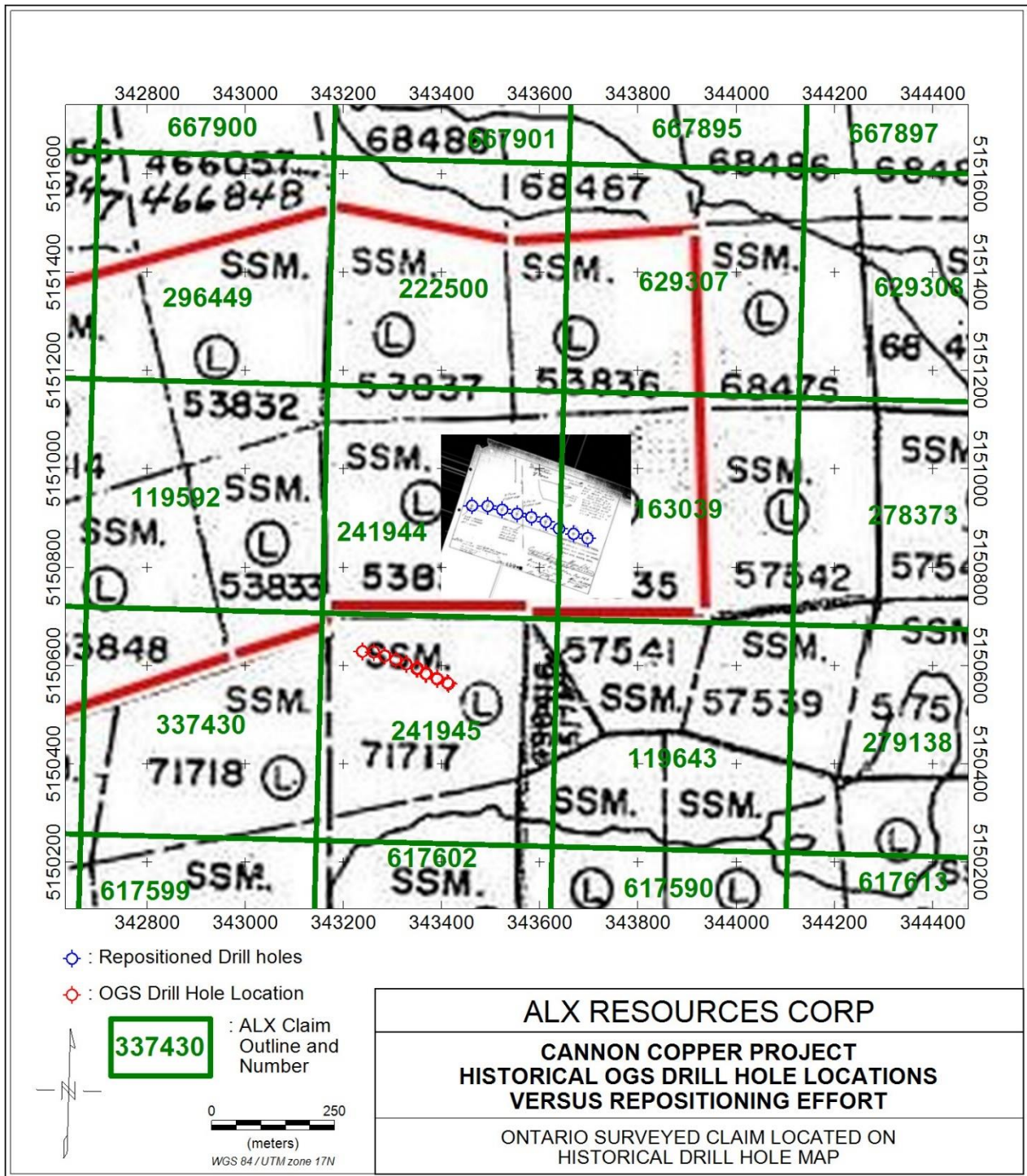


Figure 7: Example of Repositioned Historical Drill Hole Locations, May-June 2022

F. GEOLOGICAL SETTING

F.1 Cannon Copper Project Regional Geology

All rocks exposed in the surrounding region belong to the Proterozoic Huronian Supergroup metasedimentary rocks of the late Precambrian, southern province (Figure 8). The few exceptions are the diabase dikes and granitic intrusions. Unlike most other sedimentary series of Precambrian rocks, the Huronian formations have been folded only gently instead rather than tightly. Their dip tends to be low, and the members of greatest economic interest (the quartz-pebble conglomerate beds) are extensive. Steep structures within the flat-lying formations are associated with intrusives and faults (Ritchie, 1968). The Huronian Supergroup consists of (from oldest to youngest) 1) Elliot Lake group; 2) Hough Lake Group; 3) Quirke Lake Group; and 4) the Cobalt Group. The geology of Township 168 is comprised mainly of Cobalt Group of the Huronian supergroup. The Cobalt Group is a major flat-lying sedimentary assemblage of stratigraphy that underlies most of the region (Ritchie, 1968). The region is occupied by a subdivision of the Cobalt Group into the Gowganda formation. Near the corner of Township 168, diabase dikes, and presumably the quartz veining hosting the copper mineralization, strike northwesterly toward the property. This is one of the younger Precambrian intrusives of Keweenaw age, and presumably it is one of the steep structures mentioned under Regional Geology.

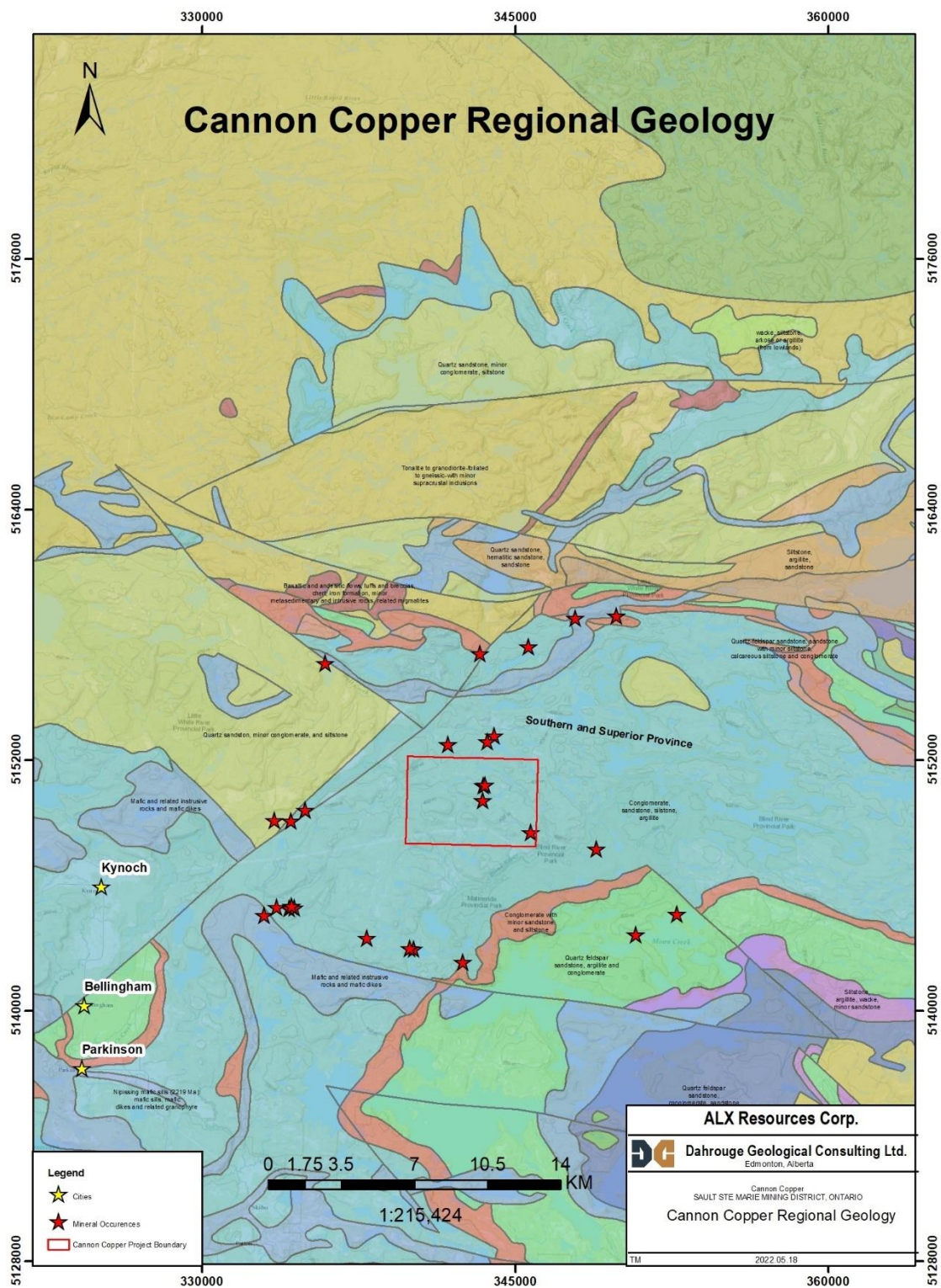


















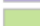




Figure 8: Regional Geology (see legend below)

Legend

	Basaltic and andesitic flows, tuffs and breccias, chert, iron formation, minor metasedimentary and intrusive rocks, related migmatites
	Conglomerate with minor sandstone and siltstone
	Conglomerate, minor sandstone, siltstone
	Conglomerate, sandstone, siltstone, argillite
	Gabbro, anorthosite
	Granite, alkali granite, granodiorite, quartz feldspar porphyry; minor related volcanic rocks (1.5 to 1.6 Ga)
	Mafic, intermediate and felsic metavolcanic rocks, intercalated metasedimentary rocks and epiclastic rocks
	Massive to foliated granodiorite to granite
	Nipissing mafic sills (2219 Ma): mafic sills, mafic dikes and related granophyre
	Quartz feldspar sandstone, conglomerate, sandstone
	Quartz sandstone, hematitic sandstone, sandstone
	Quartz sandstone, minor conglomerate, siltstone
	Quartz-feldspar sandstone, sandstone with minor siltstone, calcareous siltstone and conglomerate
	Quartz-feldspar sandstone, argillite and conglomerate
	Rhyolitic, rhyodacitic, dacitic and andesitic flows, tuffs and breccias, chert, iron formation, minor metasedimentary and intrusive rocks; related migmatites
	Siltstone, argillite, sandstone
	Siltstone, argillite, wacke, minor sandstone
	Siltstone, wacke, argillite
	Tonalite to granodiorite-foliated to gneissic-with minor supracrustal inclusions
	Wacke, siltstone, arkose, argillite, slate, mudstone, marble, chert, iron formation, minor metavolcanic rocks, conglomerate, arenite, paragneiss, migmatites
	wacke, siltstone, arkose or argillite (from lowlands)

F.2 Cannon Copper - Property Geology

The property geology consists of the Precambrian Huronian Supergroup; Cobalt Group Gowganda Formation rocks, with Keweenawan age intrusive basic dikes and quartz veining presumably hosting the copper mineralization. Below is a summarization for the Gawganda and Keweenawan formations.

F.2.1 Gowganda Formation (Ritchie, 1968).

The most common unit of the property is the Polymictic conglomerate (Gc) with or without interbedded quartzite, argillite, siltstone and greywacke. Feldspathic quartzite (Gq) with or without interbedded conglomerate, argillite, siltstone and greywacke. Greywacke (Gg) with out without interbedded conglomerate, argillite, siltstone and quartzite. Argillite, siltstone (Ga) with or without interbedded quartzite, greywacke and conglomerate. Most commonly what is seen is alternating beds of conglomerate and with narrow beds of argillite and quartzite.

F.2.2 Keweenaw Intrusives (Ritchie, 1968).

The Keweenaw rocks are represented by dikes and sills of diabase, diorite, and related rock types. These rocks are known to occur on the property, but as the property has not been mapped, their location, attitude, character, and influence are intermediate.

F.3 Cannon Copper Property Showings/Deposits

Cannon Copper is host to three significant showings: 1) "Rita" Zone; 2) "J" Showing; 3) "West" Zone. There are also two mineral occurrences 1) Andover Mining and 2) Crownbridge (Figure 9).

F.3.1 Rita Lake Zone:

The Rita Lake section has been explored by several diamond drill holes including one very short hole which did not advance far enough to intersect the potential copper zone lying near the south shore of Rita Lake. The six holes are spread at 175 ft. horizontal intervals, so the zone has been crudely tested for a strike length of 700 ft. (Chechak, 1964). The drilling done is insufficient to allow an estimate of ore reserves. There are two copper-bearing structures in the Rita Lake. One lies near the north shore of Rita Lake and shows good persistence for the known 700 ft., strike length although the widths are narrow and the grades low. The best grade was 1.8% copper across a core length of 4.1 ft. in hole CR 24 (Chechak, 1964). The second zone of copper mineralization lies near the south shore of Rita Lake and was intersected in only three of the five holes which probed deep enough to intersect the zone. Here, the widths and grades of the copper mineralization are somewhat better. The best intersection was 2.06% across 3.0 ft. of core length. Further drilling is necessary for a proper evaluation of the Rita Lake Zone (Chechak, 1964).

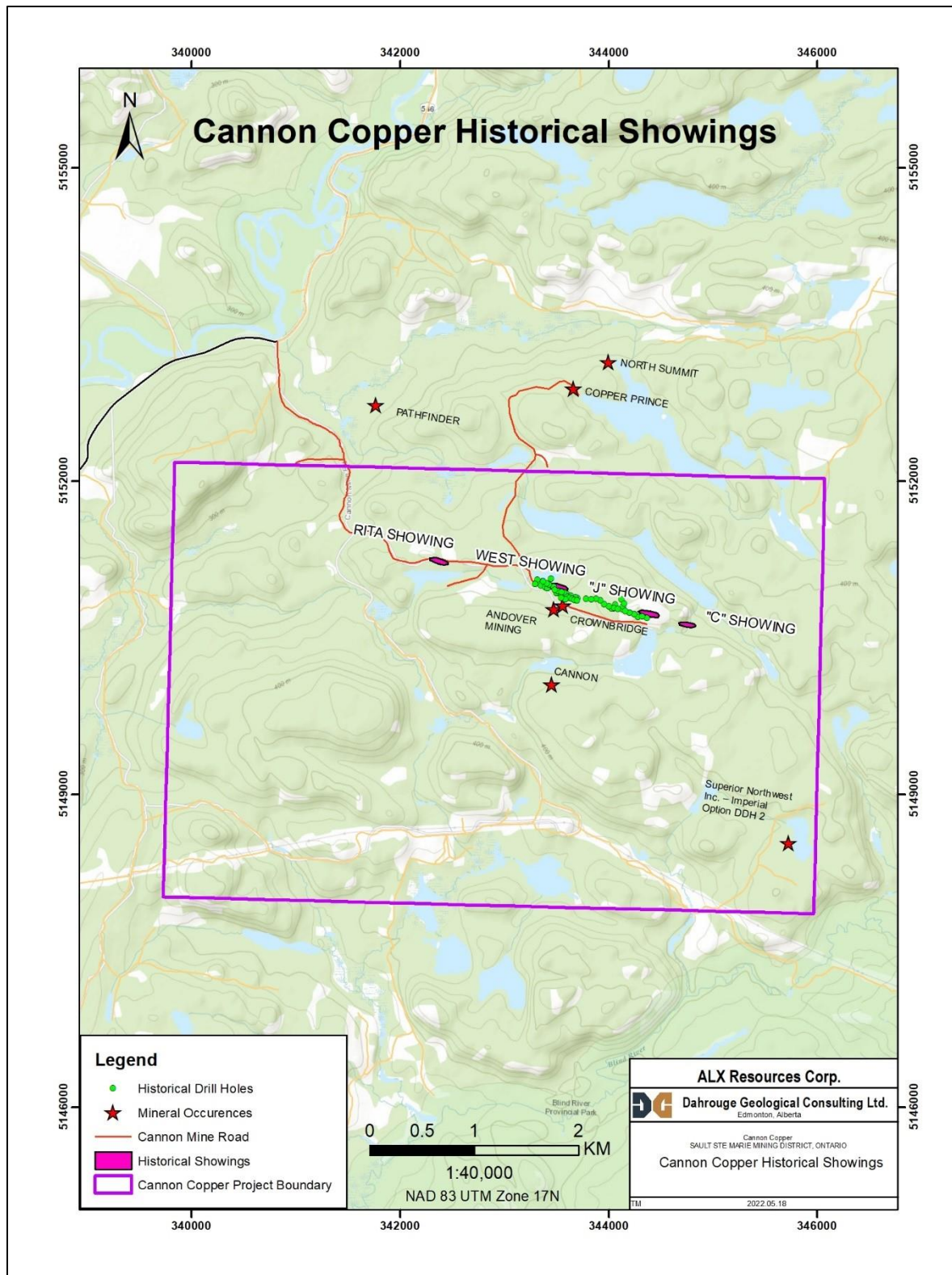


Figure 9: Cannon Copper Historical Showings and Mineral Occurrences

F.3.2 West Zone

Eight drill holes indicate that the west zone contains 142,650 tons of 1.75% copper to a depth of 1200 ft. (Chechak, 1964). Fill-in drilling should be considered within this zone, particularly between surface and 300 ft. The zone is also still considered wide open to the west. Two of the deep holes on this zone, 16-704 and GR 16, were potentially stopped short of their target. The zone provides an abundance of immediate drill targets whose exploration is deemed sensible (Chechak, 1964).

F.3.3 J Zone

There is some confusion regarding the location of some of the drill holes in this zone, which has not allowed a reliable picture of the ore potential. The historical drill holes should be re-surveyed and the drill sections re-plotted. If this work were completed, it is likely that further diamond drilling would be recommended.

F.3.4 Mineral Occurrences

The Andover Mining and Crownbridge mineral occurrences are both located in the central region of the property. Both occurrences are copper showings associated with quartz veining. The Andover Mining occurrence is associated with trenching done by the company between 1958 and 1959. The Crownbridge showing is associated with diamond drill hole assays done between 1963 and 1965. The mineralized portion of the vein system had a known strike length of 4,200 feet. The width of the vein system ranges from 1 to 30 feet and averages 6.5 feet. It has been explored by drilling to a depth of 1000 feet, although most of the drilling has been confined to depths of less than 500 feet. Drilling results show that copper mineralization is confined to multiple lenses within the vein system. To a depth of 1,000 feet, total reserves, including 10 % allowance for dilution, were reported to be 415,000 tons, grading 1.8% Cu, over an average width of 6.5 feet (Northern Miner, May 27, 1965).

G. Mineralization

Local mineralization is predominantly chalcopyrite, with minor gold, lead and silver and is dominantly seen disseminated and in seams in fractured zones in quartz and in brecciated zones or stockworks (Ritchie, 1968). Trace pyrrhotite mineralization is seen in vertically dipping diabase. The quartz and quartz breccia cuts across both the conglomerate-argillite beds and the quartzite, and it appears that the better mineralization is near the formational contact, which contact may have a controlling influence on the

formation and attitude of copper concentrations within the mineralized zone (Szetu, 1965). There are three potential deposit types present on the property.

G.1 Quartz-Sulphide Veins

This deposit type may be present on the property, main veins are seen striking East-West. This strike correlates to the “Main Vein” strike seen N60W, which also corresponds to the Moon Lake fault. Very structurally controlled deposit type.

G.1.1 Main Vein (Ritchie, 1968)

The main vein is a quartz-filled fissure-stockwork-breccia zone which has been mineralized with chalcopyrite, bornite and hematite. There are very low gold and silver values associated with the richer copper sections. The vein is marked by a weak topographic linear feature which strikes between N80W and N85W. The linear feature is traceable on-air photographs for a length of 1.5 miles. The main vein dips steeply north and locally horizontal widths of more than 25 ft., though widths of 10 ft. seem fairly common. Rarely is the full width of the vein mineralized to a degree that is economically interesting. Generally, the part of the vein carrying potentially economic quantities of mineralization occur in three places 1) at the hanging wall; 2) in the centre of the vein; 3) against the footwall. This suggests that the ore shoots within the vein are lenses. It has been noted that mineralization may be seen distributed evenly throughout the vein, as opposed to being concentrated in blobs within barren vein. Several historical drill holes have encountered minor veins in the hanging wall of the main vein and a portion of these have carried copper values of interest.

G.2 Diabase Contact Deposits

Though no deposits of this type have been found on the property, several have been found in the surrounding area. property but they have been seen throughout the area. These deposits occur as disseminated copper sulphides distributed across narrow widths of diabase and country rock along the contacts of diabase dikes and sills (Ritchie, 1968). The deposits rarely have quartz veins associated in any significant amount. Garnet, magnetite and other contact metamorphic minerals may or may not be

present. These deposits are difficult to find by geophysical methods as they seldom form continuous conductors (Ritchie, 1968).

G.3 Bedded Deposits

It has been reported in historical data that, at depth thinly bedded siliceous argillite showed very fine disseminated chalcopyrite, which was well below ore grade (Ritchie, 1968). Though below economic values, a discovery of this nature has merit. One of the largest copper mines in the world in White Pine, in the northwest corner of Michigan State, was mined as low-grade, bedded copper deposits, which then intersected a larger bedded copper deposit. Due to the similarity in age, rock type, and structure there is potential on the property for this type of copper occurrence.

H. 2021 AIRBORNE GEOPHYSICAL SURVEY SUMMARY

H.1.1 Cannon Copper Helicopter-borne VTEM™ Plus Survey

The 2021 Geotech Ltd. VTEM™ Plus magnetic and time domain electromagnetic (VTEM™ Plus) survey was completed with 4 production flights over 4 days (not including calibration, setup, stand-by days due to inclement weather, and mob/demob) beginning on July 26, 2021 and completed on August 4, 2021.

H.1.2 Magnetics

The VTEM airborne magnetic data is presented in Figures 10 and 11, showing the Total Magnetic Intensity (“TMI”) and the TMI Vertical Derivative, respectively. The survey area is dominated by roughly east-west trending features. From Ontario Geological Survey (“OGS”) geological maps and drill hole information, the basement rocks are dominated by conglomerates, siltstones, quartzites and arkose rocks. The only evidence of proximal intrusive rocks are two mafic dykes trending roughly northwest as shown in the VTEM interpretation map (Figure 20). Mineralization with economic potential on the property consists of chalcopyrite-rich structures trending roughly west-northwest. From the historical drill hole logs, it is interpreted that mafic fragments with the conglomerates are the probable source of elevated magnetic amplitudes. However, it does not appear that lithological trends cause the elevated magnetic high features. It appears more likely that east-west faulting has demagnetized the bedrock (see Figures 10, 11 and 20) and that these trends are most likely associated to the copper mineralisation.

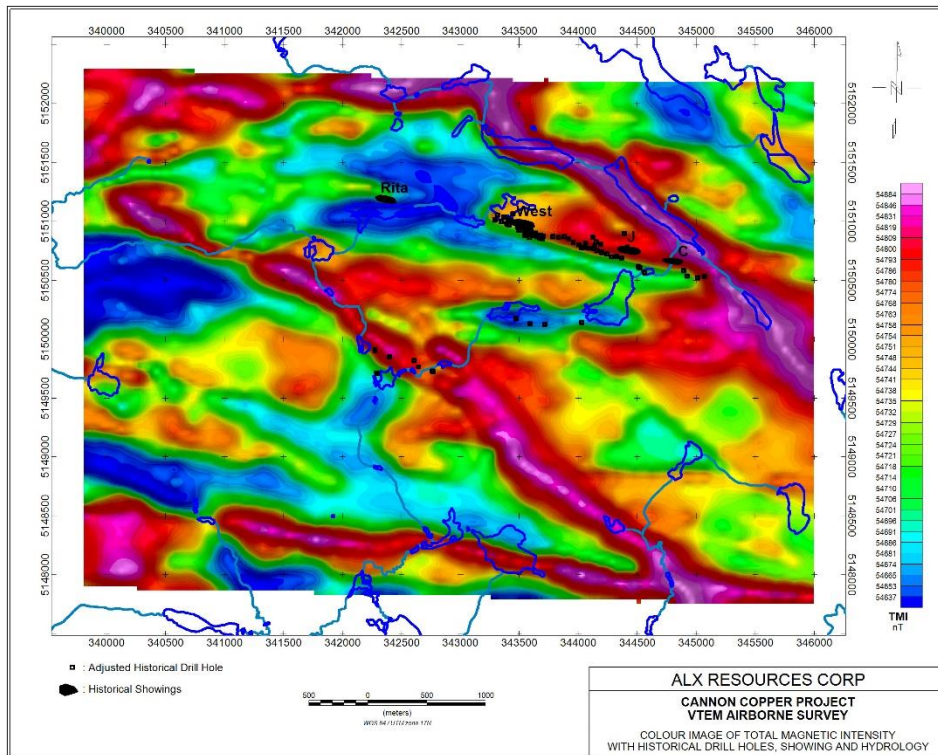


Figure 10: Total Magnetic Intensity

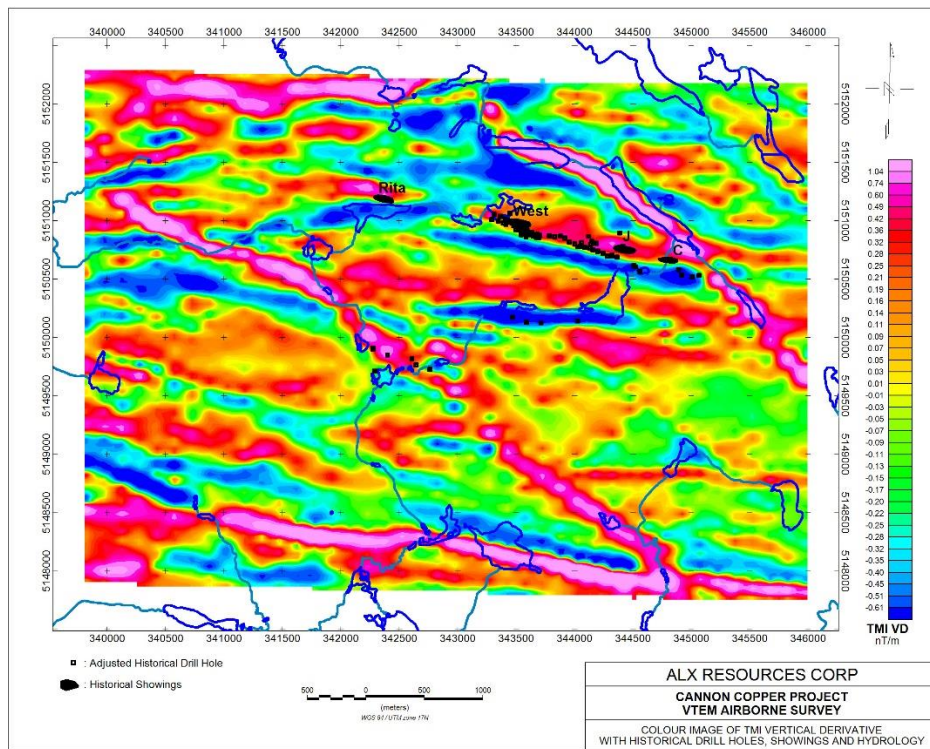


Figure 11: TMI Vertical Derivative

H.1.3 Electromagnetic Data

The airborne electromagnetic (“EM”) data is provided in 43 time channels from the earliest time Channel 4 to the latest time Channel 46. Typically, weak conductors would be detected in the early time channels only, whereas strong conductors would be present into the late time channels. Within the Cannon Copper survey block anomalous features do not endure past channel 15, which is considered as an early time channel, and as such, only weak conductive features are present. The southern border of the survey block is crossed by a powerline which is clearly shown by the powerline monitor (“PLM”) parameter presented in Figure 12.

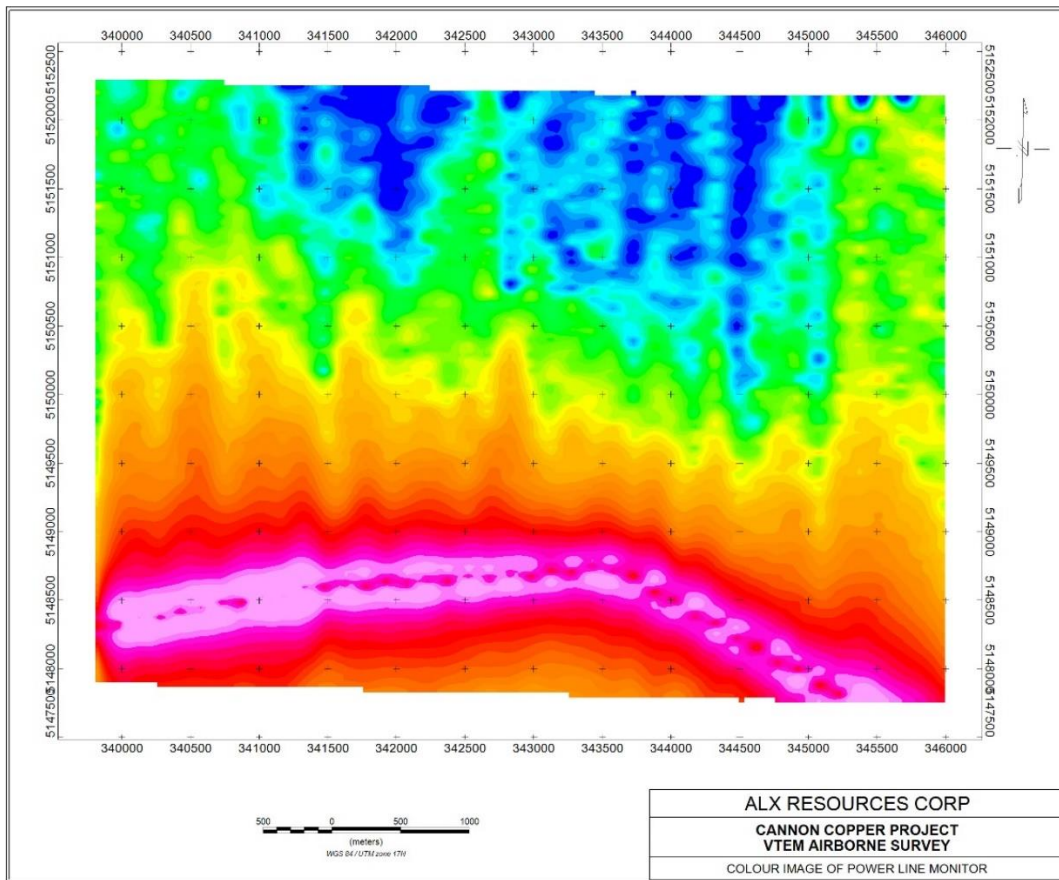


Figure 12: Powerline Monitor Parameter

Figures 13 to 19 present the colour images of Channels 5, 10, 11, 12, 13, 14 and 15. In the Channel 5 response (Figure 13) we see that hydrology dominates the elevated EM response. As we progress in the later time channels, the hydrology association diminishes and a single anomaly remains, located in the

northwest portion of the property. This anomaly may still be caused by thick overburden, however alteration and/or disseminated sulphide mineralization may also be the cause.

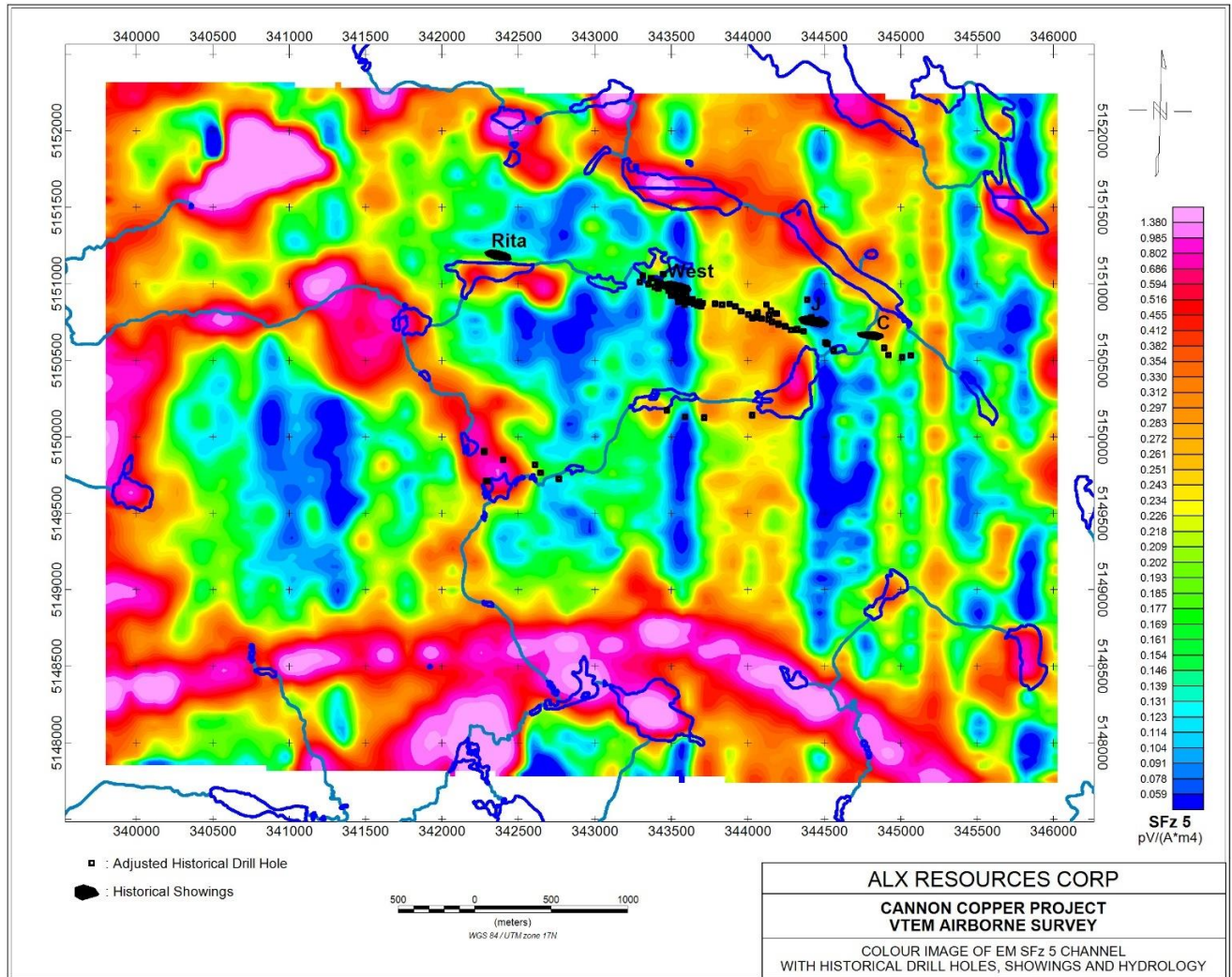


Figure 13: Channel 5 with Historical DDH, Showings and Hydrology

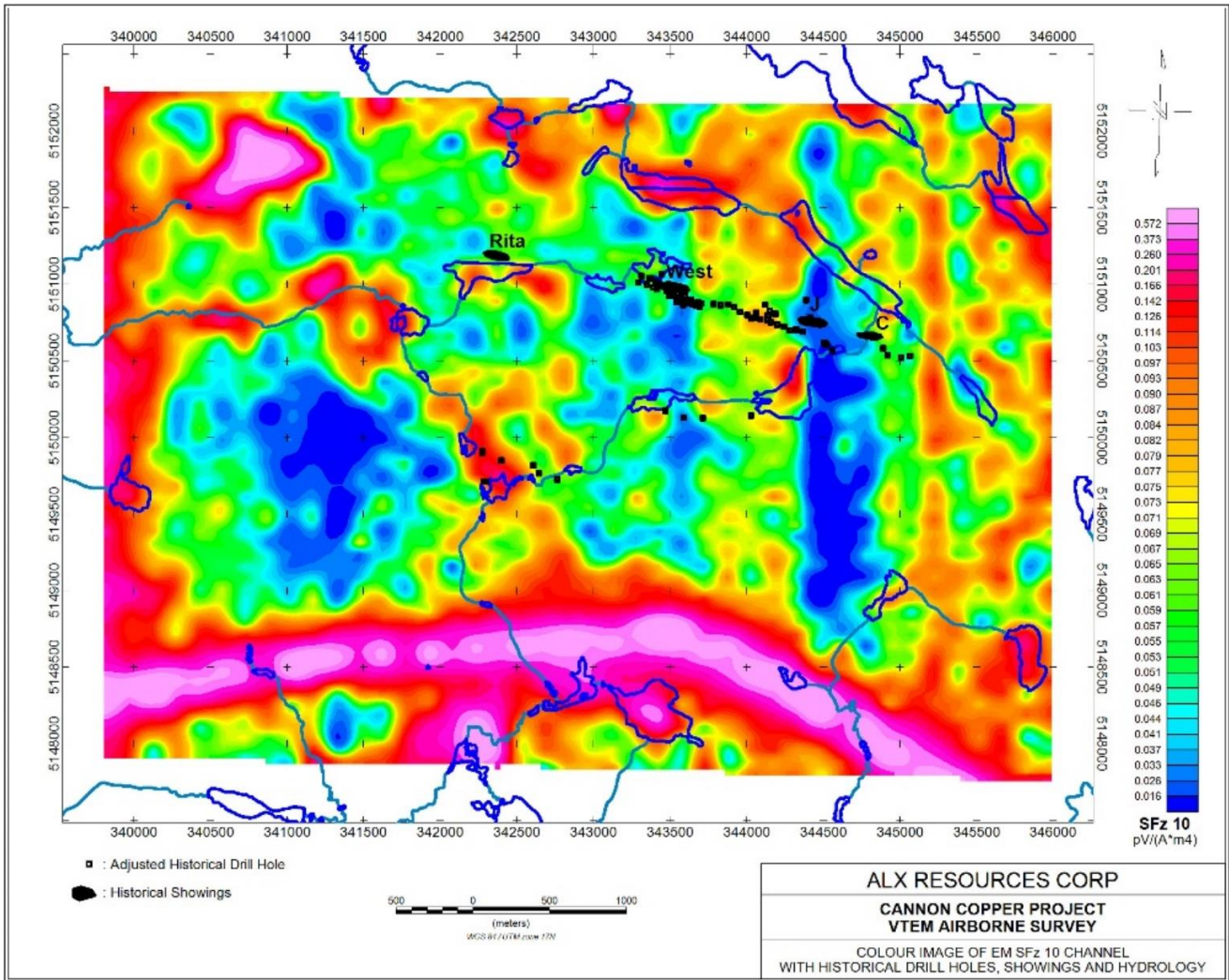


Figure 14: Channel 10 with Historical DDH, Showings and Hydrology

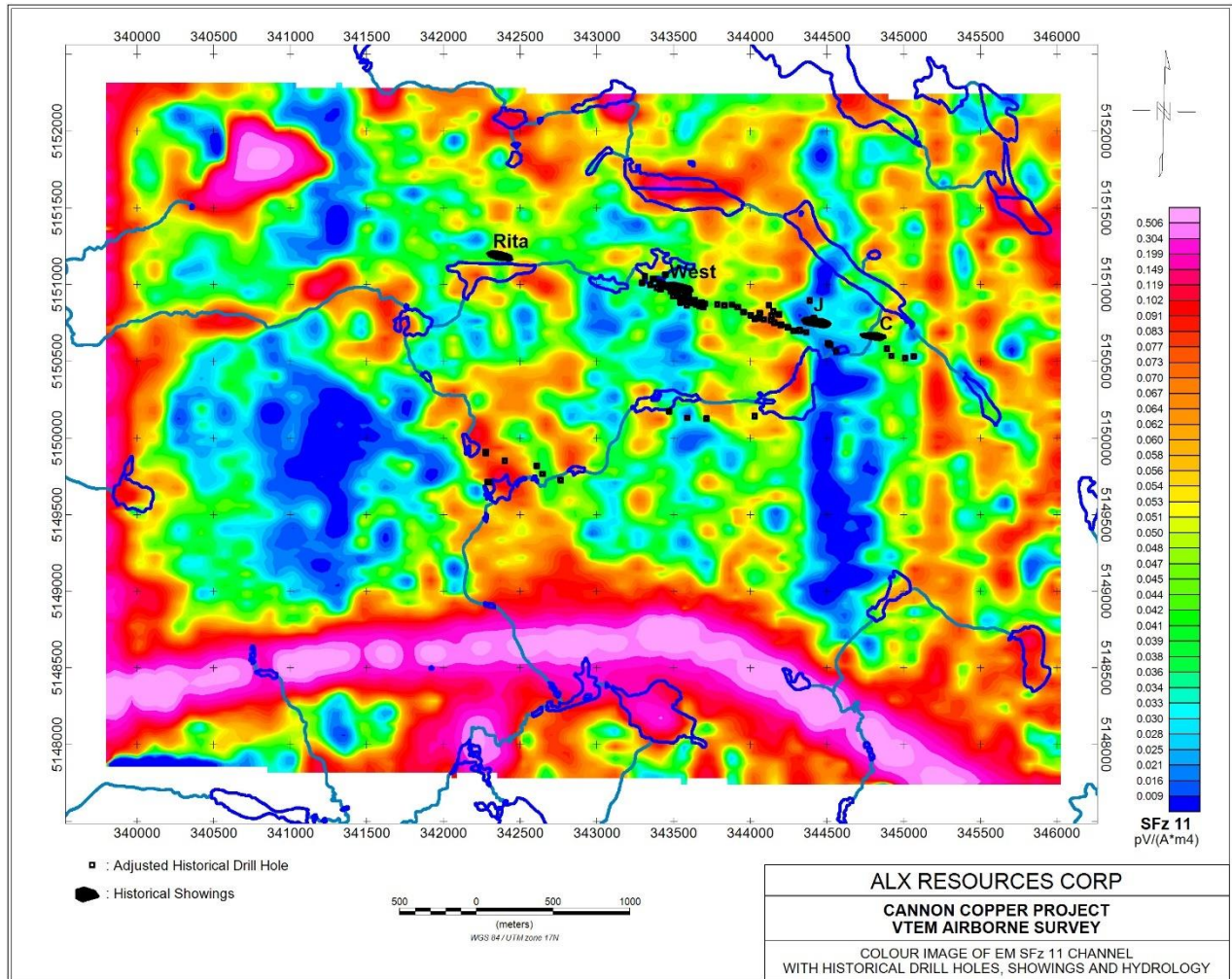


Figure 15: Channel 11 with Historical DDH, Showings and Hydrology

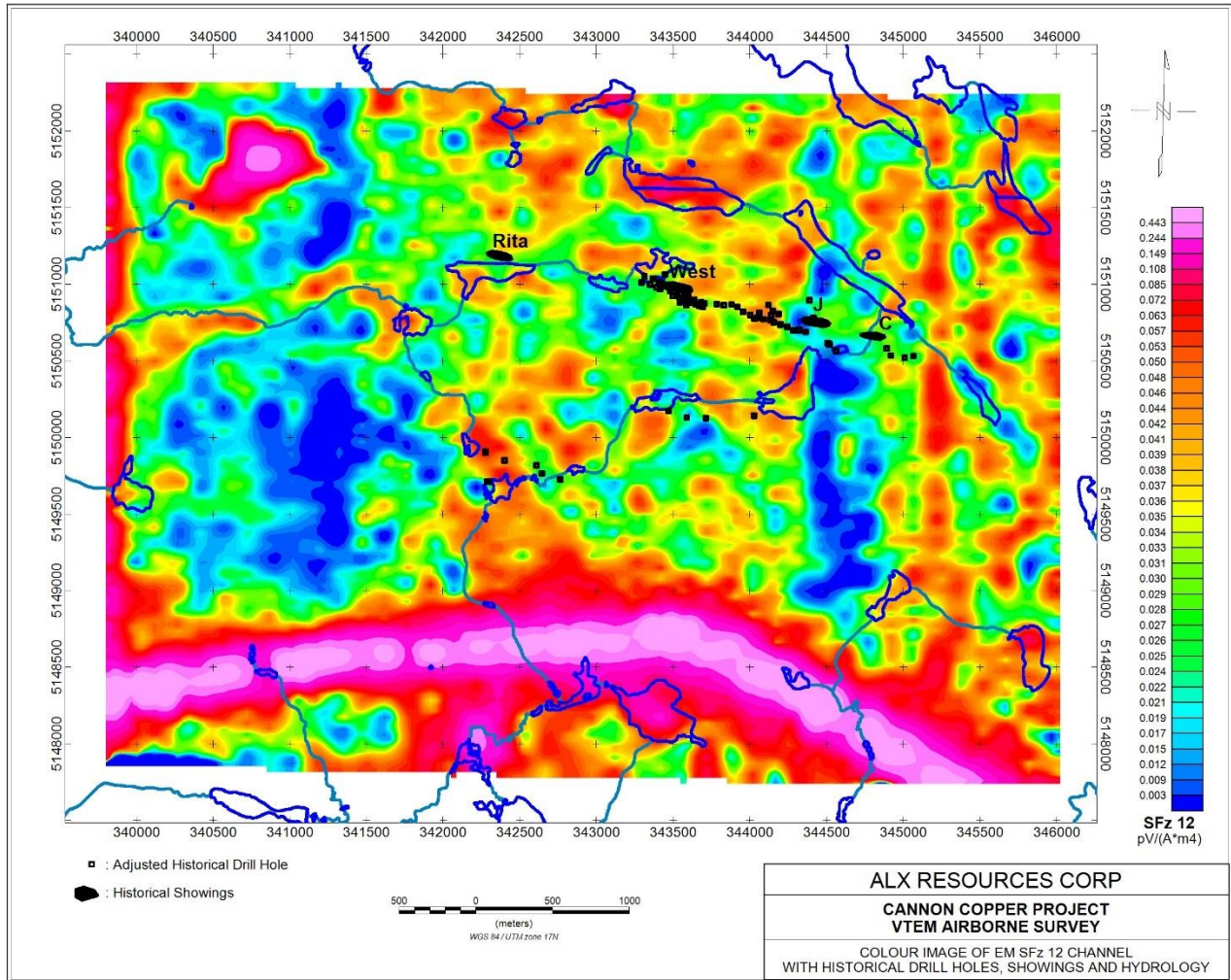


Figure 16: Channel 12 with Historical DDH, Showings and Hydrology

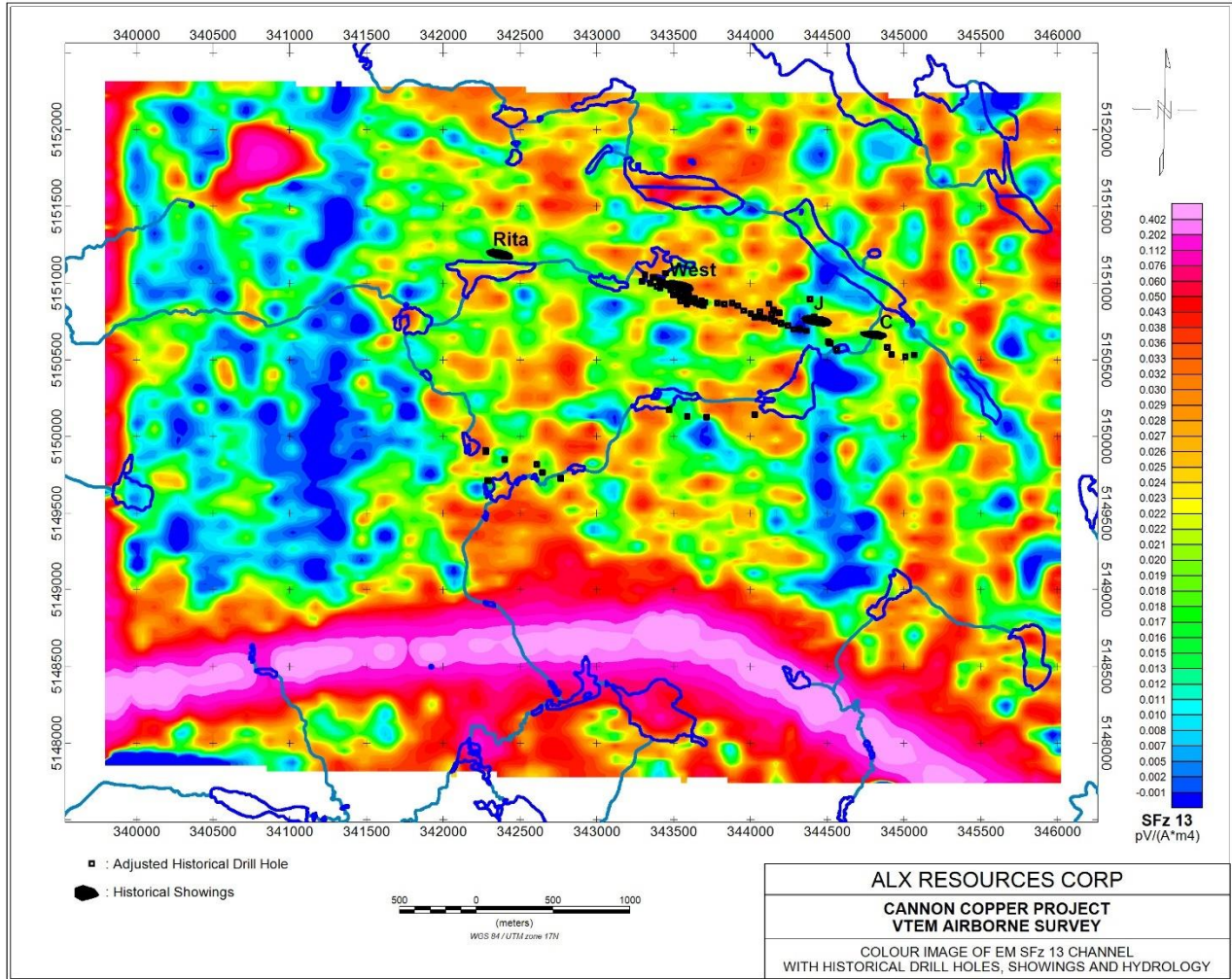


Figure 17: Channel 13 with Historical DDH, Showings and Hydrology

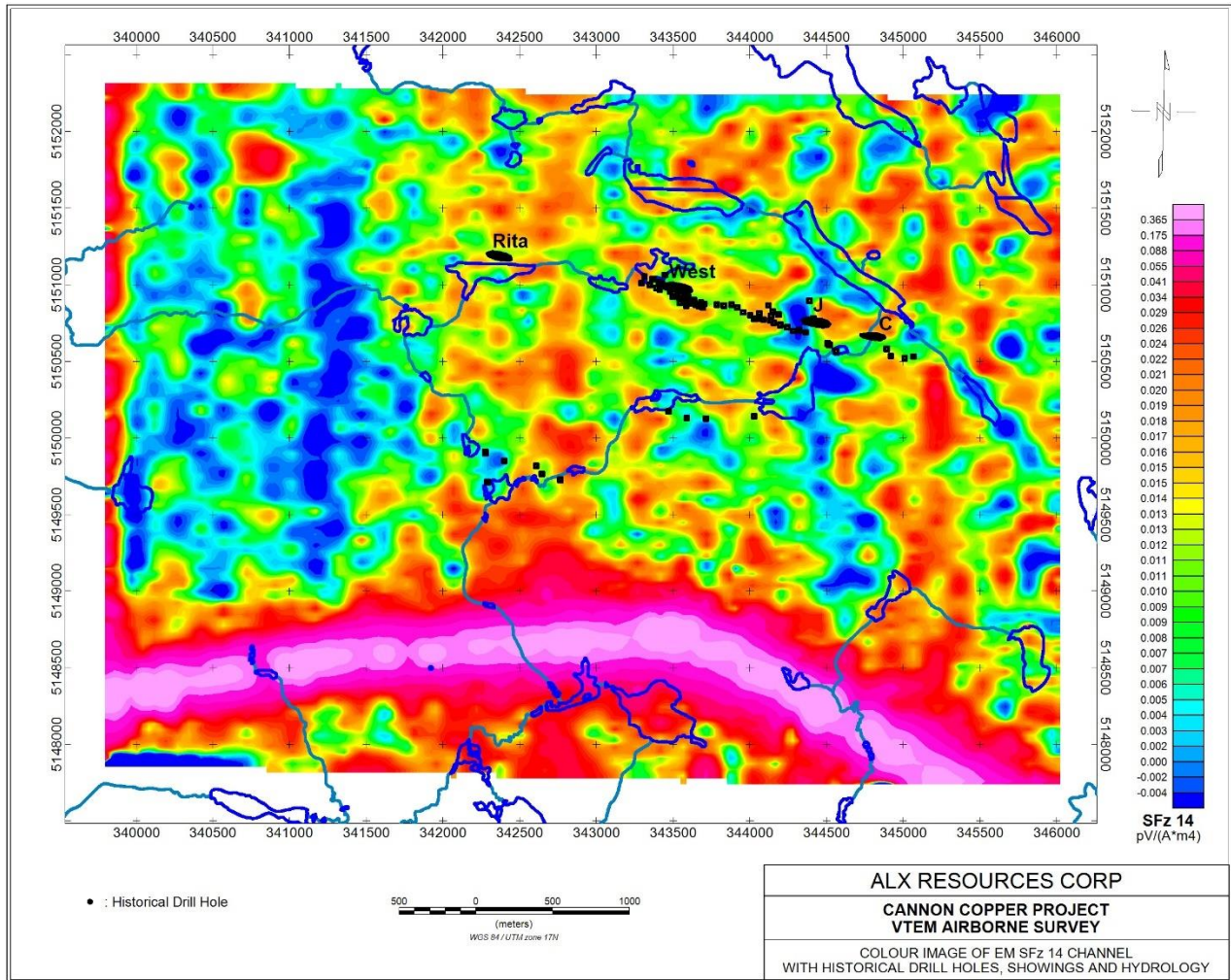


Figure 18: Channel 14 with Historical DDH, Showings and Hydrology

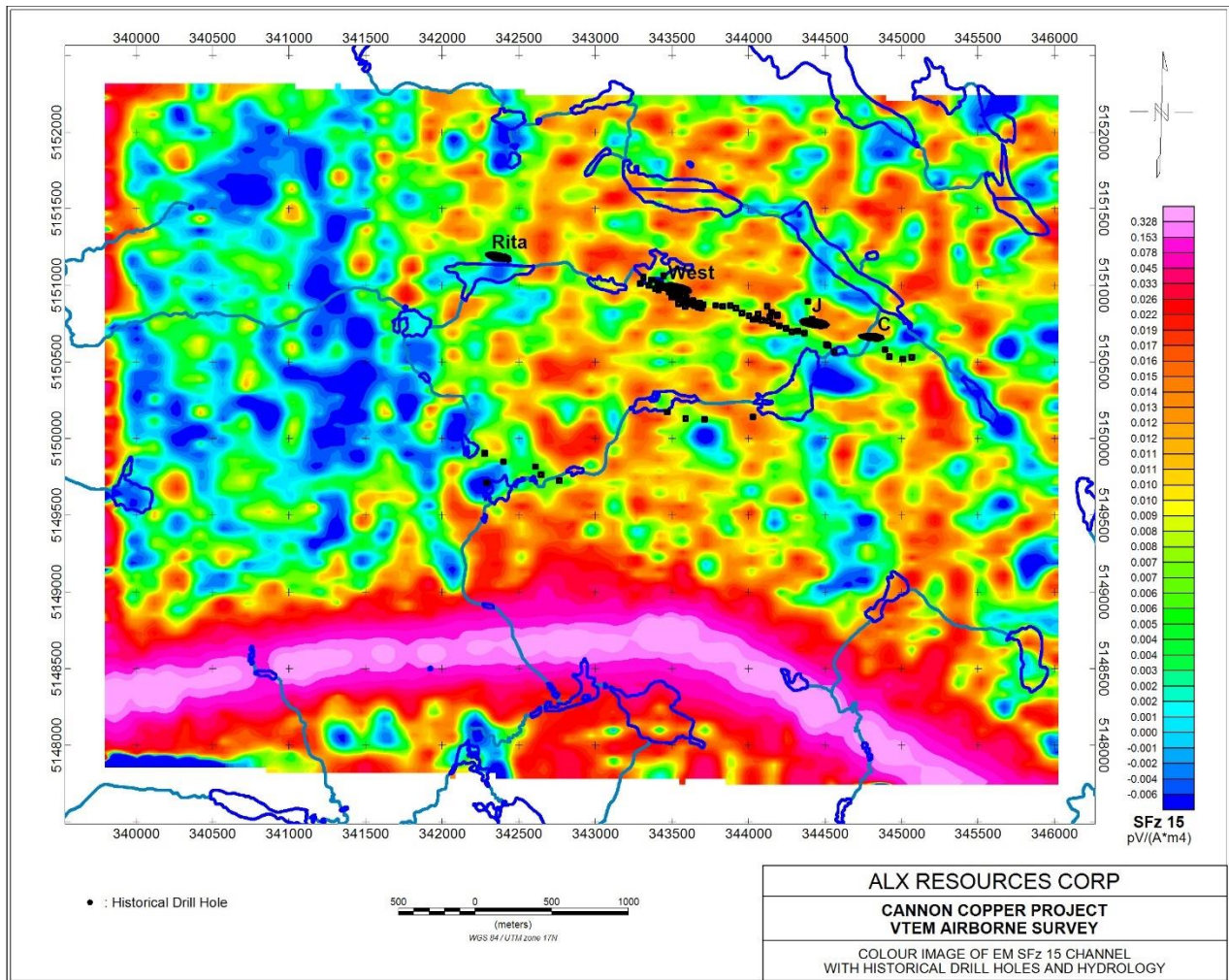


Figure 19: Channel 15 with Historical DDH, Showings and Hydrology

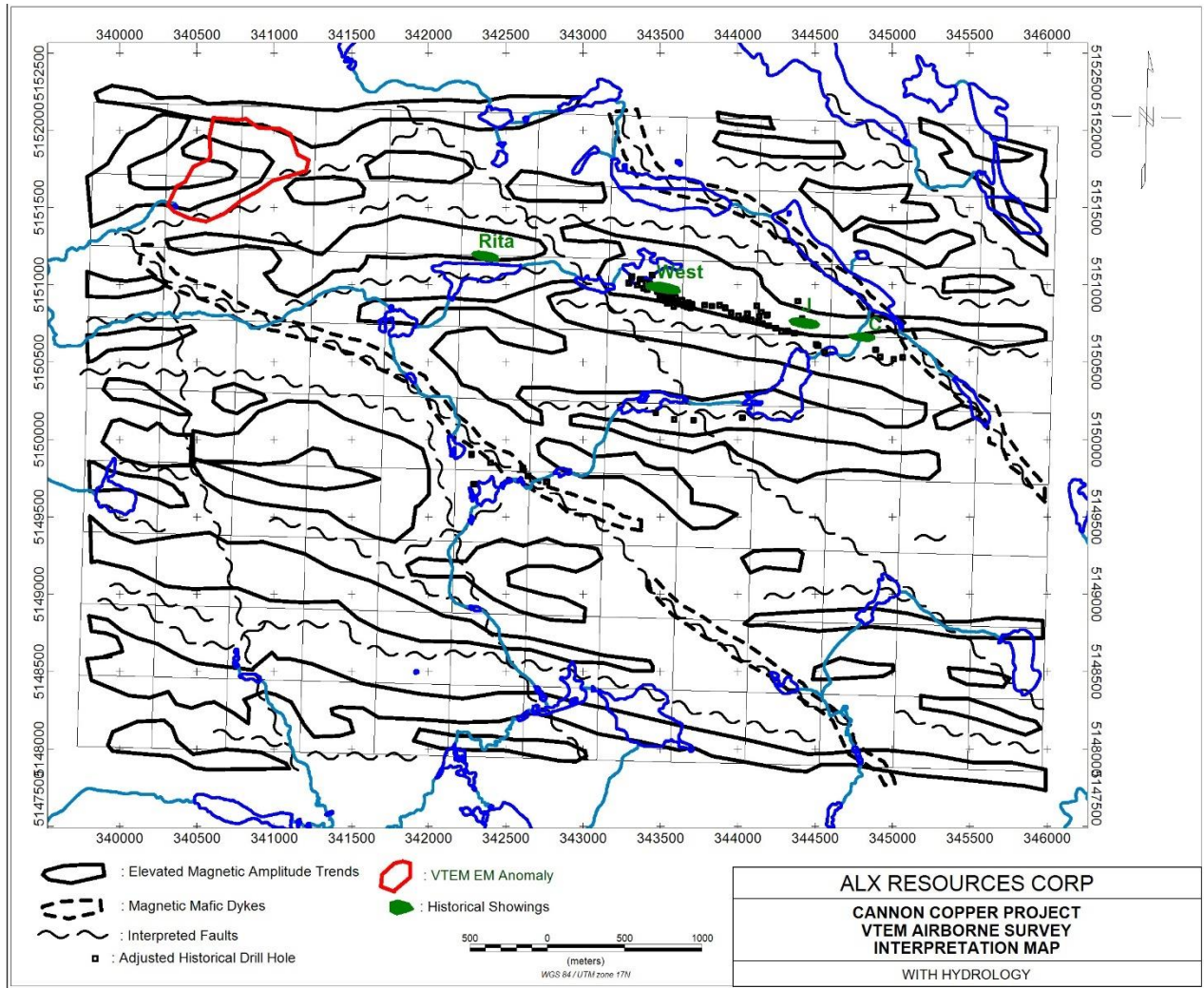


Figure 20: VTEM Airborne Survey Interpretation Map

I. SUMMARY AND RECOMMENDATIONS

I.1 Cannon Copper Property

The VTEM™ Plus EM and magnetic airborne survey has provided useful magnetic data that outlines trends parallel to known mineralization. The EM component has not detected strong conductive features associated to the known mineralization. A single early-time EM anomaly located in the northwest portion of the survey block has the potential of representing alteration and/or disseminated sulphide mineralization.

It is recommended that Induced Polarization ground geophysical surveys be carried out in order to test the detectability of the known copper mineralization. It is also recommended that the known mineral showings and historical drill holes be investigated on the ground in order to accurately locate them.

J. REFERENCES

S.S Szetu, 1965. Report on Thirty-One Claim Property for Pathfinder Copper Mines Limited. Submitted to the Ontario Securities Commission.

C.T Ritchie, 1968. Mineral Exploration Report on The Property of Cannon Mines Limited. Submitted to the Ontario Securities Commission.

B.W Chechak, 1964. Crownbridge Copper Mines Limited Summary Development Report on the Iron Bridge Property. Submitted to the Ontario Securities Commission.

Northern Miner, 1965. Northern Miner Article May 27. <https://www.northernminer.com/northern-miner-archives/>

D.C McKenzie, 1959. Prospect of Andover Mining and Exploration Limited. Submitted to the Ontario Securities Commission.

APPENDIX 1

Claim Listing – Cannon Copper Property

Tenure Number	Issue Date	Anniversary Date	Title	Owner	Area (ha)
119592	2018-04-10	2022-06-27	Single Cell Mining Claim	(100) ALX RESOURCES CORP.	22.21962
119643	2018-04-10	2022-06-27	Single Cell Mining Claim	(100) ALX RESOURCES CORP.	22.22114
163039	2018-04-10	2022-06-27	Single Cell Mining Claim	(100) ALX RESOURCES CORP.	22.21946
222373	2018-04-10	2022-06-27	Single Cell Mining Claim	(100) ALX RESOURCES CORP.	22.2197
222500	2018-04-10	2022-06-27	Single Cell Mining Claim	(100) ALX RESOURCES CORP.	22.21784
241944	2018-04-10	2022-06-27	Single Cell Mining Claim	(100) ALX RESOURCES CORP.	22.21953
241945	2018-04-10	2022-06-27	Single Cell Mining Claim	(100) ALX RESOURCES CORP.	22.22121
259018	2018-04-10	2022-06-27	Single Cell Mining Claim	(100) ALX RESOURCES CORP.	22.21801
278373	2018-04-10	2022-06-27	Single Cell Mining Claim	(100) ALX RESOURCES CORP.	22.21937
279138	2018-04-10	2022-06-27	Single Cell Mining Claim	(100) ALX RESOURCES CORP.	22.22105
296449	2018-04-10	2022-06-27	Single Cell Mining Claim	(100) ALX RESOURCES CORP.	22.21792
337430	2018-04-10	2022-06-27	Single Cell Mining Claim	(100) ALX RESOURCES CORP.	22.2213
337482	2018-04-10	2022-06-27	Single Cell Mining Claim	(100) ALX RESOURCES CORP.	22.22138
617583	2020-10-30	2022-10-30	Single Cell Mining Claim	(100) ALX RESOURCES CORP.	22.22164
617584	2020-10-30	2022-10-30	Single Cell Mining Claim	(100) ALX RESOURCES CORP.	22.21819
617585	2020-10-30	2022-10-30	Single Cell Mining Claim	(100) ALX RESOURCES CORP.	22.22316
617586	2020-10-30	2022-10-30	Single Cell Mining Claim	(100) ALX RESOURCES CORP.	22.22496
617587	2020-10-30	2022-10-30	Single Cell Mining Claim	(100) ALX RESOURCES CORP.	22.22173
617588	2020-10-30	2022-10-30	Single Cell Mining Claim	(100) ALX RESOURCES CORP.	22.22156
617589	2020-10-30	2022-10-30	Single Cell Mining Claim	(100) ALX RESOURCES CORP.	22.21811
617590	2020-10-30	2022-10-30	Single Cell Mining Claim	(100) ALX RESOURCES CORP.	22.22283
617591	2020-10-30	2022-10-30	Single Cell Mining Claim	(100) ALX RESOURCES CORP.	22.21925
617592	2020-10-30	2022-10-30	Single Cell Mining Claim	(100) ALX RESOURCES CORP.	22.22421
617593	2020-10-30	2022-10-30	Single Cell Mining Claim	(100) ALX RESOURCES CORP.	22.21974
617594	2020-10-30	2022-10-30	Single Cell Mining Claim	(100) ALX RESOURCES CORP.	22.22504
617595	2020-10-30	2022-10-30	Single Cell Mining Claim	(100) ALX RESOURCES CORP.	22.22324
617596	2020-10-30	2022-10-30	Single Cell Mining Claim	(100) ALX RESOURCES CORP.	22.22446
617597	2020-10-30	2022-10-30	Single Cell Mining Claim	(100) ALX RESOURCES CORP.	22.2243
617598	2020-10-30	2022-10-30	Single Cell Mining Claim	(100) ALX RESOURCES CORP.	22.22308
617599	2020-10-30	2022-10-30	Single Cell Mining Claim	(100) ALX RESOURCES CORP.	22.22299
617600	2020-10-30	2022-10-30	Single Cell Mining Claim	(100) ALX RESOURCES CORP.	22.21991
617601	2020-10-30	2022-10-30	Single Cell Mining Claim	(100) ALX RESOURCES CORP.	22.22487
617602	2020-10-30	2022-10-30	Single Cell Mining Claim	(100) ALX RESOURCES CORP.	22.22291
617603	2020-10-30	2022-10-30	Single Cell Mining Claim	(100) ALX RESOURCES CORP.	22.22259
617604	2020-10-30	2022-10-30	Single Cell Mining Claim	(100) ALX RESOURCES CORP.	22.22333
617605	2020-10-30	2022-10-30	Single Cell Mining Claim	(100) ALX RESOURCES CORP.	22.21999
617606	2020-10-30	2022-10-30	Single Cell Mining Claim	(100) ALX RESOURCES CORP.	22.21836
617607	2020-10-30	2022-10-30	Single Cell Mining Claim	(100) ALX RESOURCES CORP.	22.21982
617608	2020-10-30	2022-10-30	Single Cell Mining Claim	(100) ALX RESOURCES CORP.	22.22479
617609	2020-10-30	2022-10-30	Single Cell Mining Claim	(100) ALX RESOURCES CORP.	22.22148
617610	2020-10-30	2022-10-30	Single Cell Mining Claim	(100) ALX RESOURCES CORP.	22.22471
617611	2020-10-30	2022-10-30	Single Cell Mining Claim	(100) ALX RESOURCES CORP.	22.22454
617612	2020-10-30	2022-10-30	Single Cell Mining Claim	(100) ALX RESOURCES CORP.	22.22438
617613	2020-10-30	2022-10-30	Single Cell Mining Claim	(100) ALX RESOURCES CORP.	22.22275
617614	2020-10-30	2022-10-30	Single Cell Mining Claim	(100) ALX RESOURCES CORP.	22.22098
617615	2020-10-30	2022-10-30	Single Cell Mining Claim	(100) ALX RESOURCES CORP.	22.2209

667884	2021-07-09	2023-07-09	Single Cell Mining Claim	(100) ALX RESOURCES CORP.	22.22753
667885	2021-07-09	2023-07-09	Single Cell Mining Claim	(100) ALX RESOURCES CORP.	22.22844
667886	2021-07-09	2023-07-09	Single Cell Mining Claim	(100) ALX RESOURCES CORP.	22.22803
667887	2021-07-09	2023-07-09	Single Cell Mining Claim	(100) ALX RESOURCES CORP.	22.22962
667888	2021-07-09	2023-07-09	Single Cell Mining Claim	(100) ALX RESOURCES CORP.	22.22769
667889	2021-07-09	2023-07-09	Single Cell Mining Claim	(100) ALX RESOURCES CORP.	22.2165
667890	2021-07-09	2023-07-09	Single Cell Mining Claim	(100) ALX RESOURCES CORP.	22.21642
667891	2021-07-09	2023-07-09	Single Cell Mining Claim	(100) ALX RESOURCES CORP.	22.21576
667892	2021-07-09	2023-07-09	Single Cell Mining Claim	(100) ALX RESOURCES CORP.	22.21666
667893	2021-07-09	2023-07-09	Single Cell Mining Claim	(100) ALX RESOURCES CORP.	22.21584
667894	2021-07-09	2023-07-09	Single Cell Mining Claim	(100) ALX RESOURCES CORP.	22.21675
667895	2021-07-09	2023-07-09	Single Cell Mining Claim	(100) ALX RESOURCES CORP.	22.21609
667896	2021-07-09	2023-07-09	Single Cell Mining Claim	(100) ALX RESOURCES CORP.	22.21658
667897	2021-07-09	2023-07-09	Single Cell Mining Claim	(100) ALX RESOURCES CORP.	22.216
667898	2021-07-09	2023-07-09	Single Cell Mining Claim	(100) ALX RESOURCES CORP.	22.21592
667899	2021-07-09	2023-07-09	Single Cell Mining Claim	(100) ALX RESOURCES CORP.	22.21633
667900	2021-07-09	2023-07-09	Single Cell Mining Claim	(100) ALX RESOURCES CORP.	22.21625
667901	2021-07-09	2023-07-09	Single Cell Mining Claim	(100) ALX RESOURCES CORP.	22.21616

APPENDIX 2

Geotech Ltd. Logistics Report:

2021 Vertical Time-Domain Electromagnetic (“VTEM™” Plus)

Airborne Geophysical Survey

Cannon Copper Property, Ontario, Canada



VTEM™ Plus

REPORT ON A HELICOPTER-BORNE VERSATILE TIME
DOMAIN ELECTROMAGNETIC (VTEM™ Plus) AND HORIZONTAL
MAGNETIC GRADIOMETER GEOPHYSICAL SURVEY

October 2021

PROJECT: CANNON COPPER PROJECT
LOCATION: ELLIOT LAKE, ON
FOR: ALX RESOURCES CORP.
SURVEY FLOWN: JULY - AUGUST 2021
PROJECT: GL210096

Geotech Ltd.
270 Industrial Parkway South
Aurora, ON Canada L4G 3T9

Tel: +1 905 841 5004
Web: www.geotech.ca
Email: info@geotech.ca



TABLE OF CONTENTS

TABLE OF CONTENTS.....	1
LIST OF FIGURES.....	1
LIST OF TABLES	2
APPENDICES	2
EXECUTIVE SUMMARY.....	3
1. INTRODUCTION.....	4
1.1 General Considerations.....	4
1.2 Survey And System Specifications.....	5
1.3 Topographic Relief And Cultural Features.....	6
2. DATA ACQUISITION	7
2.1 Survey Area.....	7
2.2 Survey Operations.....	7
2.3 Flight Specifications.....	8
2.4 Aircraft and Equipment.....	8
2.4.1 Survey Aircraft	8
2.4.2 Electromagnetic System	8
2.4.3 Full Waveform VTEM™ Sensor Calibration	11
2.4.4 Horizontal Magnetic Gradiometer.....	12
2.4.5 Radar Altimeter	12
2.4.6 Laser Altimeter.....	12
2.4.7 GPS Navigation System	12
2.4.8 Digital Acquisition System.....	12
2.5 Base Station.....	13
3. PERSONNEL.....	14
4. DATA PROCESSING AND PRESENTATION.....	15
4.1 Flight Path.....	15
4.2 Electromagnetic Data	15
4.3 Horizontal Magnetic Gradiometer Data.....	17
4.4 Tau Parameter and CVG Calculation	17
5. DELIVERABLES.....	18
5.1 Survey Report.....	18
5.2 Maps	18
5.3 Digital Data	19
6. CONCLUSIONS AND RECOMMENDATIONS.....	23

LIST OF FIGURES

Figure 1: Survey location	4
Figure 2: Survey area location map on Google Earth.....	5
Figure 3: Cannon Copper Project flight paths over a Google Earth Image.....	6
Figure 4: VTEM™ Transmitter Current Waveform.....	9
Figure 5: VTEM™ plus System Configuration.....	11
Figure 6: Z, X and Fraser filtered X (FFx) components for "thin" target.....	16

LIST OF TABLES

Table 1: Survey Specifications	7
Table 2: Survey schedule.....	7
Table 3: Off-Time Decay Sampling Scheme.....	9
Table 4: VTEM™ System Specifications.....	10
Table 5: Acquisition Sampling Rates.....	13
Table 6: Geosoft GDB Data Format	19
Table 7: Geosoft Resistivity Depth Image GDB Data Format.....	21
Table 8: Geosoft database for the VTEM waveform.....	22

APPENDICES

A. Survey Location Maps.....	A1
B. Survey Survey Area Coordinates	B1
C. Geophysical Maps	C1
D. Generalized Modelling Results of the VTEM System.....	D1
E. TAU Analysis	E1
F. TEM Resistivity Depth Imaging (RDI)	F1
G. Resistivity Depth Images (RDI).....	G1

EXECUTIVE SUMMARY

CANNON COPPER PROJECT ELLIOT LAKE, ON

Between July 10th and August 5th, 2021, Geotech Ltd. carried out a helicopter-borne geophysical survey over the Cannon Copper Project area near Elliot Lake, ON.

Principal geophysical sensors included a versatile time domain electromagnetic (VTEM™ Plus) system and a horizontal magnetic gradiometer with two caesium sensors. Ancillary equipment included a GPS navigation system and a radar altimeter. A total of 203 line-kilometres of geophysical data for the Cannon Copper block were acquired during the survey.

In-field data quality assurance and preliminary processing were carried out on a daily basis during the acquisition phase. Preliminary and final data processing, including generation of final digital data and map products were undertaken from the office of Geotech Ltd. in Aurora, Ontario.

The preliminary processed survey results are presented as the following maps:

- Electromagnetic stacked profiles of the B-field Z Component
- Electromagnetic stacked profiles of dB/dt Z Component
- B-Field Z Component Channel grid
- dB/dt Z Component Channel grid
- Fraser Filtered X Component Channel grid
- Total Magnetic Intensity (TMI)
- Calculated Time Constant (Tau) with Calculated Vertical Derivative of TMI contours
- Calculated Vertical Derivative of TMI (CVG)
- Magnetic Total Horizontal Gradient (TotHG)
- Magnetic Tilt-Angle Derivative (TiltDrv)
- Resistivity Depth Imaging (RDI) sections and depth-slices are presented.

Digital data include all electromagnetic and magnetic products, plus ancillary data including the waveform.

The survey report describes the procedures for data acquisition, equipment used, processing, preliminary image presentation and the specifications for the digital data set.

1. INTRODUCTION

1.1 GENERAL CONSIDERATIONS

Geotech Ltd. performed a helicopter-borne geophysical survey over the Cannon Copper Project near Elliot Lake, ON (Figure 1 & Figure 2).

Warren W. Stanyer represented ALX Resources Corp. during the data acquisition and data processing phases of this project.

The geophysical surveys consisted of helicopter borne EM using the versatile time-domain electromagnetic (VTEM™) plus system with Full-Waveform processing. Measurements consisted of Vertical (Z) and In-line Horizontal (X) components of the EM fields using an induction coil and a horizontal magnetic gradiometer using two caesium magnetometers. A total of 203 line-km of geophysical data were acquired during the survey.

The crew was based out of Elliot Lake, ON (Figure 2) for the acquisition phase of the survey. Survey flying started on July 10th and was completed on August 5th, 2021.

Data quality control and quality assurance, and preliminary data processing were carried out on a daily basis during the acquisition phase of the project. Final data processing followed immediately after the end of the survey. Final reporting, data presentation and archiving were completed in October 2021.

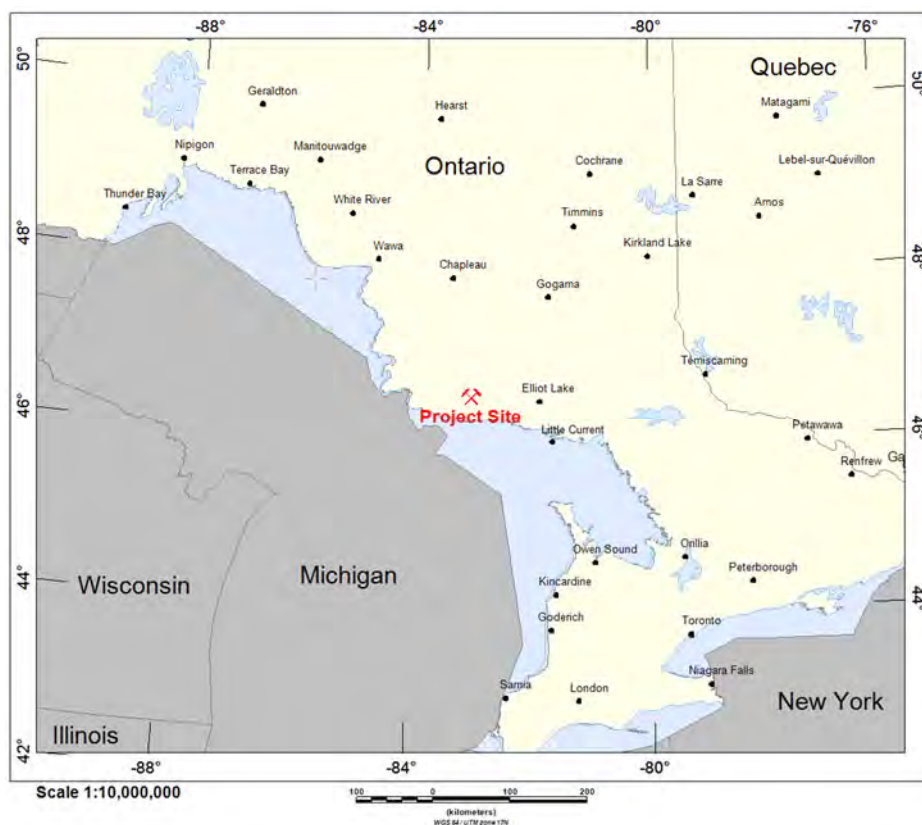


Figure 1: Survey location

1.2 SURVEY AND SYSTEM SPECIFICATIONS

The survey area is located approximately 29 km northwest of Elliot Lake, ON (Figure 2).



Figure 2: Survey area location map on Google Earth.

The Cannon Copper survey area was flown in a north to south ($N 0^{\circ} E$ azimuth) direction with traverse line spacings of 150 metres, as depicted in Figure 3. Tie lines were flown perpendicular to the traverse lines at 1500 metres spacing. For more detailed information on the flight spacings and directions, see Table 1.

1.3 TOPOGRAPHIC RELIEF AND CULTURAL FEATURES

Topographically, the survey area exhibits relief with elevations ranging from 274 to 449 metres over an area of 27 square kilometres (Figure 3).

There are signs of culture, such as roads within the Cannon Copper survey area.

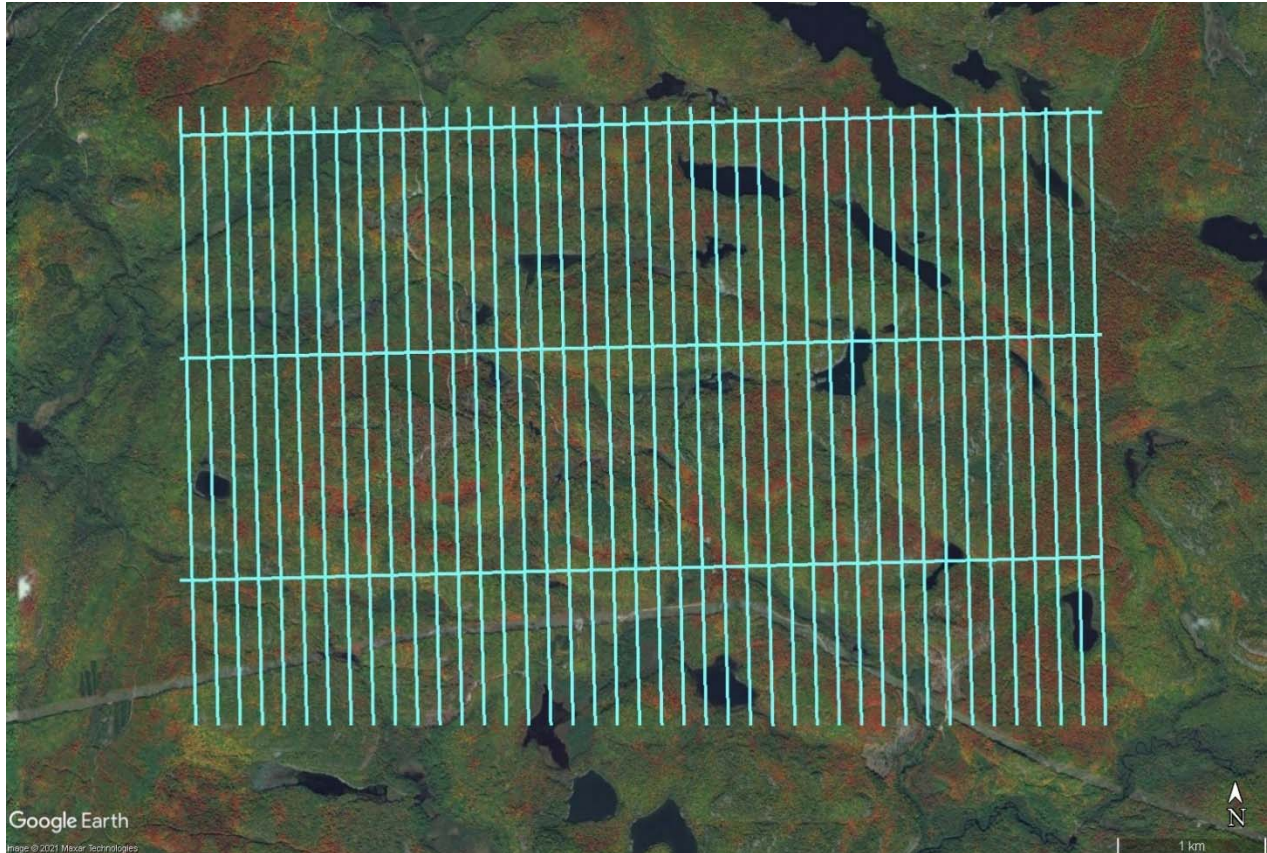


Figure 3: Cannon Copper Project flight paths over a Google Earth Image.

2. DATA ACQUISITION

2.1 SURVEY AREA

The survey area (see Figure 3 and Appendix A) and general flight specifications are as follows:

Table 1: Survey Specifications

Survey block	Line spacing (m)	Area (km ²)	Planned ¹ Line-km	Actual Line-km	Flight direction	Line numbers
Cannon Copper	Traverse: 150	27	194	203	N 0° E / N 180° E	L1000 – L1410
	Tie: 1500				N 90° E / N 270° E	T2000 – T2020
Total		27	194	203		

Survey area boundaries co-ordinates are provided in Appendix B.

2.2 SURVEY OPERATIONS

Survey operations were based out of Elliot Lake, ON (see Figure 2). The following table shows the timing of the flying.

Table 2: Survey schedule

Date	Comments
10-July	Crew arrived Elliot Lake
11-July	System assembly
12-July	System assembly and base station setup
13-July	Helicopter arrival
14-July	System assembly
15-July	Helicopter installation completed
16-July	Geometry, altimeter and flight test completed
17-July	System calibration, radar altimeter and test flight completed
18-July	Test flight and system troubleshooting
19-July	Test flight with geometry adjustments
20-July	Standby due to poor weather
21-July	Standby due to poor weather and radar altimeter troubleshooting
22-July	Radar altimeter installation and testing
23-July	Test flights
24-July	Standby due to poor weather
25-July	System calibration
26-July	Production Flight – 62.5 km flown
27-July	Production Flight – 41.7 km flown
28-July	Production Flight – 47.94 km flown
29-July	Standby due to poor weather
30-July	System troubleshooting due to elevated noise level
31-July	Standby due to poor weather
01-August	Standby due to poor weather

¹ Note: Actual Line kilometres represent the total line kilometres in the final database.

Date	Comments
02-August	System troubleshooting
03-August	Test flights
04-August	Production Flight – 38.0 km flown
05-August	Demobilization

2.3 FLIGHT SPECIFICATIONS

During the survey, the helicopter was maintained at a mean altitude of 115 metres above the ground with an average survey speed of 72 km/hour. This allowed for an actual average Transmitter-receiver loop terrain clearance of 60 metres and a magnetic sensor clearance of 70 metres.

The on-board operator was responsible for monitoring the system integrity. He also maintained a detailed flight log during the survey, tracking the times of the flight as well as any unusual geophysical or topographic features.

On return of the aircrew to the base camp the survey data was transferred from a compact flash card (PCMCIA) to the data processing computer. The data were then uploaded via ftp to the Geotech office in Aurora for daily quality assurance and quality control by qualified personnel.

2.4 AIRCRAFT AND EQUIPMENT

2.4.1 SURVEY AIRCRAFT

The survey was flown using a Eurocopter Aerospatiale (A-Star) 350 B2 helicopter, registration C-GVMU. The helicopter is owned and operated by Geotech Aviation Ltd. Installation of the geophysical and ancillary equipment was carried out by a Geotech Ltd. crew.

2.4.2 ELECTROMAGNETIC SYSTEM

The electromagnetic system was a Geotech Time Domain EM (VTEM™ Plus) full receiver-waveform streamed data recorded system. The “full waveform VTEM system” uses the streamed half-cycle recording of transmitter and receiver waveforms to obtain a complete system response calibration throughout the entire survey flight. VTEM with the serial number 32 had been used for the survey. The VTEM™ transmitter current waveform is shown diagrammatically in Figure 4.

The VTEM™ Receiver and transmitter coils were in concentric-coplanar and Z-direction oriented configuration. The receiver system for the project also included coincident-coaxial X-direction coil to measure the in-line dB/dt and calculate B-Field responses. The Transmitter-receiver loop was towed at a mean distance of 55 metres below the aircraft as shown in Figure 5.

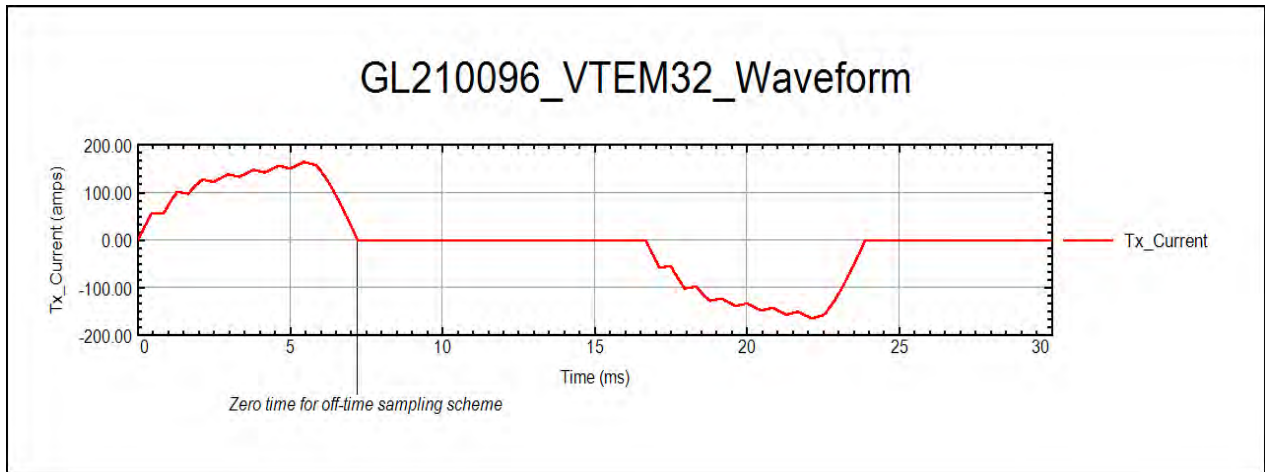


Figure 4: VTEM™ Transmitter Current Waveform

The VTEM™ decay sampling scheme is shown in Table 3 below. Forty-three-time measurement gates were used for the final data processing in the range from 0.021 to 8.083 msec. Zero time for the off-time sampling scheme is equal to the current pulse width and is defined as the time near the end of the turn-off ramp where the di/dt waveform falls to 1/2 of its peak value.

Table 3: Off-Time Decay Sampling Scheme

VTEM™ Decay Sampling Scheme				
Index	Start	End	Middle	Width
Milliseconds				
4	0.018	0.023	0.021	0.005
5	0.023	0.029	0.026	0.005
6	0.029	0.034	0.031	0.005
7	0.034	0.039	0.036	0.005
8	0.039	0.045	0.042	0.006
9	0.045	0.051	0.048	0.007
10	0.051	0.059	0.055	0.008
11	0.059	0.068	0.063	0.009
12	0.068	0.078	0.073	0.010
13	0.078	0.090	0.083	0.012
14	0.090	0.103	0.096	0.013
15	0.103	0.118	0.110	0.015
16	0.118	0.136	0.126	0.018
17	0.136	0.156	0.145	0.020
18	0.156	0.179	0.167	0.023
19	0.179	0.206	0.192	0.027
20	0.206	0.236	0.220	0.030
21	0.236	0.271	0.253	0.035
22	0.271	0.312	0.290	0.040
23	0.312	0.358	0.333	0.046

VTEM™ Decay Sampling Scheme				
Index	Start	End	Middle	Width
Milliseconds				
24	0.358	0.411	0.383	0.053
25	0.411	0.472	0.440	0.061
26	0.472	0.543	0.505	0.070
27	0.543	0.623	0.580	0.081
28	0.623	0.716	0.667	0.093
29	0.716	0.823	0.766	0.107
30	0.823	0.945	0.880	0.122
31	0.945	1.086	1.010	0.141
32	1.086	1.247	1.161	0.161
33	1.247	1.432	1.333	0.185
34	1.432	1.646	1.531	0.214
35	1.646	1.891	1.760	0.245
36	1.891	2.172	2.021	0.281
37	2.172	2.495	2.323	0.323
38	2.495	2.865	2.667	0.370
39	2.865	3.292	3.063	0.427
40	3.292	3.781	3.521	0.490
41	3.781	4.341	4.042	0.560
42	4.341	4.987	4.641	0.646
43	4.987	5.729	5.333	0.742
44	5.729	6.581	6.125	0.852
45	6.581	7.560	7.036	0.979
46	7.560	8.685	8.083	1.125

Z Component: 4-46 time gates
X Component: 20-46 time gates

Table 4: VTEM™ System Specifications

Transmitter	Receiver
<ul style="list-style-type: none"> • Transmitter loop diameter: 26 m • Number of turns: 4 • Effective Transmitter loop area: 2123.7 m² • Transmitter base frequency: 30 Hz • Peak current: 164 A • Pulse width: 7.22 ms • Waveform shape: Bi-polar trapezoid • Peak dipole moment: 348,289 nIA • Average transmitter-receiver loop terrain clearance: 60 metres 	<ul style="list-style-type: none"> • X -Coil diameter: 0.32 m • Number of turns: 245 • Effective coil area: 19.69 m² • Z-Coil diameter: 1.2 m • Number of turns: 100 • Effective coil area: 113.04 m²

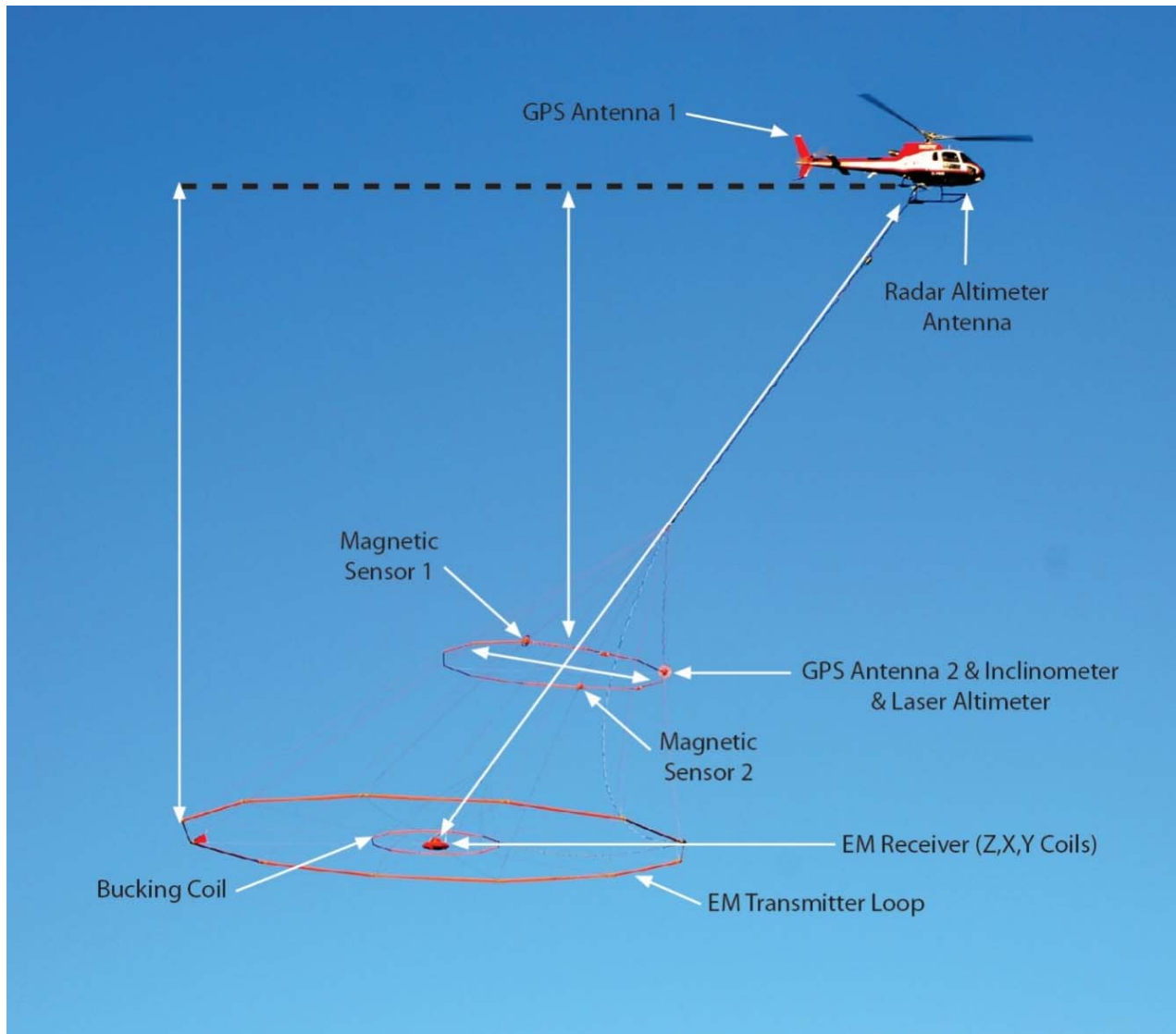


Figure 5: VTEM™plus System Configuration.

2.4.3 FULL WAVEFORM VTEM™ SENSOR CALIBRATION

The calibration is performed on the complete VTEM™ system installed in and connected to the helicopter, using special calibration equipment. This calibration takes place on the ground at the start of the project prior to surveying.

The procedure takes half-cycle files acquired and calculates a calibration file consisting of a single stacked half-cycle waveform. The purpose of the stacking is to attenuate natural and man-made magnetic signals, leaving only the response to the calibration signal.

This calibration allows the transfer function between the EM receiver and data acquisition system and the transfer function between the current monitor and data acquisition system to be determined. These calibration results are then used in VTEM full waveform processing.

2.4.4 HORIZONTAL MAGNETIC GRADIOMETER

The horizontal magnetic gradiometer consists of two Geometrics split-beam field magnetic sensors with a sampling interval of 0.1 seconds. These sensors are mounted 12.5 metres apart on a separate loop, 10 metres above the Transmitter-receiver loop. A GPS antenna and Gyro Inclinator is installed on the separate loop to accurately record the tilt and position of the magnetic gradiometer sensors.

2.4.5 RADAR ALTIMETER

A Terra TRA 3000/TRI 40 radar altimeter was used to record terrain clearance. The antenna was mounted beneath the bubble of the helicopter cockpit (Figure 5).

2.4.6 LASER ALTIMETER

A Schmitt Industries AR300 laser altimeter was used. Altitude range 0.5 to 300m and accuracy ± 5 cm.

2.4.7 GPS NAVIGATION SYSTEM

The navigation system used was a Geotech PC104 based navigation system utilizing a NovAtel's WAAS(Wide Area Augmentation System) enabled GPS receiver, Geotech navigate software, a full screen display with controls in front of the pilot to direct the flight and a NovAtel GPS antenna mounted on the helicopter tail (Figure 5). As many as 11 GPS and two WAAS satellites may be monitored at any one time. The positional accuracy or circular error probability (CEP) is 1.8 m, with WAAS active, it is 1.0 m. The coordinates of the survey area were set-up prior to the survey and the information was fed into the airborne navigation system. The second GPS antenna is installed on the additional magnetic loop together with Gyro Inclinator.

2.4.8 DIGITAL ACQUISITION SYSTEM

A Geotech data acquisition system recorded the digital survey data on an internal compact flash card. Data is displayed on an LCD screen as traces to allow the operator to monitor the integrity of the system. The data type and sampling interval as provided in Table 5

Table 5: Acquisition Sampling Rates

Data Type	Sampling
TDEM	0.1 sec
Magnetometer	0.1 sec
GPS Position	0.2 sec
Radar Altimeter	0.2 sec
Inclinometer	0.1 sec
Laser	0.1 sec

2.5 BASE STATION

A combined magnetometer/GPS base station was utilized on this project. A Geometrics Caesium vapour magnetometer was used as a magnetic sensor with a sensitivity of 0.001 nT. The base station was recording the magnetic field together with the GPS time at 1 Hz on a base station computer.

The base station magnetometer sensor was installed in a secured location away from electric transmission lines and moving ferrous objects such as motor vehicles. The base station data were backed-up to the data processing computer at the end of each survey day.

3. PERSONNEL

The following Geotech Ltd. personnel were involved in the project.

FIELD:

Project Manager:	Tai-Chyi Shei
Data QC:	Marta Orta
Crew chief:	Adolf Masiyandima
Operator:	Timothy Rideout

The survey pilot and the mechanical engineer were employed directly by the helicopter operator – Geotech Aviation Ltd.

Pilot:	Rob Girard
Mechanical Engineer:	n/a

OFFICE:

Preliminary Data Processing:	Marta Orta
Final Data Processing:	Mike Finlayson
Data QA/QC:	Emily Data Jean Legault
Reporting/Mapping:	Oreva Oputeh

Processing and Interpretation phases were carried out under the supervision of Emily Data & Jean M. Legault, M.Sc.A, P.Geo (OGQ)– Chief Geophysicist. The customer relations were looked after by David Hitz.

4. DATA PROCESSING AND PRESENTATION

Data compilation and processing were carried out by the application of Geosoft OASIS Montaj and programs proprietary to Geotech Ltd.

4.1 FLIGHT PATH

The flight path, recorded by the acquisition program as WGS 84 latitude/longitude, was converted into the NAD83 Datum, UTM Zone 17N coordinate system in Oasis Montaj.

The flight path was drawn using linear interpolation between x, y positions from the navigation system. Positions are updated every second and expressed as UTM easting's (x) and UTM northing's (y).

4.2 ELECTROMAGNETIC DATA

The Full Waveform EM specific data processing operations included:

- Half cycle stacking (performed at time of acquisition).
- System response correction.
- Parasitic and drift removal.

A three-stage digital filtering process was used to reject major spheric events and to reduce noise levels. Local spheric activity can produce sharp, large amplitude events that cannot be removed by conventional filtering procedures. Smoothing or stacking will reduce their amplitude but leave a broader residual response that can be confused with geological phenomena. To avoid this possibility, a computer algorithm searches out and rejects the major spheric events.

The signal to noise ratio was further improved by the application of a low pass linear digital filter. This filter has zero phase shift which prevents any lag or peak displacement from occurring, and it suppresses only variations with a wavelength less than about 1 second or 15 metres. This filter is a symmetrical 1 sec linear filter.

The results are presented as stacked profiles of EM voltages for the time gates, in linear - logarithmic scale for the B-field Z component and dB/dt responses in the Z and X components. B-field Z component time channels recorded at 0.880 milliseconds after the termination of the impulse is also presented as a colour image. Calculated Time Constant (TAU) with Calculated Vertical Derivative contours is presented in Appendix C. Resistivity Depth Image (RDI) is also presented in Appendix G.

VTEM™ has two receiver coil orientations. Z-axis coil is oriented parallel to the transmitter coil axis, and both are horizontal to the ground. The X-axis coil is oriented parallel to the ground and along the line-of-flight. The combination of the X and Z coils configuration provides information on the position, depth, dip, and thickness of a conductor. Generalized modeling results of VTEM data are shown in Appendix D.

In general X-component data produce cross-over type anomalies: from “+ to -” in flight direction of flight for “thin” sub vertical targets and from “- to +” in direction of flight for “thick” targets. Z component data produce double peak type anomalies for “thin” sub vertical targets and single peak for “thick” targets. The limits and change-over of “thin-thick” depends on dimensions of a TEM system (Appendix D, Figure D-16).

Because of X component polarity is under line-of-flight, convolution Fraser Filter (Figure 6) is applied to X component data to represent axes of conductors in the form of grid map. In this case positive FF anomalies always correspond to “plus-to-minus” X data crossovers independent of the flight direction.

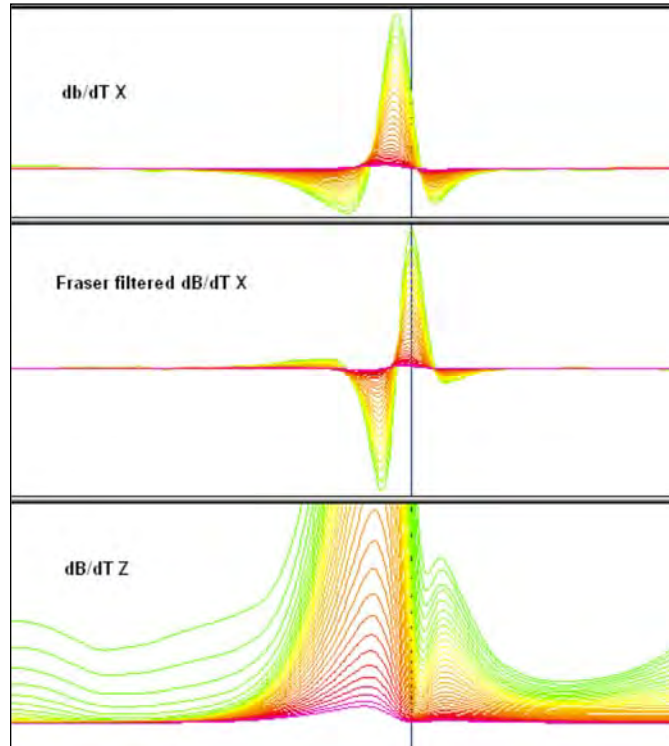


Figure 6: Z, X and Fraser filtered X (FFx) components for “thin” target.

4.3 HORIZONTAL MAGNETIC GRADIOMETER DATA

The horizontal gradients data from the VTEM™ Plus are measured by two magnetometers 12.5 m apart on an independent bird mounted 10m above the VTEM™ loop. A GPS and a Gyro Inclinometer help to determine the positions and orientations of the magnetometers. The data from the two magnetometers are corrected for position and orientation variations, as well as for the diurnal variations using the base station data.

The position of the centre of the horizontal magnetic gradiometer bird is calculated from the GPS utilizing in-house processing tool in Geosoft. Following that total magnetic intensity is calculated at the center of the bird by calculating the mean values from both sensors. In addition to the total intensity advanced processing is done to calculate the in-line and crossline (or lateral) horizontal gradient which enhance the understanding of magnetic targets. The in-line (longitudinal) horizontal gradient is calculated from the difference of two consecutive total magnetic field readings divided by the distance along the flight line direction, while the crossline (lateral) horizontal magnetic gradient is calculated from the difference in the magnetic readings from both magnetic sensors divided by their horizontal separation.

Two advanced magnetic derivative products, the total horizontal derivative (THDR), and tilt angle derivative and are also created. The total horizontal derivative or gradient is defined as:

$THDR = \sqrt{H_x^2 + H_y^2}$, where H_x and H_y are crossline and in-line horizontal gradients.

The tilt angle derivative (TDR) is defined as:

$TDR = \arctan (V_z/THDR)$, where THDR is the total horizontal derivative, and V_z is the vertical derivative.

Measured crossline gradients can help to enhance crossline linear features during gridding.

4.4 TAU PARAMETER AND CVG CALCULATION

The processed VTEM survey results are presented as a calculated dB/dt time constant (Tau), which is an indicator of geological unit's electrical conductance.

An explanation of the EM time constant calculation is provided in Appendix E. The TAU dB/dt map is presented in Appendix C. The map is accompanied by an overlay of the calculated vertical gradient of TMI anomaly contours for tracing possible EM-MAG anomaly correlations.

The CVG contour layer, on the top of TAU color grid, is generally more representative of the smaller scale and shallower magnetic sources in comparison with the TMI. The calculated vertical derivative (CVG) is designed to emphasize structures and lithological units that may not otherwise be seen on the TMI due to the nearby presence of stronger magnetic responses, showing a high resolution in terms of individual structures.

5. DELIVERABLES

5.1 SURVEY REPORT

The survey report describes the data acquisition, processing, and final presentation of the survey results. The survey report is provided in two paper copies and digitally in PDF format.

5.2 MAPS

Final maps were produced at scale of 1:7,000 for best representation of the survey size and line spacing. The coordinate/projection system used was WGS84 Datum, UTM Zone 17N. All maps show the flight path trace and topographic data, latitude and longitude.

The results of the survey are presented as EM profiles, a late-time gate gridded EM channel, and a colour magnetic TMI contour map.

- Maps at 1:7,000 in Geosoft MAP format, as follows:

GL210096_7K_dBdt:	dB/dt profiles Z Component, Time Gates 0.220 – 7.036 ms in linear – logarithmic scale.
GL210096_7K_BField:	B-field profiles Z Component, Time Gates 0.220 – 7.036 ms in linear – logarithmic scale.
GL210096_7K_BFz30:	B-field Z Component Channel 30, Time Gate 0.880 ms colour image.
GL210096_7K_SFz10:	VTEM dB/dt Z Component Channel 10, Time Gate 0.055 ms colour image
GL210096_7K_SFz35:	VTEM dB/dt Z Component Channel 35, Time Gate 1.760 ms colour image
GL210096_7K_SFxFF25:	Fraser Filtered dB/dt X Component Channel 25, Time Gate 0.440 ms colour image.
GL210096_7K_TMI:	Total Magnetic Intensity (TMI) colour image and contours.
GL210096_7K_CVG:	Calculated Vertical Derivative (CVG) of TMI colour image.
GL210096_7K_TauSF_CVG:	dB/dt Calculated Time Constant (Tau) with Calculated Vertical Derivative contours.
GL210096_7K_TotHG:	Magnetic Total Horizontal Gradient colour image
GL210096_7K_TiltDrv:	Magnetic Tilt Angle Derivative colour image

- Maps are also presented in PDF format.
- The topographic data base was derived from 1:250,000 CANVEC Data. Inset data is from Geocommunities (www.geocomm.com)
- A Google Earth file *GL210096_ALX.kmz* showing the flight path of the block is included. Free versions of Google Earth software from: <http://earth.google.com/download-earth.html>

5.3 DIGITAL DATA

Two copies of the data and maps on DVD were prepared to accompany the report. Each DVD contains a digital file of the line data in GDB Geosoft Montaj format as well as the maps in Geosoft Montaj Map and PDF format.

- DVD structure.

Data contains databases, grids and maps, as described below.
 Report contains a copy of the report and appendices in PDF format.

Databases in Geosoft GDB format, containing the channels listed in Table 6.

Table 6: Geosoft GDB Data Format

Channel name	Units	Description
X	metres	Easting WGS84 Zone 17N
Y	metres	Northing WGS84 Zone 17N
Longitude	Decimal Degrees	WGS84 Longitude data
Latitude	Decimal Degrees	WGS84 Latitude data
Z	metres	GPS antenna elevation
Zb	metres	EM bird elevation
Radar	metres	Helicopter terrain clearance from radar altimeter
Radarb	metres	Calculated EM transmitter-receiver loop terrain clearance from radar altimeter
DEM	metres	Digital Elevation Model
Gtime	Seconds of the day	GPS time
Mag1L	nT	Measured Total Magnetic field data (left sensor)
Mag1R	nT	Measured Total Magnetic field data (right sensor)
Basemag	nT	Magnetic diurnal variation data
Mag2LZ	nT	Z corrected (w.r.t. loop center) and diurnal corrected magnetic field left mag
Mag2RZ	nT	Z corrected (w.r.t. loop center) and diurnal corrected magnetic field right mag
TMI2	nT	Calculated from diurnal corrected total magnetic field intensity of the centre of the loop
TMI3	nT	Microleveled total magnetic field intensity of the centre of the loop
Hginline		Calculated in-line gradient
Hgcxline		Measured cross-line gradient
CVG	nT/m	Calculated Magnetic Vertical Gradient of TMI
SFz[4]	pV/(A*m ⁴)	Z dB/dt 0.021 millisecond time channel
SFz[5]	pV/(A*m ⁴)	Z dB/dt 0.026 millisecond time channel
SFz[6]	pV/(A*m ⁴)	Z dB/dt 0.031 millisecond time channel
SFz[7]	pV/(A*m ⁴)	Z dB/dt 0.036 millisecond time channel
SFz[8]	pV/(A*m ⁴)	Z dB/dt 0.042 millisecond time channel
SFz[9]	pV/(A*m ⁴)	Z dB/dt 0.048 millisecond time channel
SFz[10]	pV/(A*m ⁴)	Z dB/dt 0.055 millisecond time channel
SFz[11]	pV/(A*m ⁴)	Z dB/dt 0.063 millisecond time channel
SFz[12]	pV/(A*m ⁴)	Z dB/dt 0.073 millisecond time channel
SFz[13]	pV/(A*m ⁴)	Z dB/dt 0.083 millisecond time channel
SFz[14]	pV/(A*m ⁴)	Z dB/dt 0.096 millisecond time channel

Channel name	Units	Description
SFz[15]	pV/(A*m ⁴)	Z dB/dt 0.110 millisecond time channel
SFz[16]	pV/(A*m ⁴)	Z dB/dt 0.126 millisecond time channel
SFz[17]	pV/(A*m ⁴)	Z dB/dt 0.145 millisecond time channel
SFz[18]	pV/(A*m ⁴)	Z dB/dt 0.167 millisecond time channel
SFz[19]	pV/(A*m ⁴)	Z dB/dt 0.192 millisecond time channel
SFz[20]	pV/(A*m ⁴)	Z dB/dt 0.220 millisecond time channel
SFz[21]	pV/(A*m ⁴)	Z dB/dt 0.253 millisecond time channel
SFz[22]	pV/(A*m ⁴)	Z dB/dt 0.290 millisecond time channel
SFz[23]	pV/(A*m ⁴)	Z dB/dt 0.333 millisecond time channel
SFz[24]	pV/(A*m ⁴)	Z dB/dt 0.383 millisecond time channel
SFz[25]	pV/(A*m ⁴)	Z dB/dt 0.440 millisecond time channel
SFz[26]	pV/(A*m ⁴)	Z dB/dt 0.505 millisecond time channel
SFz[27]	pV/(A*m ⁴)	Z dB/dt 0.580 millisecond time channel
SFz[28]	pV/(A*m ⁴)	Z dB/dt 0.667 millisecond time channel
SFz[29]	pV/(A*m ⁴)	Z dB/dt 0.766 millisecond time channel
SFz[30]	pV/(A*m ⁴)	Z dB/dt 0.880 millisecond time channel
SFz[31]	pV/(A*m ⁴)	Z dB/dt 1.010 millisecond time channel
SFz[32]	pV/(A*m ⁴)	Z dB/dt 1.161 millisecond time channel
SFz[33]	pV/(A*m ⁴)	Z dB/dt 1.333 millisecond time channel
SFz[34]	pV/(A*m ⁴)	Z dB/dt 1.531 millisecond time channel
SFz[35]	pV/(A*m ⁴)	Z dB/dt 1.760 millisecond time channel
SFz[36]	pV/(A*m ⁴)	Z dB/dt 2.021 millisecond time channel
SFz[37]	pV/(A*m ⁴)	Z dB/dt 2.323 millisecond time channel
SFz[38]	pV/(A*m ⁴)	Z dB/dt 2.667 millisecond time channel
SFz[39]	pV/(A*m ⁴)	Z dB/dt 3.063 millisecond time channel
SFz[40]	pV/(A*m ⁴)	Z dB/dt 3.521 millisecond time channel
SFz[41]	pV/(A*m ⁴)	Z dB/dt 4.042 millisecond time channel
SFz[42]	pV/(A*m ⁴)	Z dB/dt 4.641 millisecond time channel
SFz[43]	pV/(A*m ⁴)	Z dB/dt 5.333 millisecond time channel
SFz[44]	pV/(A*m ⁴)	Z dB/dt 6.125 millisecond time channel
SFz[45]	pV/(A*m ⁴)	Z dB/dt 7.036 millisecond time channel
SFz[46]	pV/(A*m ⁴)	Z dB/dt 8.083 millisecond time channel
SFx[20]	pV/(A*m ⁴)	X dB/dt 0.220 millisecond time channel
SFx[21]	pV/(A*m ⁴)	X dB/dt 0.253 millisecond time channel
SFx[22]	pV/(A*m ⁴)	X dB/dt 0.290 millisecond time channel
SFx[23]	pV/(A*m ⁴)	X dB/dt 0.333 millisecond time channel
SFx[24]	pV/(A*m ⁴)	X dB/dt 0.383 millisecond time channel
SFx[25]	pV/(A*m ⁴)	X dB/dt 0.440 millisecond time channel
SFx[26]	pV/(A*m ⁴)	X dB/dt 0.505 millisecond time channel
SFx[27]	pV/(A*m ⁴)	X dB/dt 0.580 millisecond time channel
SFx[28]	pV/(A*m ⁴)	X dB/dt 0.667 millisecond time channel
SFx[29]	pV/(A*m ⁴)	X dB/dt 0.766 millisecond time channel
SFx[30]	pV/(A*m ⁴)	X dB/dt 0.880 millisecond time channel
SFx[31]	pV/(A*m ⁴)	X dB/dt 1.010 millisecond time channel
SFx[32]	pV/(A*m ⁴)	X dB/dt 1.161 millisecond time channel
SFx[33]	pV/(A*m ⁴)	X dB/dt 1.333 millisecond time channel
SFx[34]	pV/(A*m ⁴)	X dB/dt 1.531 millisecond time channel
SFx[35]	pV/(A*m ⁴)	X dB/dt 1.760 millisecond time channel
SFx[36]	pV/(A*m ⁴)	X dB/dt 2.021 millisecond time channel
SFx[37]	pV/(A*m ⁴)	X dB/dt 2.323 millisecond time channel

Channel name	Units	Description
SFx[38]	pV/(A*m ⁴)	X dB/dt 2.667 millisecond time channel
SFx[39]	pV/(A*m ⁴)	X dB/dt 3.063 millisecond time channel
SFx[40]	pV/(A*m ⁴)	X dB/dt 3.521 millisecond time channel
SFx[41]	pV/(A*m ⁴)	X dB/dt 4.042 millisecond time channel
SFx[42]	pV/(A*m ⁴)	X dB/dt 4.641 millisecond time channel
SFx[43]	pV/(A*m ⁴)	X dB/dt 5.333 millisecond time channel
SFx[44]	pV/(A*m ⁴)	X dB/dt 6.125 millisecond time channel
SFx[45]	pV/(A*m ⁴)	X dB/dt 7.036 millisecond time channel
SFx[46]	pV/(A*m ⁴)	X dB/dt 8.083 millisecond time channel
BFz	(pV*ms)/(A*m ⁴)	Z B-Field data for time channels 4 to 46
BFX	(pV*ms)/(A*m ⁴)	X B-Field data for time channels 20 to 46
SFxFF	pV/(A*m ⁴)	Fraser Filtered X dB/dt
NchanBF		Latest time channels of TAU calculation
TauBF	ms	Time constant B-Field
NchanSF		Latest time channels of TAU calculation
TauSF	ms	Time constant dB/dt
PLM		60 Hz power line monitor

Electromagnetic B-field and dB/dt Z component data is found in array channel format between indexes 4 – 46, and X component data from 20 – 46, as described above.

- Database of the Resistivity Depth Images in Geosoft GDB format, containing the following channels:

Table 7: Geosoft Resistivity Depth Image GDB Data Format

Channel name	Units	Description
Xg	metres	Easting WGS84 Zone 17N
Yg	metres	Northing WGS84 Zone 17N
Dist	metres	Distance from the beginning of the line
Depth	metres	array channel, depth from the surface
Z	metres	array channel, depth
AppRes	Ohm-m	array channel, Apparent Resistivity
TR	metres	EM system height
Topo	metres	digital elevation model
Radarb	metres	Calculated EM transmitter-receiver loop terrain clearance from radar altimeter
SF	pV/(A*m ⁴)	array channel, Z dB/dT
MAG	nT	TMI data
CVG	nT/m	CVG data
DOI	metres	Depth of Investigation: a measure of VTEM depth effectiveness
PLM		60Hz Power Line Monitor

- Database of the VTEM Waveform “GL210056_Waveform.gdb” in Geosoft GDB format, containing the following channels:

Table 8: Geosoft database for the VTEM waveform

Channel name	Units	Description
Time	milliseconds	Sampling rate interval, 5.2083 microseconds
Tx_Current	amps	Output current of the transmitter

- Geosoft Resistivity Depth Image Products:

Sections: Apparent resistivity sections along each line in .GRD and .PDF format
 Slices: Apparent resistivity slices at selected depths from 25m to depth of investigation, at an increment of 25m in .GRD and .PDF format
 Voxel: 3D Voxel imaging of apparent resistivity data clipped by digital elevation and depth of investigation

- Grids in Geosoft GRD and GeoTIFF format, as follows:

GL210096_BFz30: B-Field Z Component Channel 30(Time Gate 0.880 ms)
 GL210096_SFxFF25: Fraser Filtered dB/dt X Component Channel 25 (Time Gate 0.440ms)
 GL210096_SFz10: dB/dt Z Component Channel 10 (Time Gate 0.055 ms)
 GL210096_SFz25: dB/dt Z Component Channel 25 (Time Gate 0.440 ms)
 GL210096_SFz35: dB/dt Z Component Channel 35 (Time Gate 1.760 ms)
 GL210096_SFz45: dB/dt Z Component Channel 45 (Time Gate 7.036 ms)
 GL210096_TauBF: B-Field Z Component, Calculated Time Constant (ms)
 GL210096_TauSF: dB/dt Z Component, Calculated Time Constant (ms)
 GL210096_TMI: Total Magnetic Intensity (nT)
 GL210096_CVG: Calculated Vertical Derivative(nT/m)
 GL210096_Hgcxline: Measured Cross-Line Gradient (nT/m)
 GL210096_Hginline: Measured In-Line Gradient (nT/m)
 GL210096_TotHGrad: Magnetic Total Horizontal Gradient (nT/m)
 GL210096_TiltDrv: Magnetic Tilt derivative (radians)
 GL210096_DEM: Digital Elevation Model (m)
 GL210096_PLM: 60Hz Power Line Monitor

A Geosoft .GRD file has a .GI metadata file associated with it, containing grid projection information. A grid cell size of 37.5 metres was used.

6. CONCLUSIONS AND RECOMMENDATIONS

A helicopter-borne versatile time domain electromagnetic (VTEM™plus) horizontal magnetic gradiometer geophysical survey has been completed over the Cannon Copper Project near Elliot Lake, ON, on behalf of ALX Resources Corp.

The total area coverage is 27km² and the total survey line coverage is 203 line kilometres over one survey block. The principal sensors included a Time Domain EM system, and a horizontal magnetic gradiometer system with two caesium magnetometers. Results have been presented as stacked profiles, and contour colour images at a scale of 1:7,000. A formal interpretation has not been included in this study, however RDI resistivity-depth imaging have been performed in support of the VTEM data.

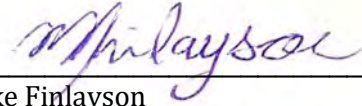
Based on the geophysical results obtained, a number of conductive and magnetic anomalies have been identified at Cannon Copper Project. Magnetically, the block is host to low to moderately-strongly magnetic host rocks, with a measured range of approx. 250 nT. The area features generally east-west oriented, alternating low and high magnetic elongated trends, that extend across the block. These are in turn cross-cut by NW-SE discordant, magnetic high and low lineaments – possibly a mix late dyke swarms and structures, respectively. A prominent cross-shaped low is noticeable in the north central part of the block that coincides with the known deposit region. Magnetic derivatives enhance the primary E-W trends and NW-SE discordant trends. Electromagnetically, the property is dominated by a prominent, gently curving, east-westerly, strongly anomalous lineament response that directly correlates with a visible powerline at the southern end of the block. In addition to being inductively coupled, the powerline appears to have also imparted high level of late-channel EM noise that affects the VTEM data across the block. Away from the powerline, much of the block is largely resistive, with no coherent late-channel EM anomalies discerned, except for negative decays from AIIP (airborne inductive induced polarization) effects. A number of short to medium strike-length (~300-500m), early channel (<ch15) conductive anomalies are defined throughout the block, some of which are aligned and without obvious geomorphologic explanation. Overall, these EM anomalies lack direct magnetic associations. The relationship between the EM and magnetic signatures are highlighted in the TAU and CVG contour maps (Appendix C) and the resistivity-depth image (RDI) sections (Appendix G). Away from the powerline, conductive anomalies feature peak late channel EM dBz/dt time constants of <0.15 ms, indicating low conductivities. Based on the RDI imaging results, apparent resistivities of range from as low as approx. 2 ohm-m and reach as high as approx. 4500-6000 ohm-m. Estimated burial depth to the top of the anomalous zones is within the near surface and maximum depths of depths of investigation (DOI) from ~250m to >650m depths.

The Cannon Copper Project is prospective for high grade, disseminated to massive copper mineralization in quartz-vein and quartz breccias, including the Cannon (Crownbridge) Copper Mine that lies on the property (www.alxresources.com). As a result, both the EM and magnetic results are likely to be of exploration interest. We recommend that EM anomaly picking be performed to define features of interest; Maxwell EM plate modeling may not be necessary or applicable. The combination of 1D and possibly 3D EM inversion could prove useful in better defining the conductive and resistive resistivity contrasts related to shear-hosted copper targets. CET-type magnetic lineament analysis and 3D MVI magnetic inversions may prove useful for mapping structure, alteration, and lithology in 2D-3D space across the blocks. We recommend that more advanced, integrated interpretation be performed on these geophysical data and these results further evaluated against the known geology for future targeting. Ground follow-up with IP or EM is also recommended prior to drill testing.

Respectfully submitted².



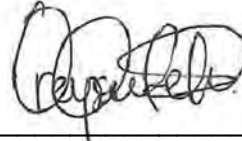
Marta Orta
Geotech Ltd.



Mike Finlayson
Geotech Ltd.



Jean M. Legault, M.Sc.A, P.Eng, P.Geo
Geotech Ltd.



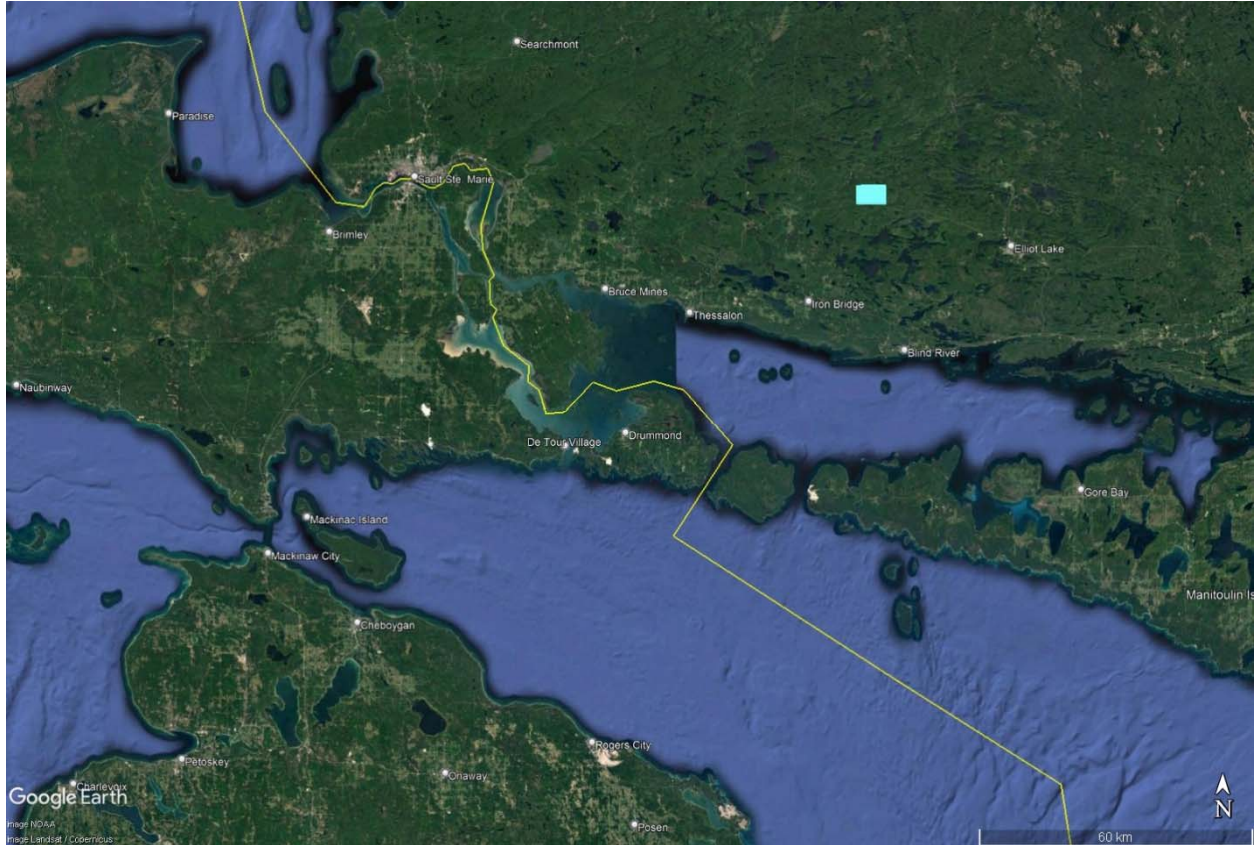
Ovea Oputeh
Geotech Ltd.

October 2021

²Final data processing of the EM and magnetic data was carried out by Mike Finlayson, from the offices of Geotech Ltd. in Aurora, Ontario, under the supervision of Emily Data & Jean M. Legault, Chief Geophysicist.

APPENDIX A

SURVEY AREA LOCATION MAP



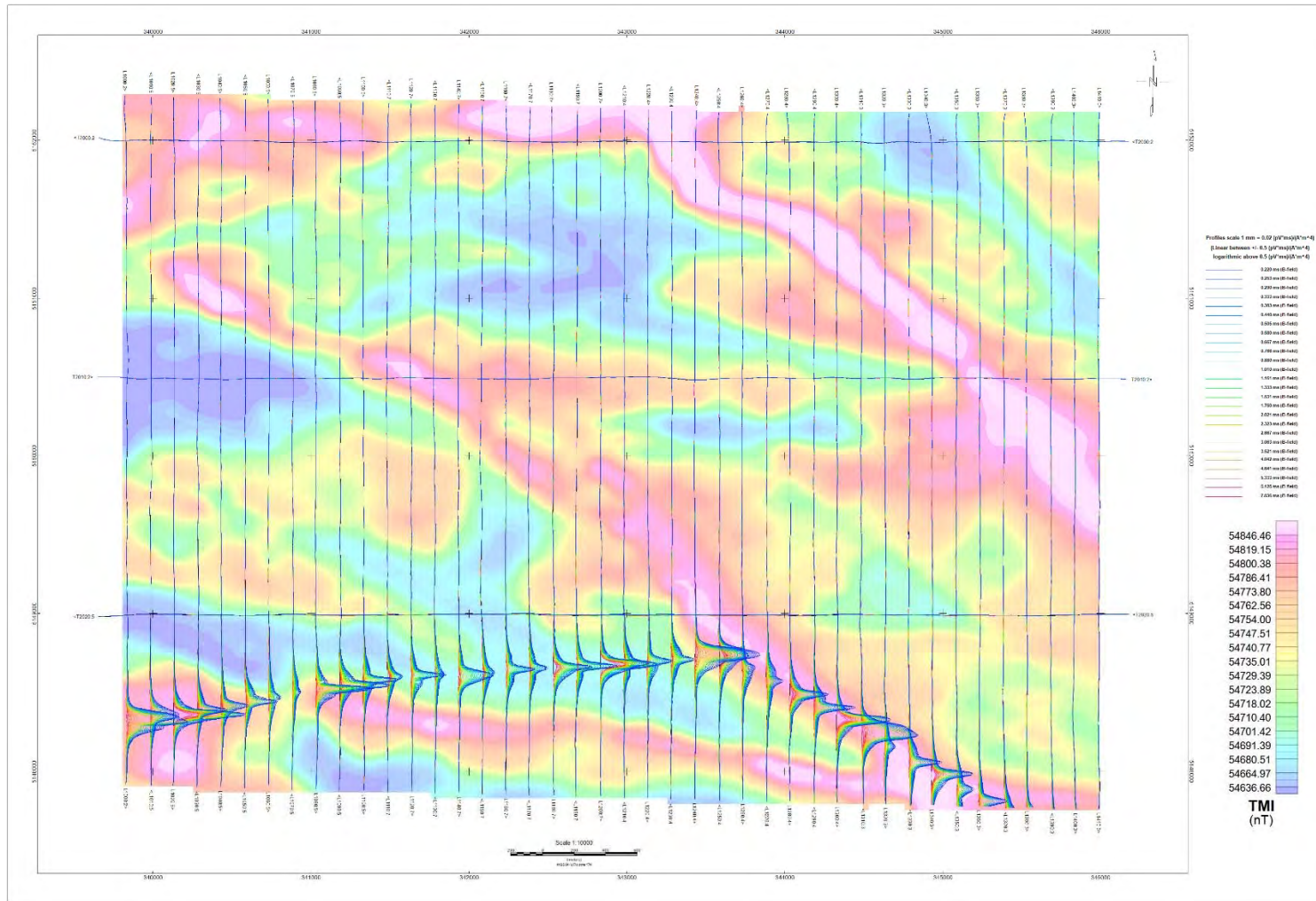
Overview of the Survey Area

APPENDIX B

SURVEY AREA COORDINATES (NAD83 UTM Zone 17N)

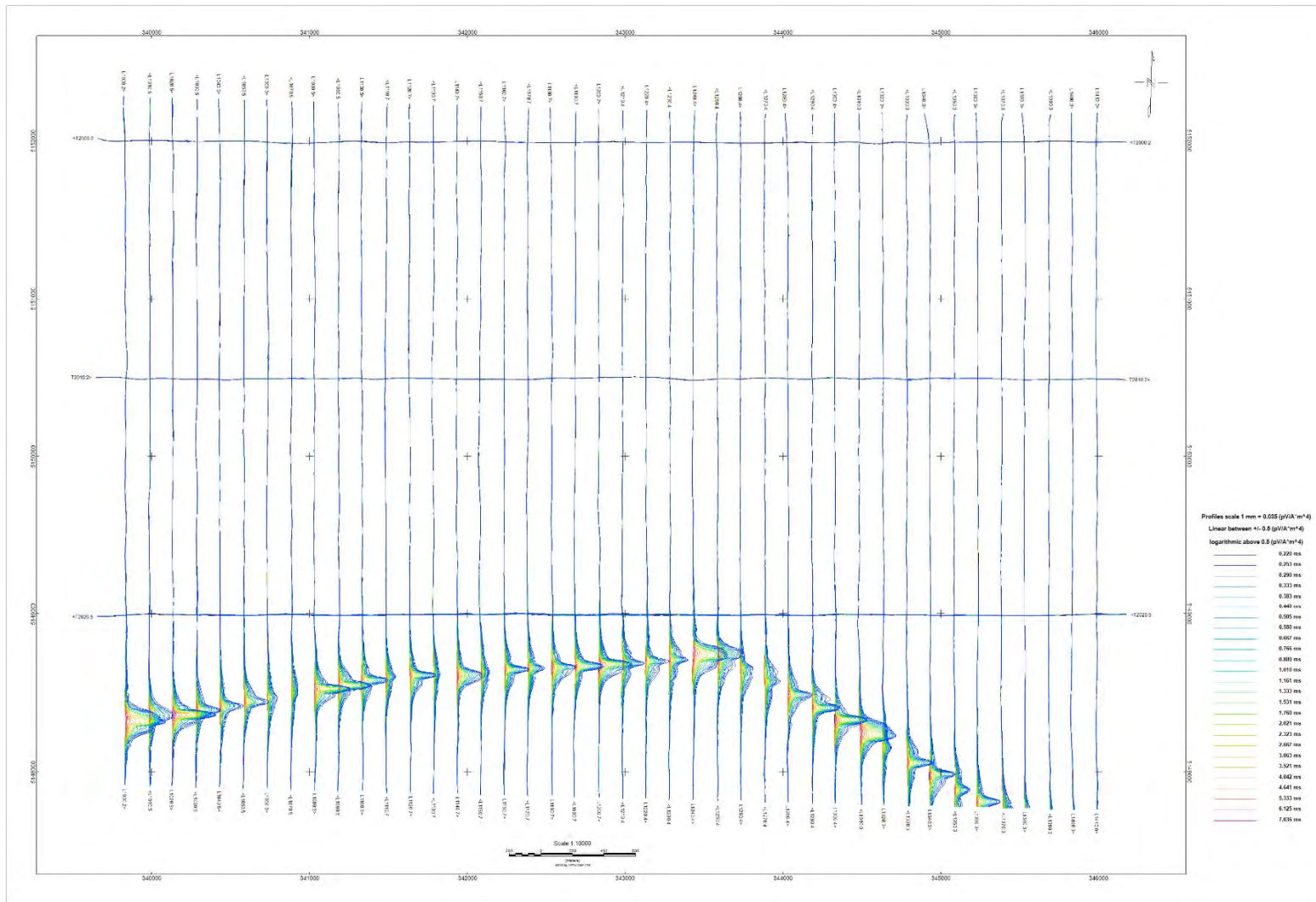
Cannon Copper Project	
X	Y
345964	5147855
339726	5148017
339836	5152183
346070	5152022

APPENDIX C - GEOPHYSICAL MAPS¹

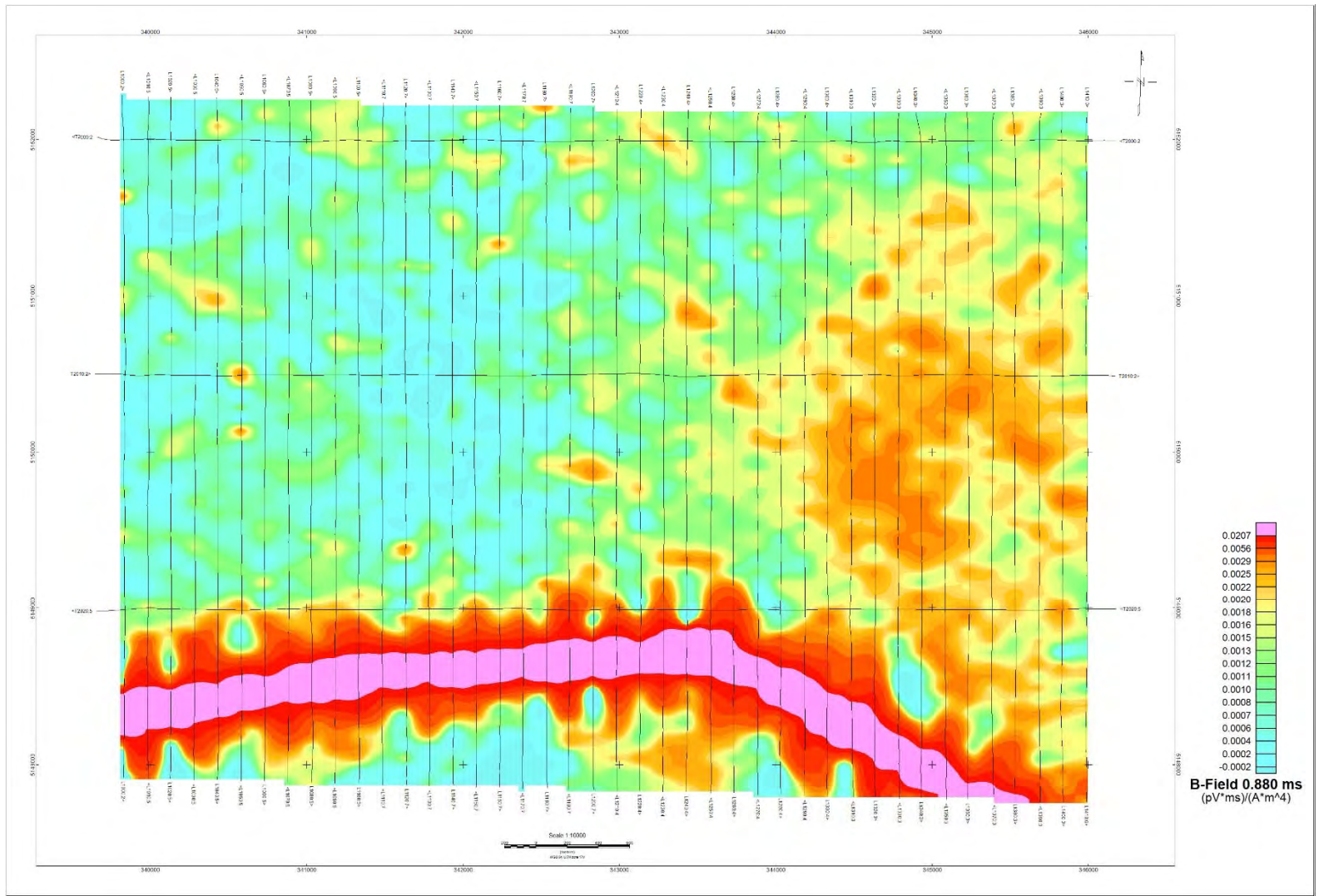


Z Component dB/dt profiles, Time Gates 0.220 – 7.036 ms

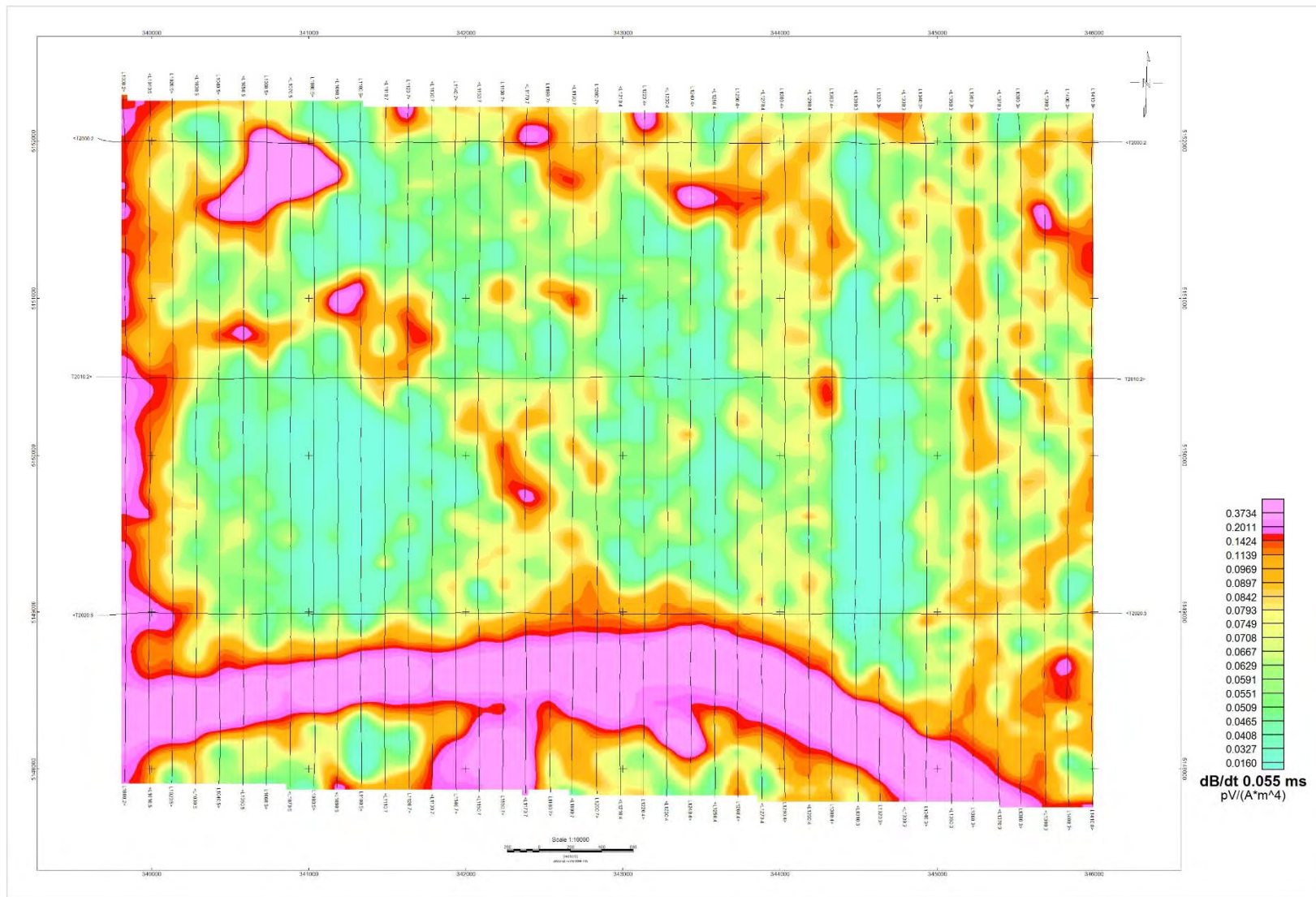
¹Complete full size geophysical maps are also available in PDF format located in the final data maps folder.



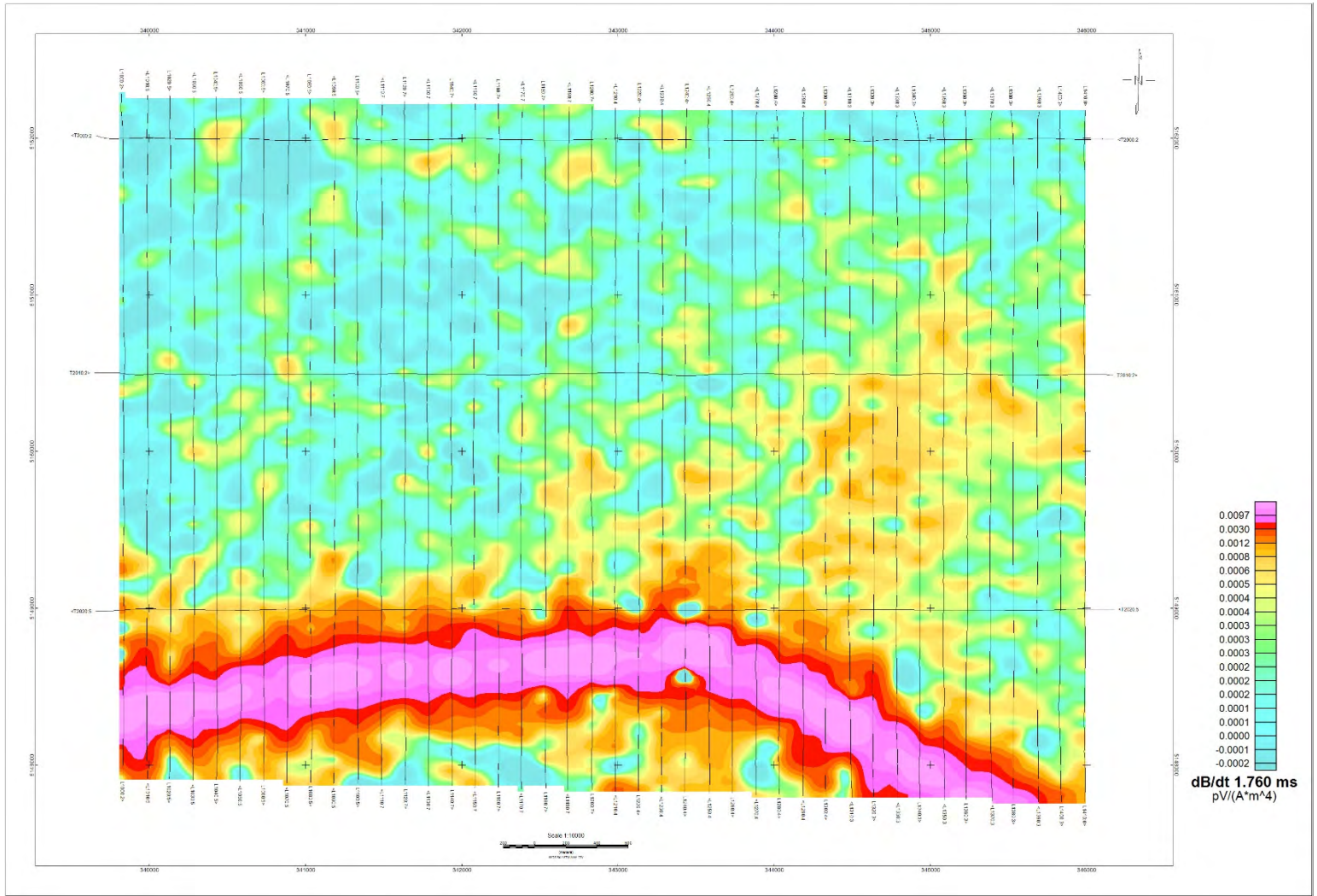
Z Component B-field profiles, Time Gates 0.220 – 7.036 ms over TMI colour image



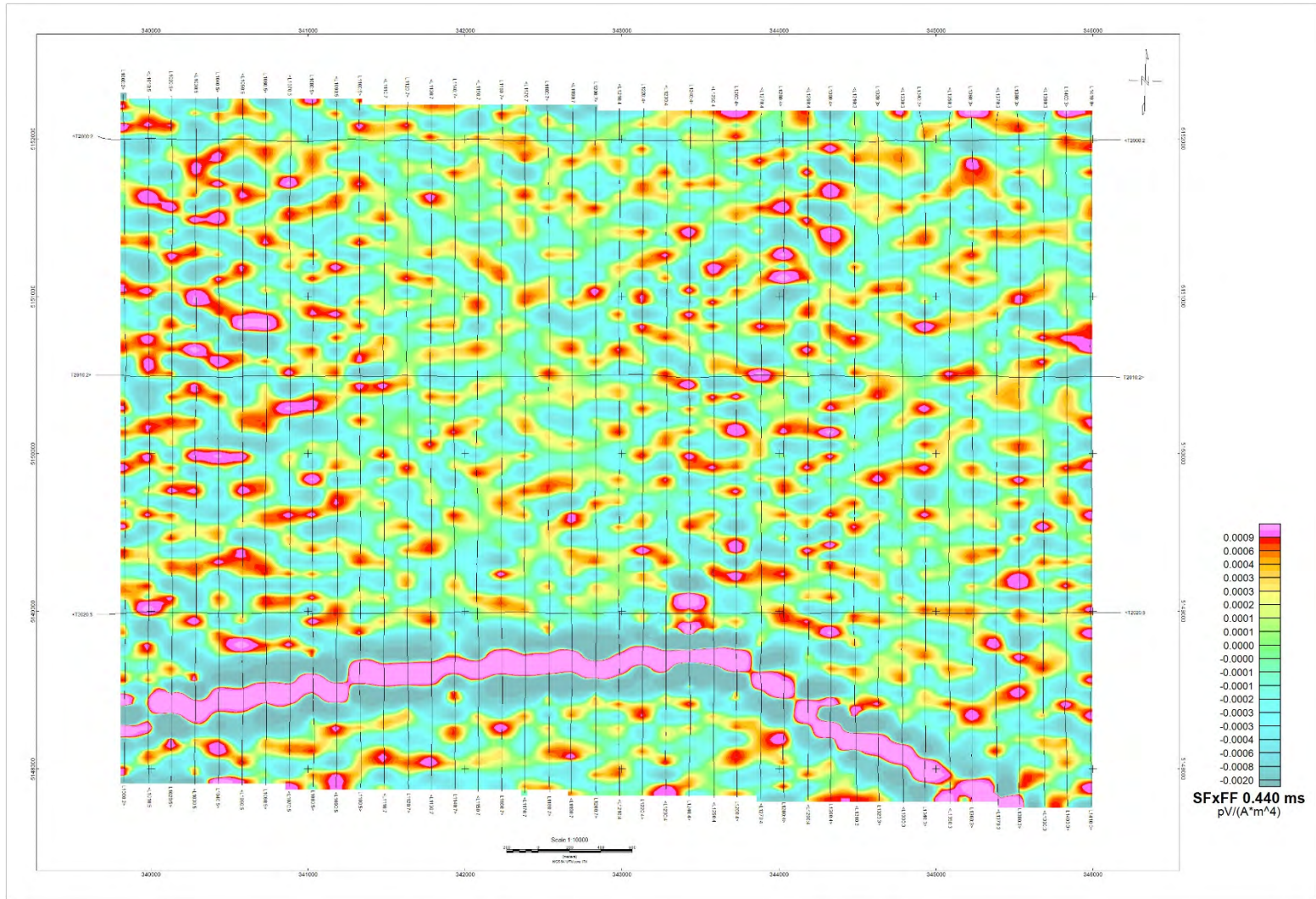
B-field Z Component Channel 30, Time Gate 0.880 ms colour image



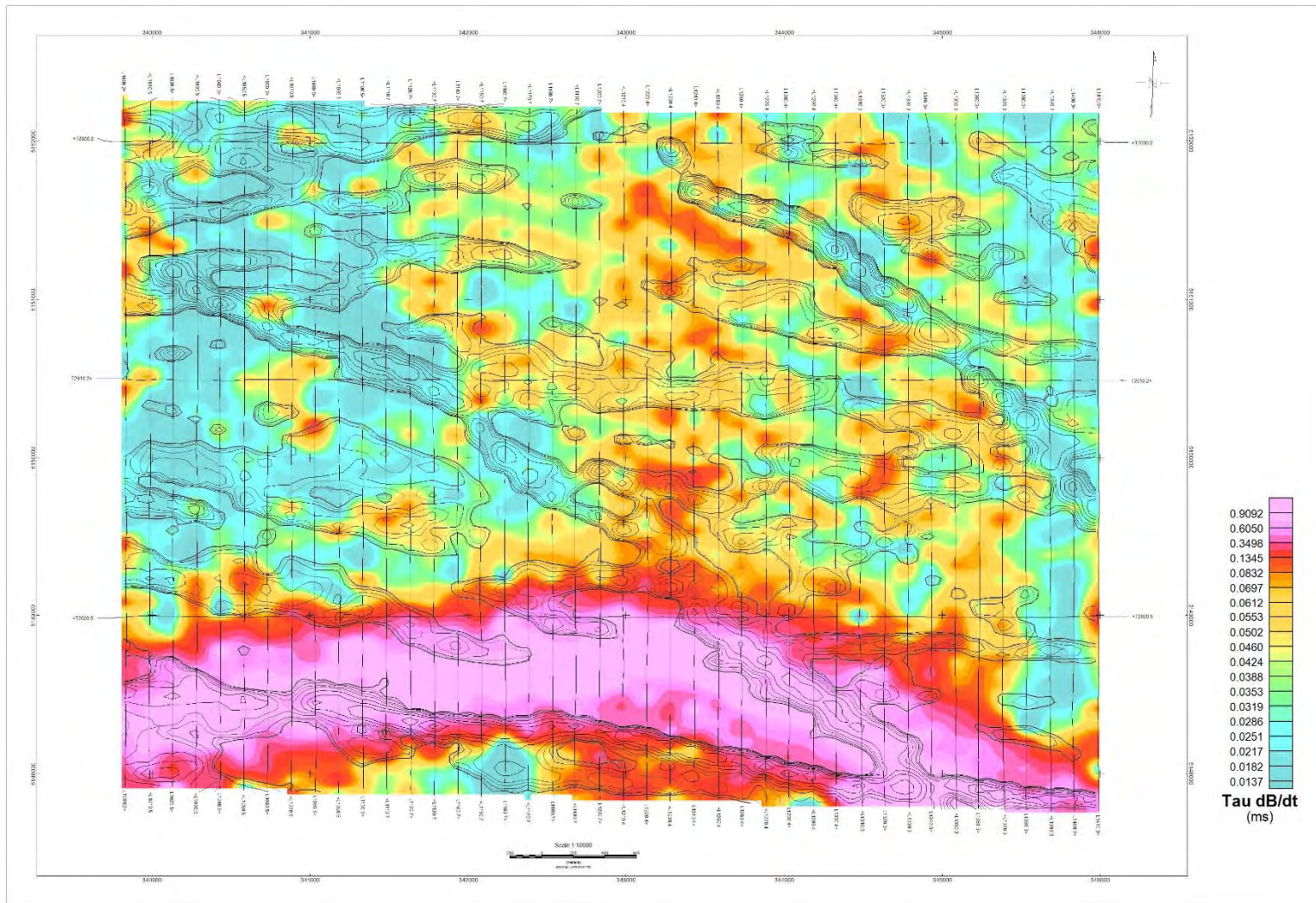
VTEM dB/dt Z Component Channel 10, Time Gate 0.055 ms colour image



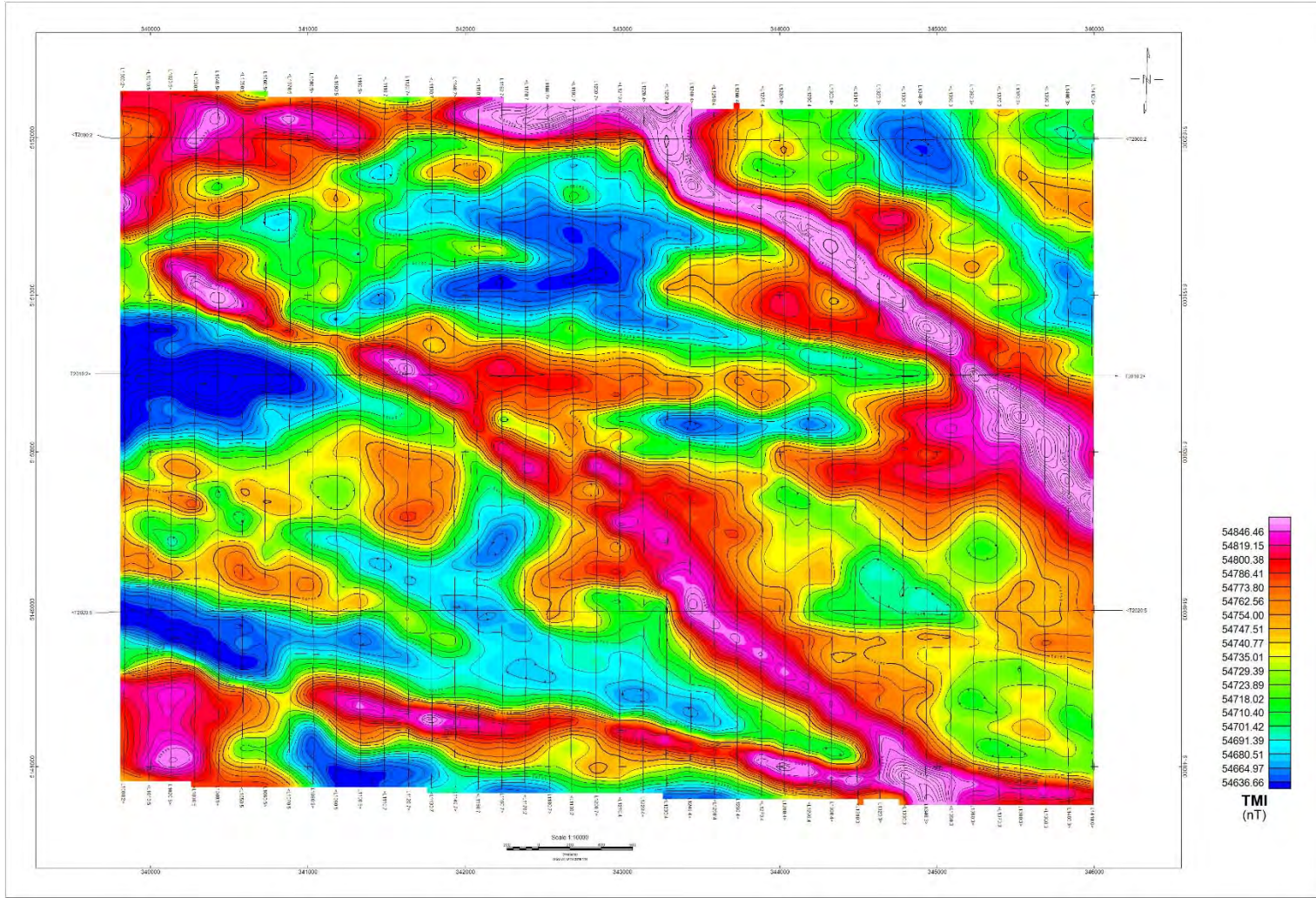
VTEM dB/dt Z Component Channel 35, Time Gate 1.760 ms colour image



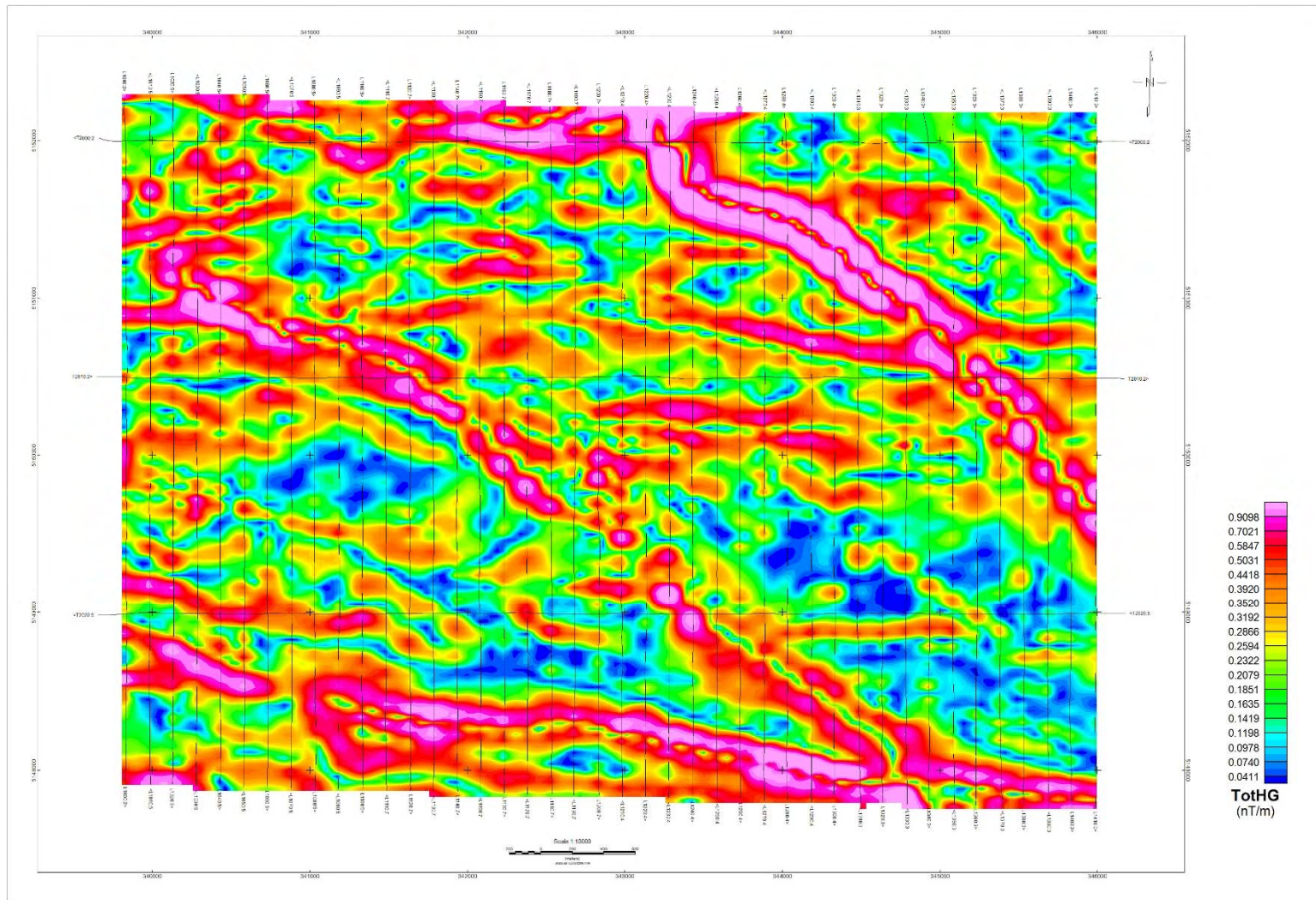
Fraser Filtered dB/dt X Component Channel 25, Time Gate 0.440 ms colour image



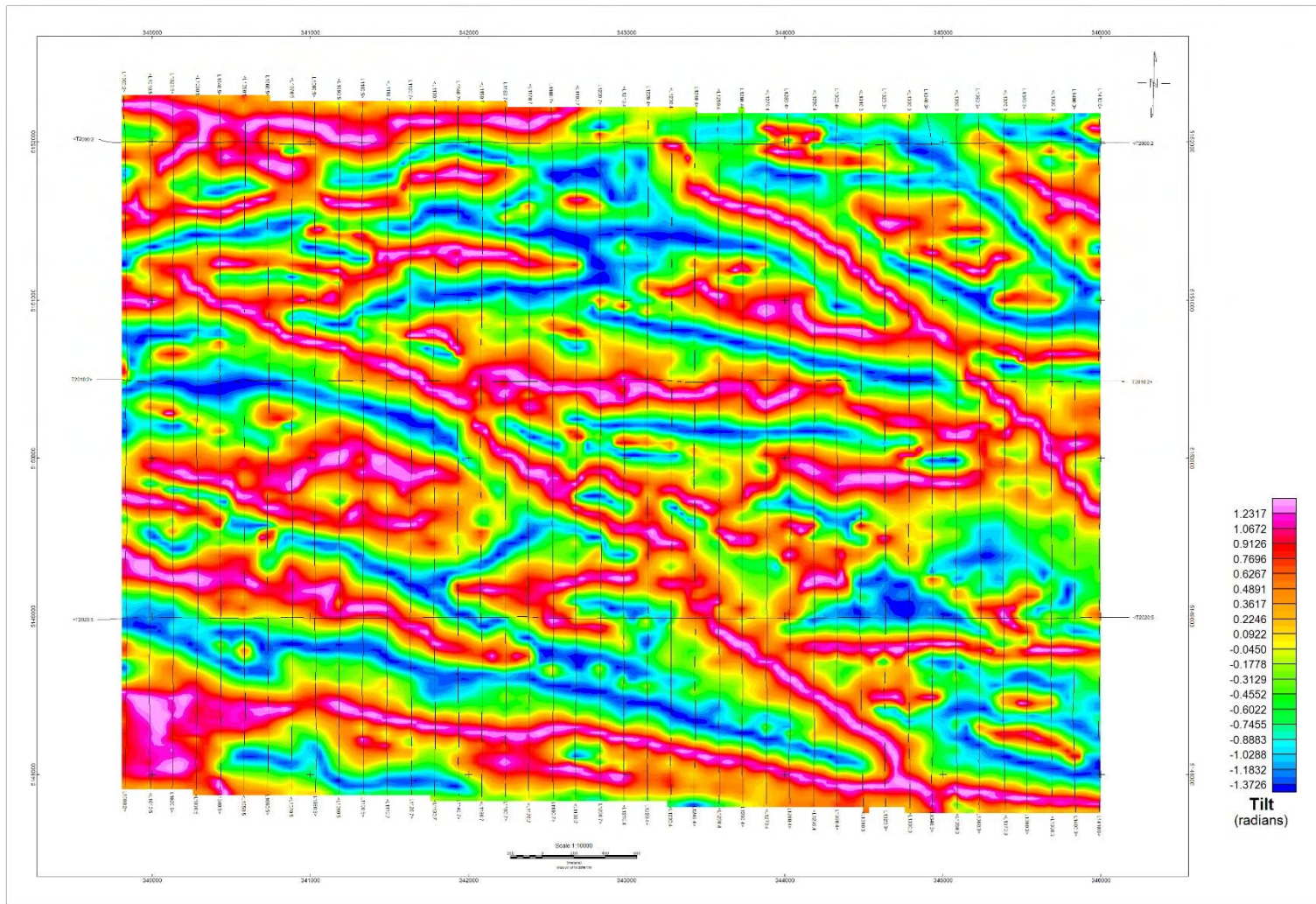
dB/dT Z-Component Calculated Time Constant (Tau) with Calculated Vertical Gradient (CVG) contours



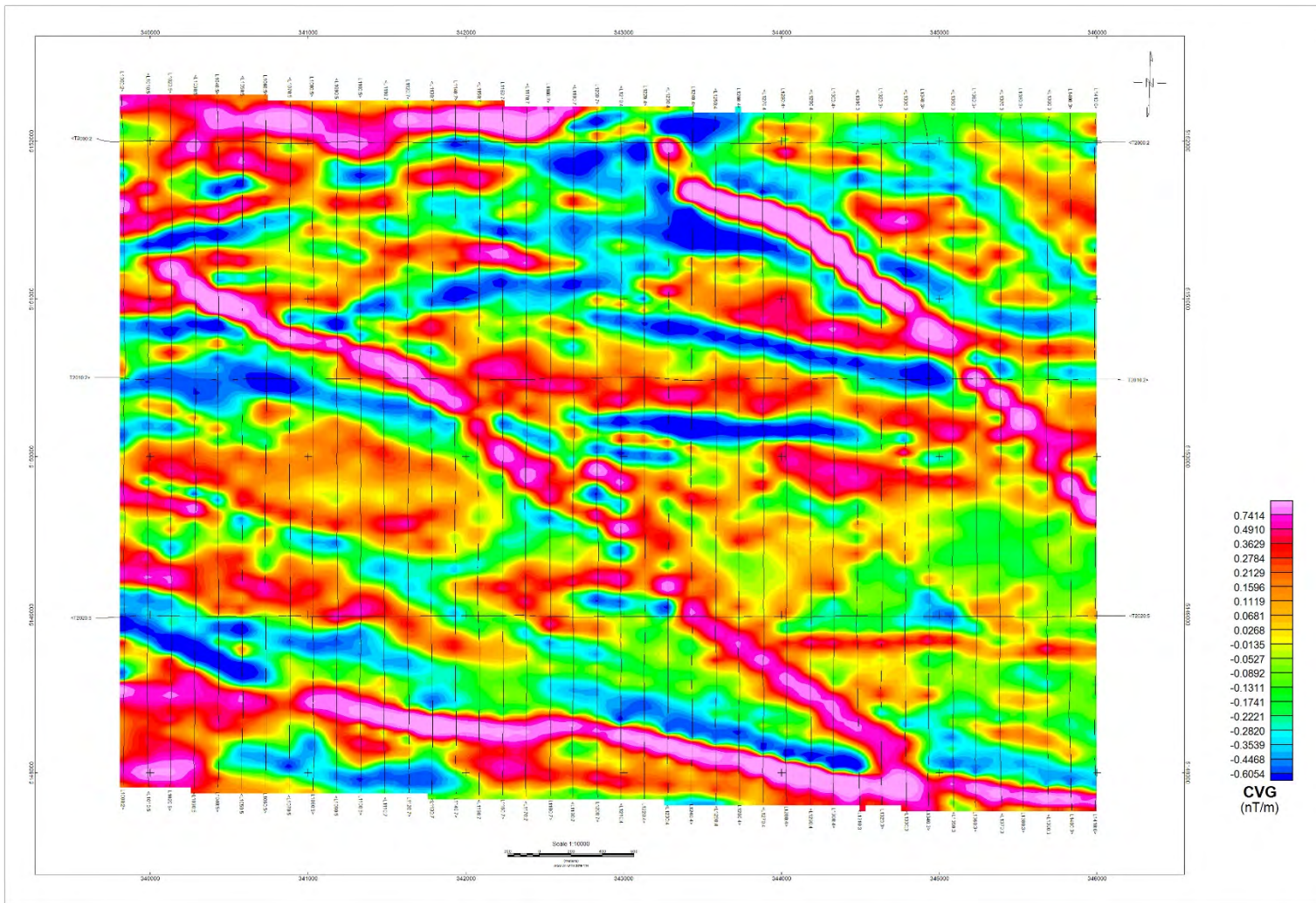
Total Magnetic Intensity (TMI) colour image and contours



Magnetic Total Horizontal Gradient colour image

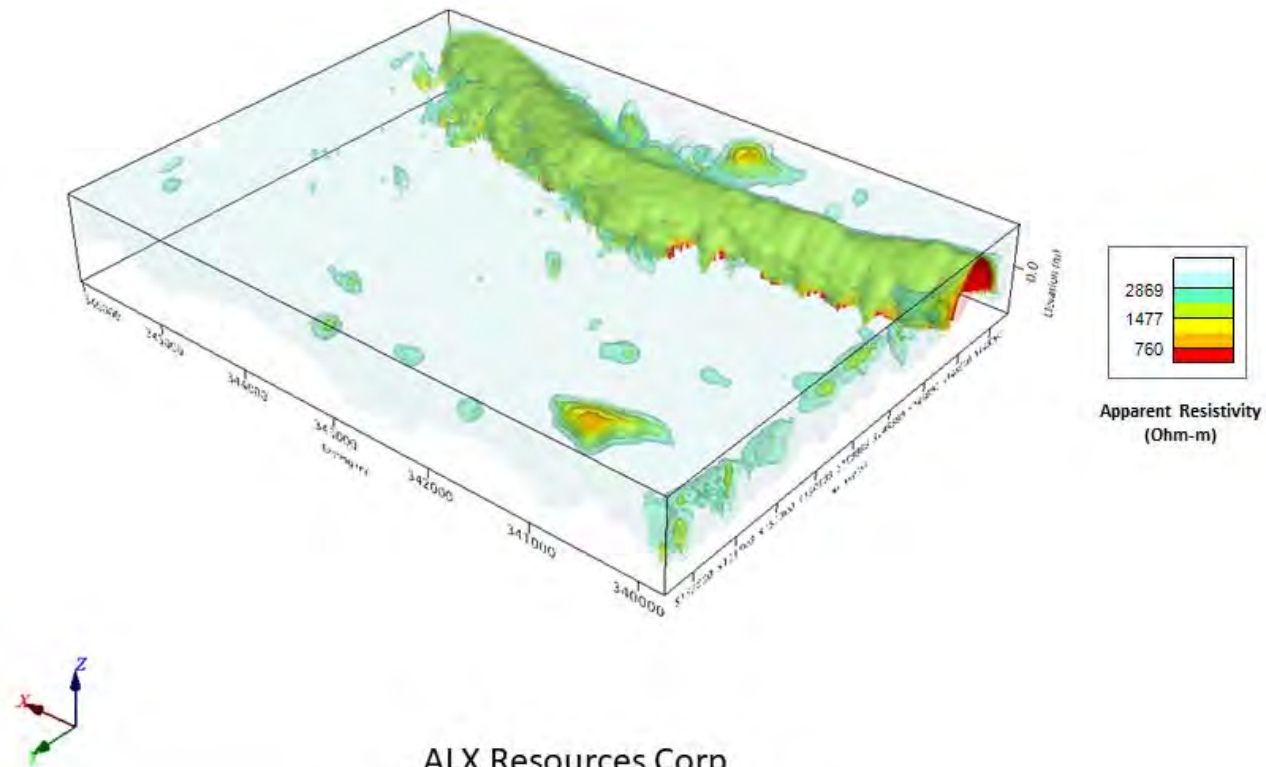


Magnetic Tilt Angle Derivative colour image



Calculated Vertical Gradient (CVG)

3D View of RDI Apparent Resistivity Voxel



ALX Resources Corp
Cannon Copper Project
Elliot Lake, ON

3D view of Resistivity-Depth-Image (RDI), Apparent Resistivity Voxel

APPENDIX D

GENERALIZED MODELING RESULTS OF THE VTEM SYSTEM INTRODUCTION

The VTEM system is based on a concentric or central loop design, whereby, the receiver is positioned at the centre of a transmitter loop that produces a primary field. The wave form is a bi-polar, modified square wave with a turn-on and turn-off at each end.

During turn-on and turn-off, a time varying field is produced (dB/dt) and an electro-motive force (emf) is created as a finite impulse response. A current ring around the transmitter loop moves outward and downward as time progresses. When conductive rocks and mineralization are encountered, a secondary field is created by mutual induction and measured by the receiver at the centre of the transmitter loop.

Efficient modeling of the results can be carried out on regularly shaped geometries, thus yielding close approximations to the parameters of the measured targets. The following is a description of a series of common models made for the purpose of promoting a general understanding of the measured results.

A set of models has been produced for the Geotech VTEM™ system dB/dT Z and X components (see models D1 to D15). The Maxwell™ modeling program (EMIT Technology Pty. Ltd. Midland, WA, AU) used to generate the following responses assumes a resistive half-space. The reader is encouraged to review these models, so as to get a general understanding of the responses as they apply to survey results. While these models do not begin to cover all possibilities, they give a general perspective on the simple and most commonly encountered anomalies.

As the plate dips and departs from the vertical position, the peaks become asymmetrical.

As the dip increases, the aspect ratio (Min/Max) decreases, and this aspect ratio can be used as an empirical guide to dip angles from near 90° to about 30° . The method is not sensitive enough where dips are less than about 30° .

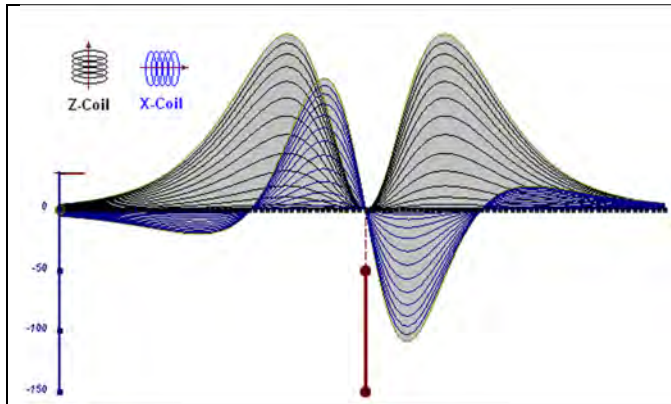


Figure D-1: vertical thin plate

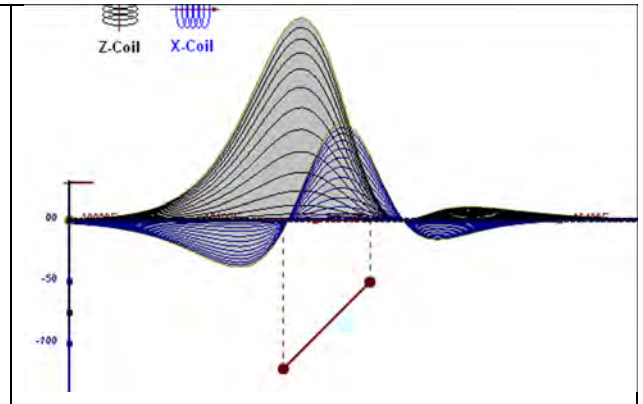


Figure D-2: inclined thin plate

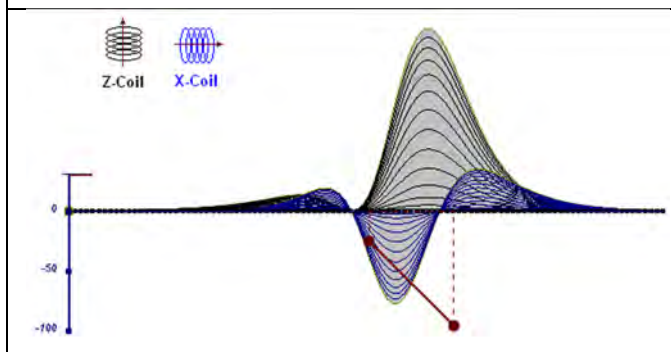


Figure D-3: inclined thin plate

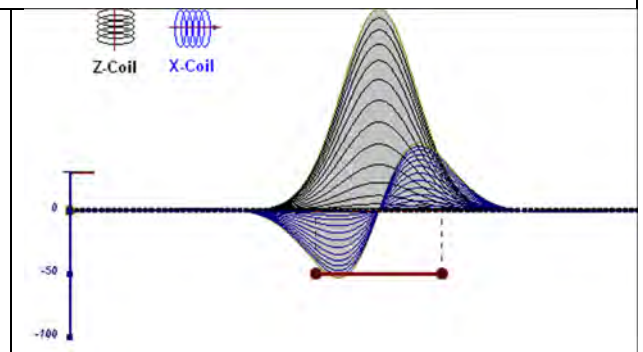


Figure D-4: horizontal thin plate

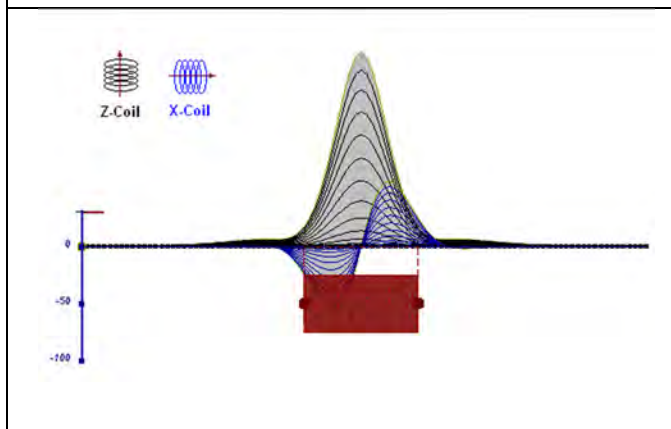


Figure D-5: horizontal thick plate (linear scale of the response)

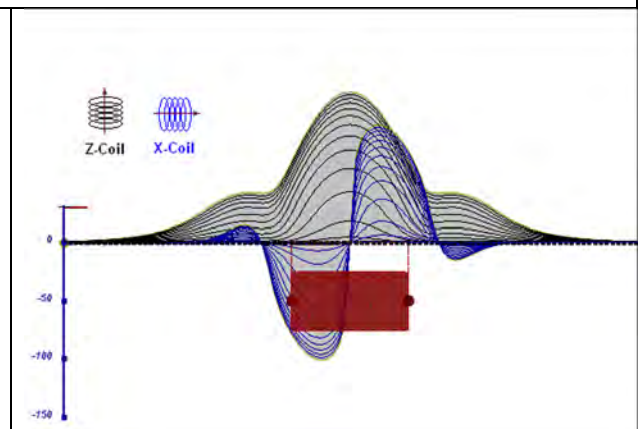


Figure D-6: horizontal thick plate (log scale of the response)

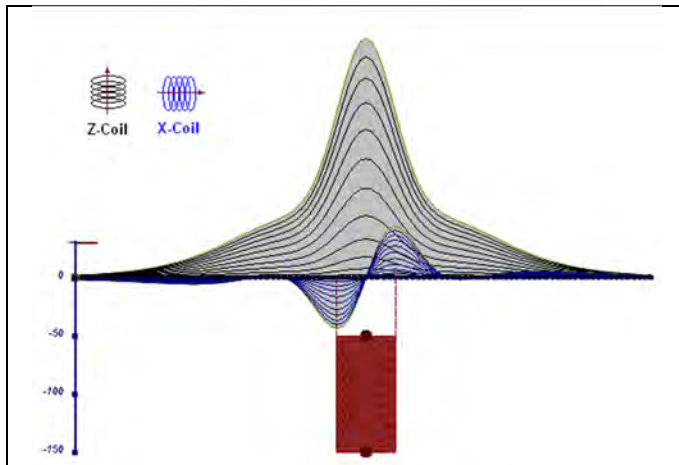


Figure D-7: vertical thick plate (linear scale of the response). 50 m depth

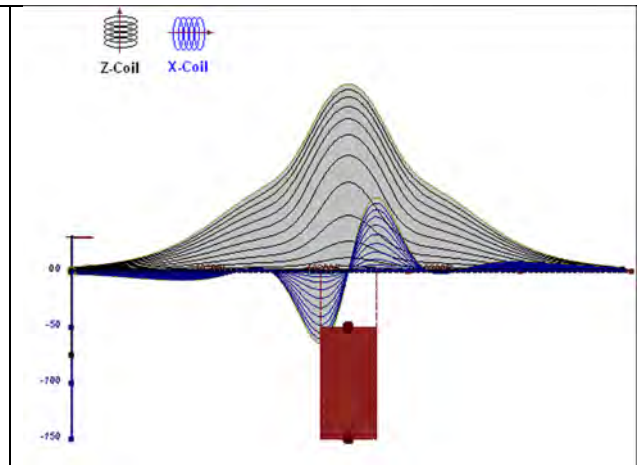


Figure D-8: vertical thick plate (log scale of the response). 50 m depth

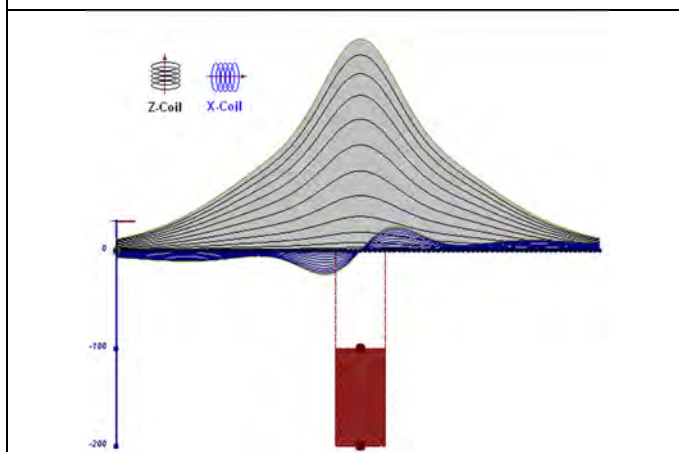


Figure D-9: vertical thick plate (linear scale of the response). 100 m depth

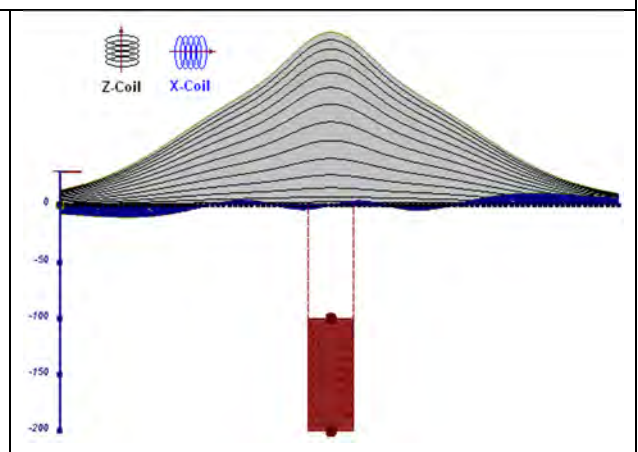


Figure D-10: vertical thick plate (linear scale of the response). Depth / horizontal thickness=2.5

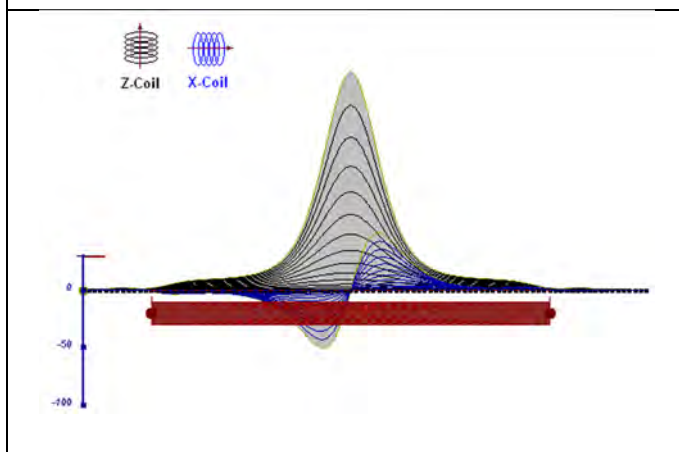


Figure D-11: horizontal thick plate (linear scale of the response)

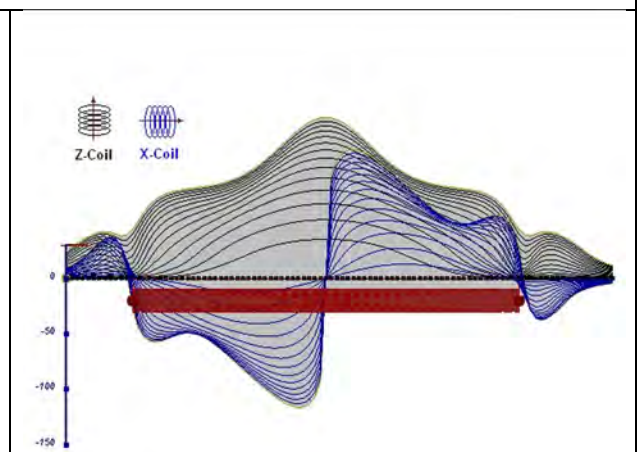


Figure D-12: horizontal thick plate (log scale of the response)

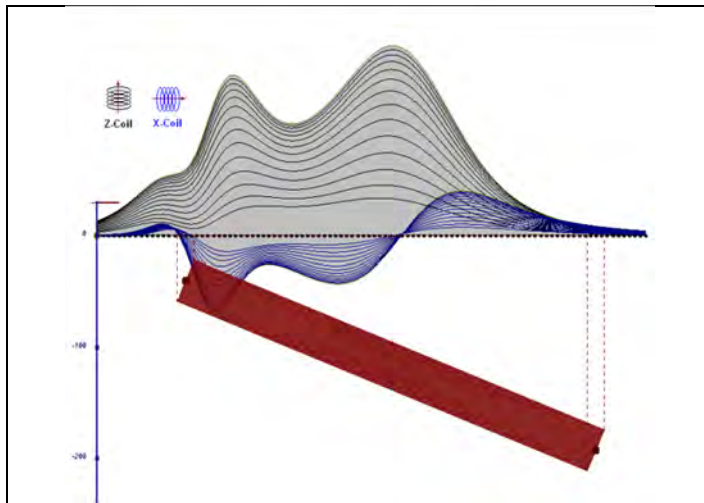


Figure D-13: inclined long thick plate

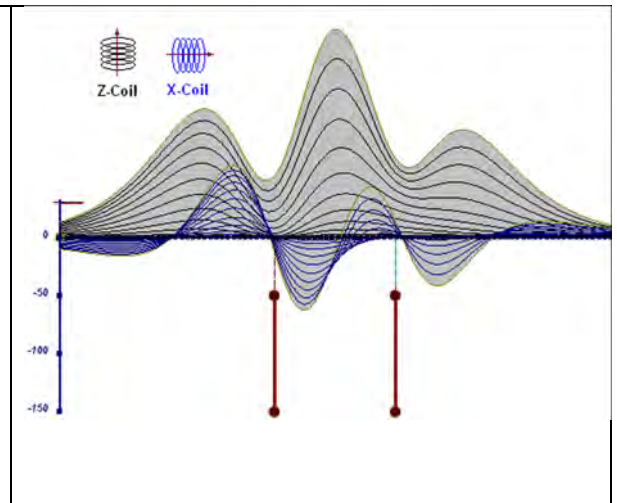


Figure D-14: two vertical thin plates

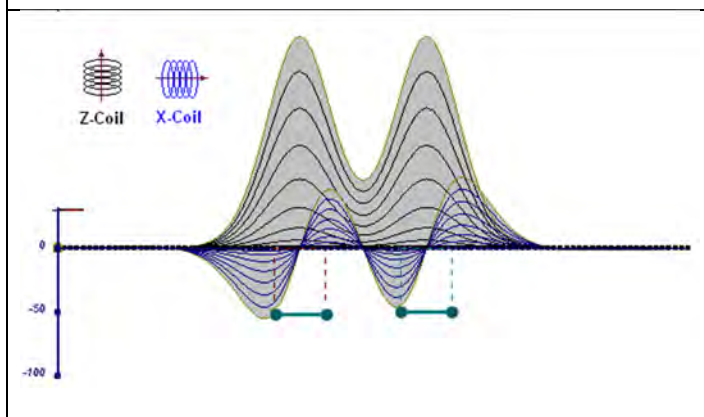


Figure D-15: two horizontal thin plates

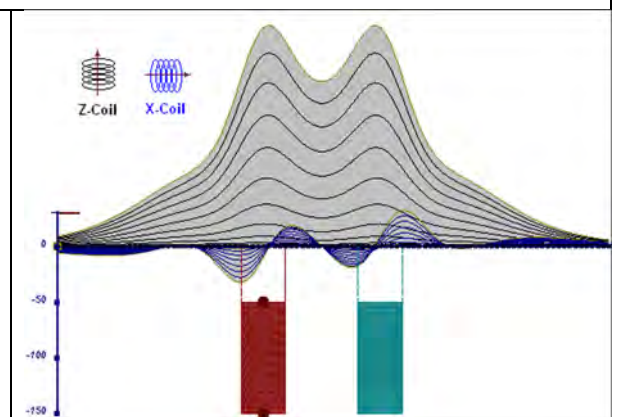


Figure D-16: two vertical thick plates

The same type of target but with different thickness, for example, creates different form of the response:

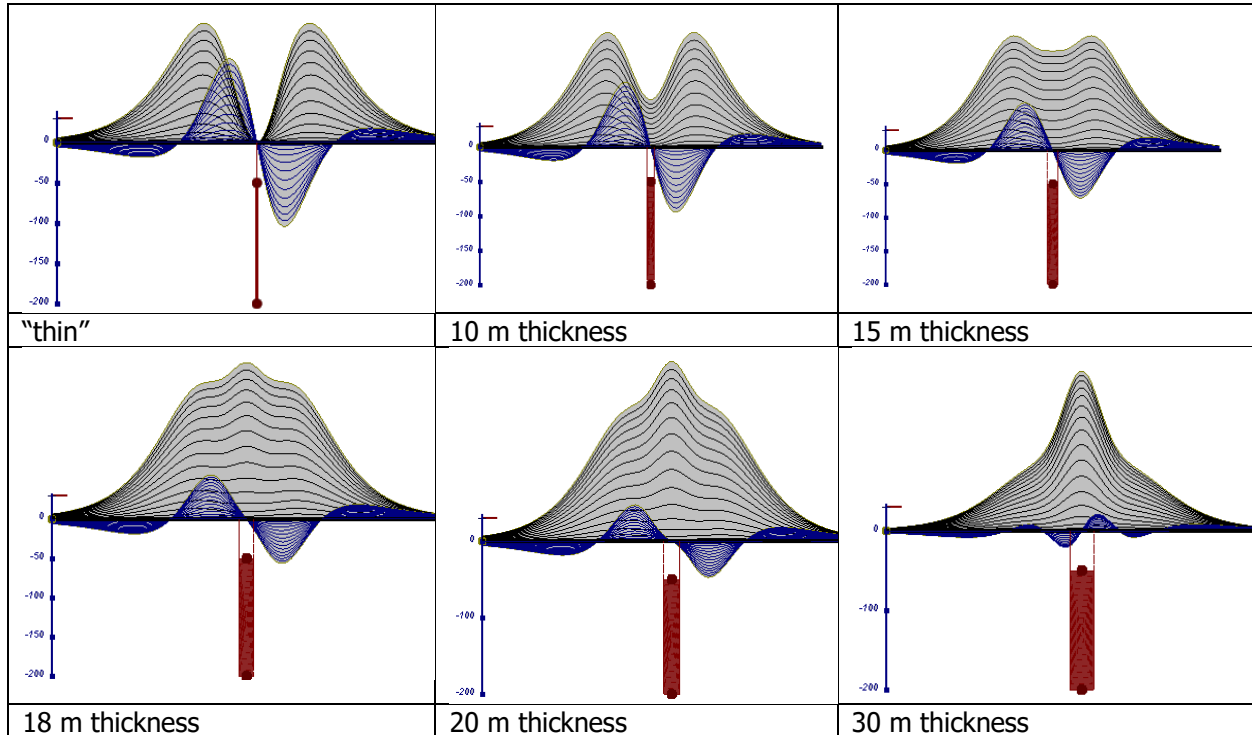


Figure E-17: Conductive vertical plate, depth 50 m, strike length 200 m, depth extends 150 m.

Geotech Ltd.

September 2010

APPENDIX E

EM TIME CONSTANT (TAU) ANALYSIS

Estimation of time constant parameter¹ in transient electromagnetic method is one of the steps toward the extraction of the information about conductances beneath the surface from TEM measurements.

The most reliable method to discriminate or rank conductors from overburden, background or one and other is by calculating the EM field decay time constant (TAU parameter), which directly depends on conductance despite their depth and accordingly amplitude of the response.

Theory

As established in electromagnetic theory, the magnitude of the electro-motive force (emf) induced is proportional to the time rate of change of primary magnetic field at the conductor. This emf causes eddy currents to flow in the conductor with a characteristic transient decay, whose Time Constant (Tau) is a function of the conductance of the survey target or conductivity and geometry (including dimensions) of the target. The decaying currents generate a proportional secondary magnetic field, the time rate of change of which is measured by the receiver coil as induced voltage during the Off time.

The receiver coil output voltage (e_0) is proportional to the time rate of change of the secondary magnetic field and has the form,

$$e_0 \propto (1 / \tau) e^{-(t/\tau)}$$

Where,

$\tau = L/R$ is the characteristic time constant of the target (TAU)

R = resistance

L = inductance

From the expression, conductive targets that have small value of resistance and hence large value of τ yield signals with small initial amplitude that decays relatively slowly with progress of time. Conversely, signals from poorly conducting targets that have large resistance value and small τ , have high initial amplitude but decay rapidly with time¹(Fig. E1).

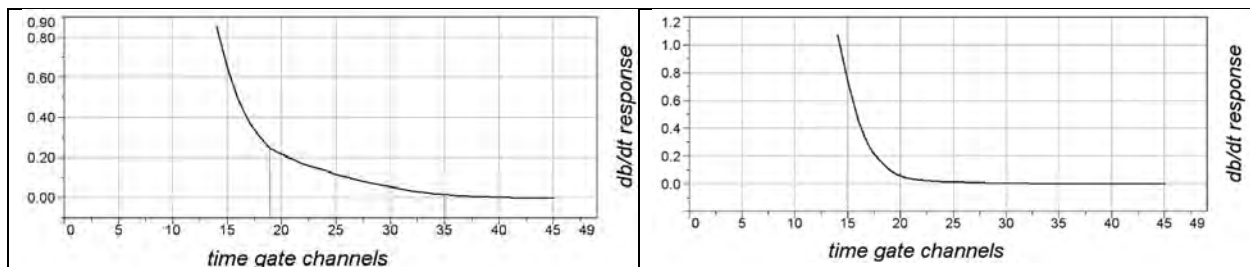


Figure E-1: Left – presence of good conductor, right – poor conductor.

¹McNeill, JD, 1980, "Applications of Transient Electromagnetic Techniques", Technical Note TN-7 page 5, Geonics Limited, Mississauga, Ontario.

EM Time Constant (Tau) Calculation

The EM Time-Constant (TAU) is a general measure of the speed of decay of the electromagnetic response and indicates the presence of eddy currents in conductive sources as well as reflecting the “conductance quality” of a source. Although TAU can be calculated using either the measured dB/dt decay or the calculated B-field decay, dB/dt is commonly preferred due to better stability (S/N) relating to signal noise. Generally, TAU calculated on base of early time response reflects both near surface overburden and poor conductors whereas, in the late ranges of time, deep and more conductive sources, respectively. For example, early time TAU distribution in an area that indicates conductive overburden is shown in Figure 2.

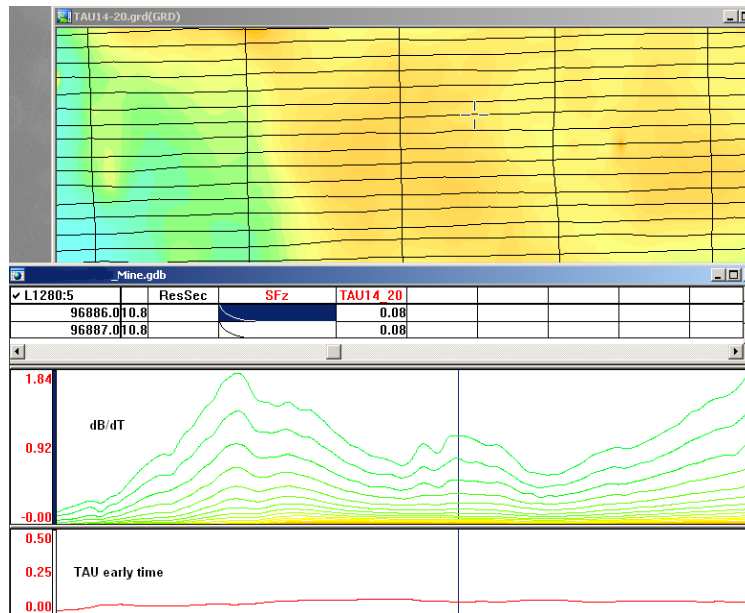


Figure E-2: Map of early time TAU. Area with overburden conductive layer and local sources.

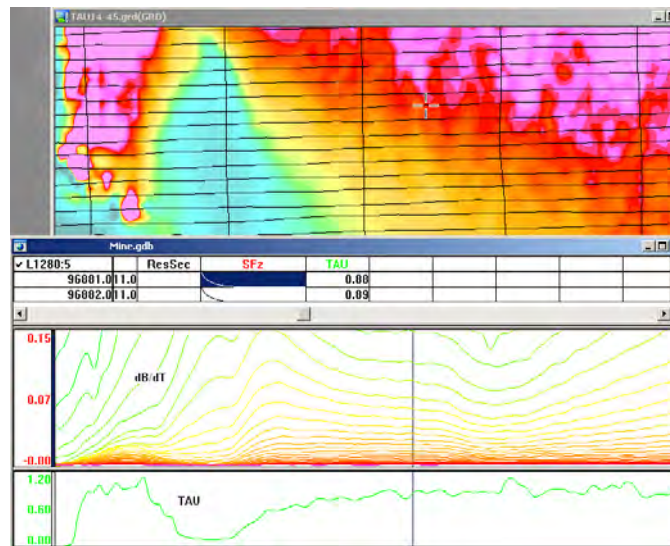


Figure E-3: Map of full-time range TAU with EM anomaly due to deep highly conductive target.

There are many advantages of TAU maps:

- TAU depends only on one parameter (conductance) in contrast to response magnitude.
- TAU is integral parameter, which covers time range, and all conductive zones and targets are displayed independently of their depth and conductivity on a single map.
- Very good differential resolution in complex conductive places with many sources with different conductivity.
- Signs of the presence of good conductive targets are amplified and emphasized independently of their depth and level of response accordingly.

In the example shown in Figure 4 and 5, three local targets are defined, each of them with a different depth of burial, as indicated on the resistivity depth image (RDI). All are very good conductors, but the deeper target (number 2) has a relatively weak dB/dt signal yet also features the strongest total TAU (Figure 4). This example highlights the benefit of TAU analysis in terms of an additional target discrimination tool.

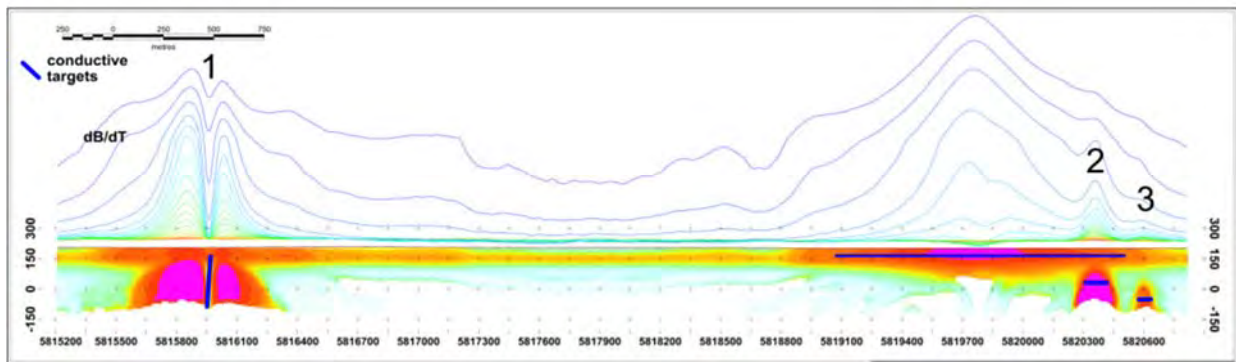


Figure E-4: dB/dt profile and RDI with different depths of targets.

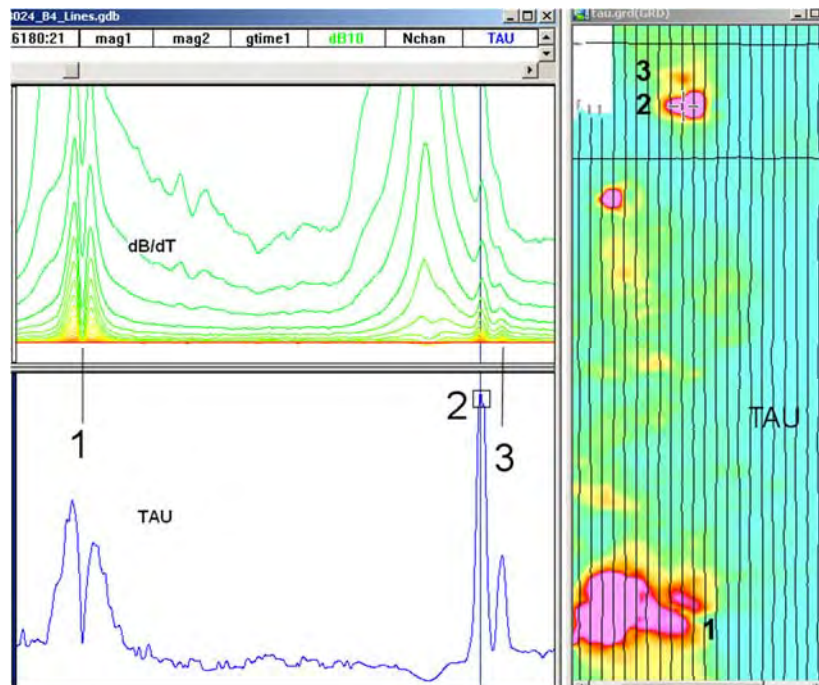


Figure E-5: Map of total TAU and dB/dt profile.

The EM Time Constants for dB/dt and B-field were calculated using the “sliding Tau” in-house program developed at Geotech. The principle of the calculation is based on using of time window (4 time channels) which is sliding along the curve decay and looking for latest time channels which have a response above the level of noise and decay. The EM decays are obtained from all available decay channels, starting at the latest channel. Time constants are taken from a least square fit of a straight-line (log/linear space) over the last 4 gates above a pre-set signal threshold level (Figure E6). Threshold settings are pointed in the “label” property of TAU database channels. The sliding Tau method determines that, as the amplitudes increase, the time-constant is taken at progressively later times in the EM decay. Conversely, as the amplitudes decrease, Tau is taken at progressively earlier times in the decay. If the maximum signal amplitude falls below the threshold or becomes negative for any of the 4 time gates, then Tau is not calculated and is assigned a value of “dummy” by default.

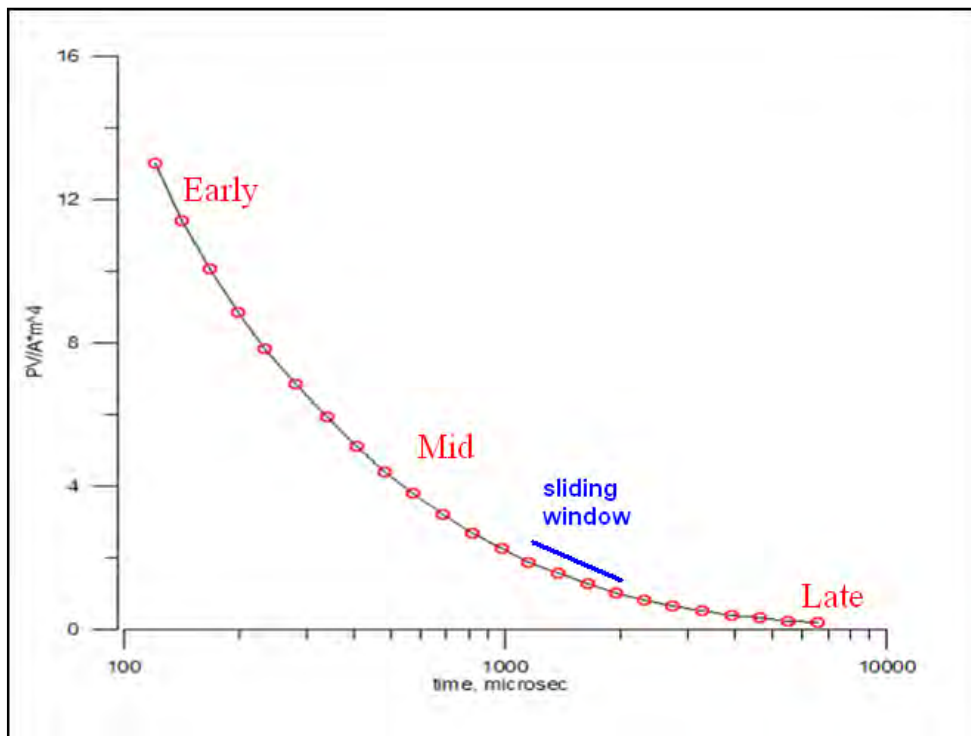


Figure E-6: Typical dB/dt decays of Vtem data

Geotech Ltd.

September 2010

APPENDIX F

TEM RESISTIVITY DEPTH IMAGING (RDI)

Resistivity depth imaging (RDI) is a technique used to rapidly convert EM profile decay data into an equivalent resistivity versus depth cross-section, by deconvolving the measured TEM data. The used RDI algorithm of Resistivity-Depth transformation is based on the scheme of the apparent resistivity transform of Meju (1998)¹ and TEM response from a conductive half-space. The program is developed by Alexander Prikhodko and depth calibrated based on forward plate modeling for VTEM system configuration (Fig. 1-10).

RDIs provide reasonable indications of conductor relative depth and vertical extent, as well as accurate 1D layered-earth apparent conductivity/resistivity structure across VTEM flight lines. Approximate depth of investigation of a TEM system, image of secondary field distribution in half space, effective resistivity, initial geometry and position of conductive targets is the information obtained on the basis of the RDIs.

Maxwell plate EM forward modeling with RDI sections from the synthetic responses (VTEM system) are presented below.

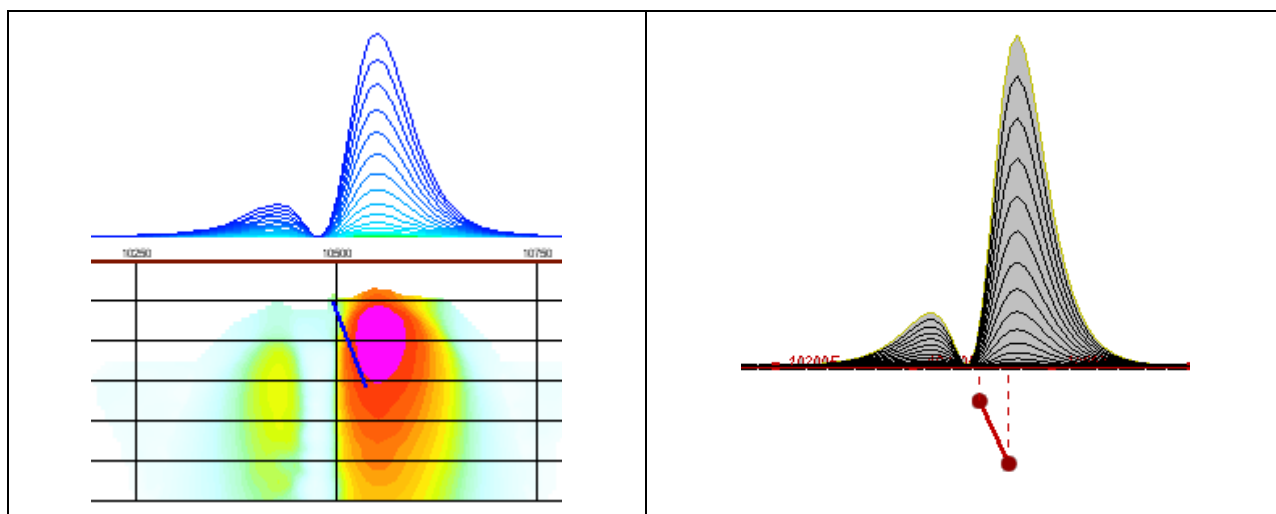


Figure F-1: Maxwell plate model and RDI from the calculated response for a conductive "thin" plate (depth 50 m, dip 65 degrees, depth extend 100 m).

¹Maxwell A.Meju, 1998, Short Note: A simple method of transient electromagnetic data analysis, *Geophysics*, **63**, 405–410.

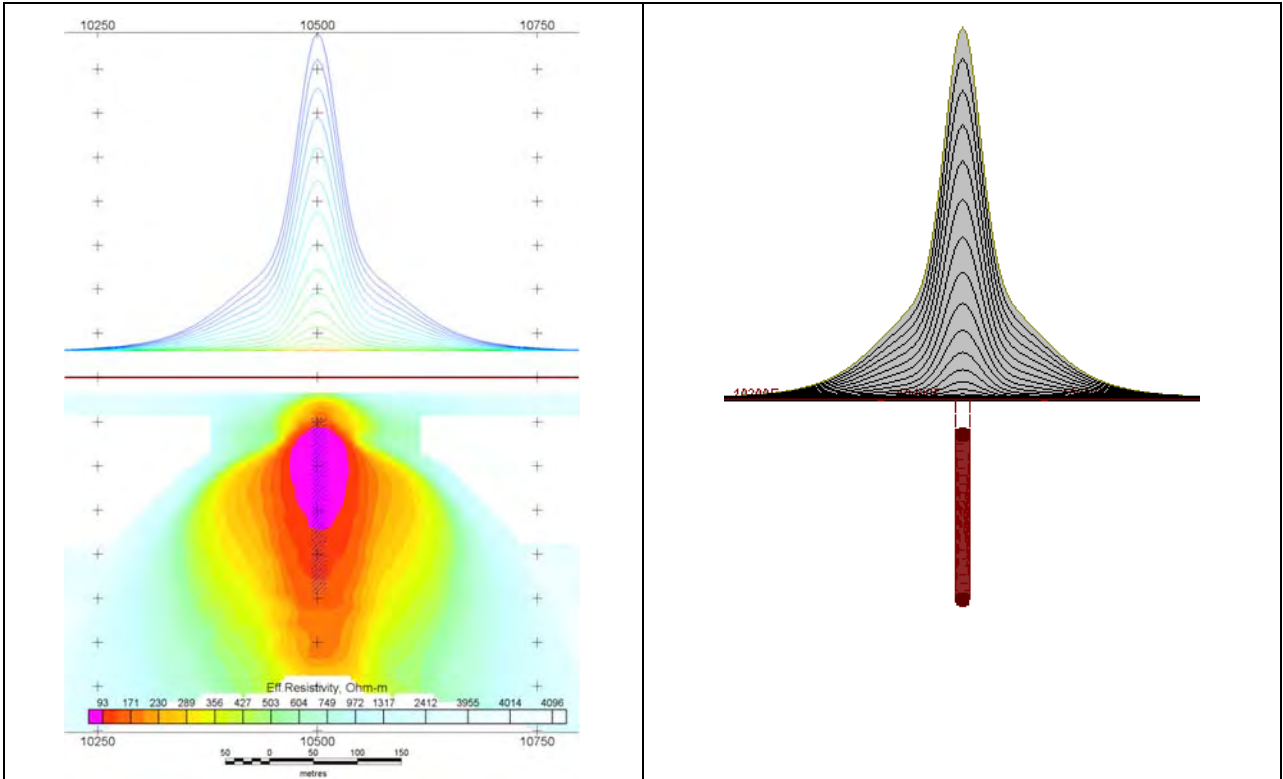


Figure F-2: Maxwell plate model and RDI from the calculated response for "thick" plate 18 m thickness, depth 50 m, depth extend 200 m).

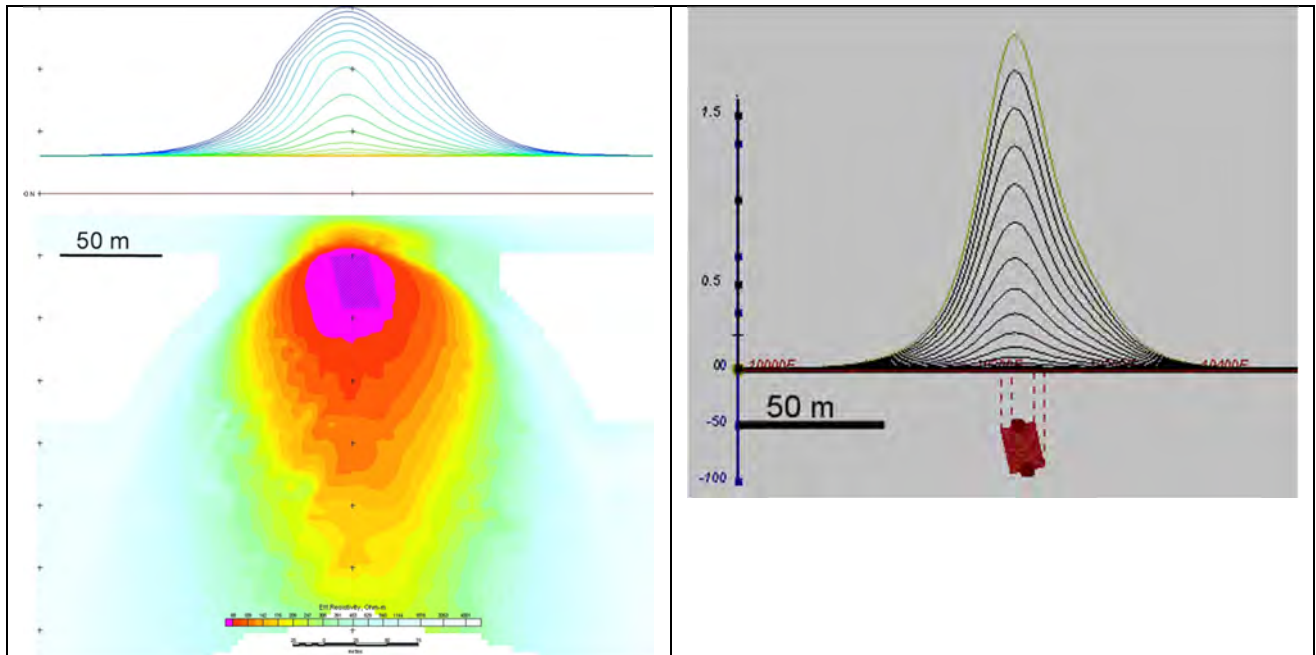


Figure F-3: Maxwell plate model and RDI from the calculated response for bulk ("thick") 100 m length, 40 m depth extend, 30 m thickness.

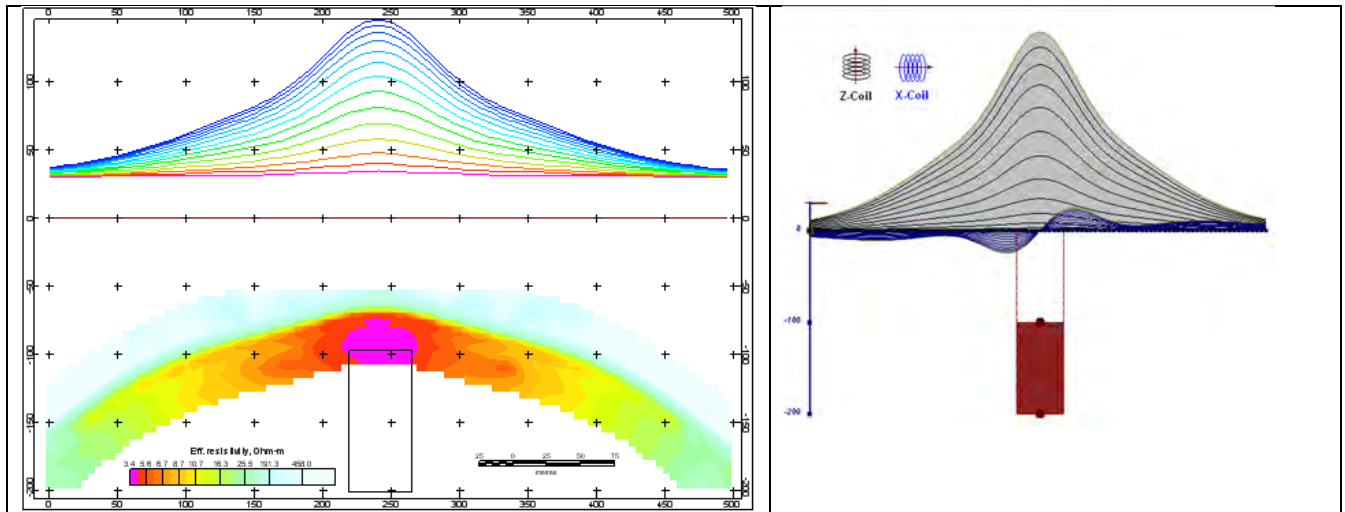


Figure F-4: Maxwell plate model and RDI from the calculated response for “thick” vertical target (depth 100 m, depth extend 100 m). 19-44 chan.

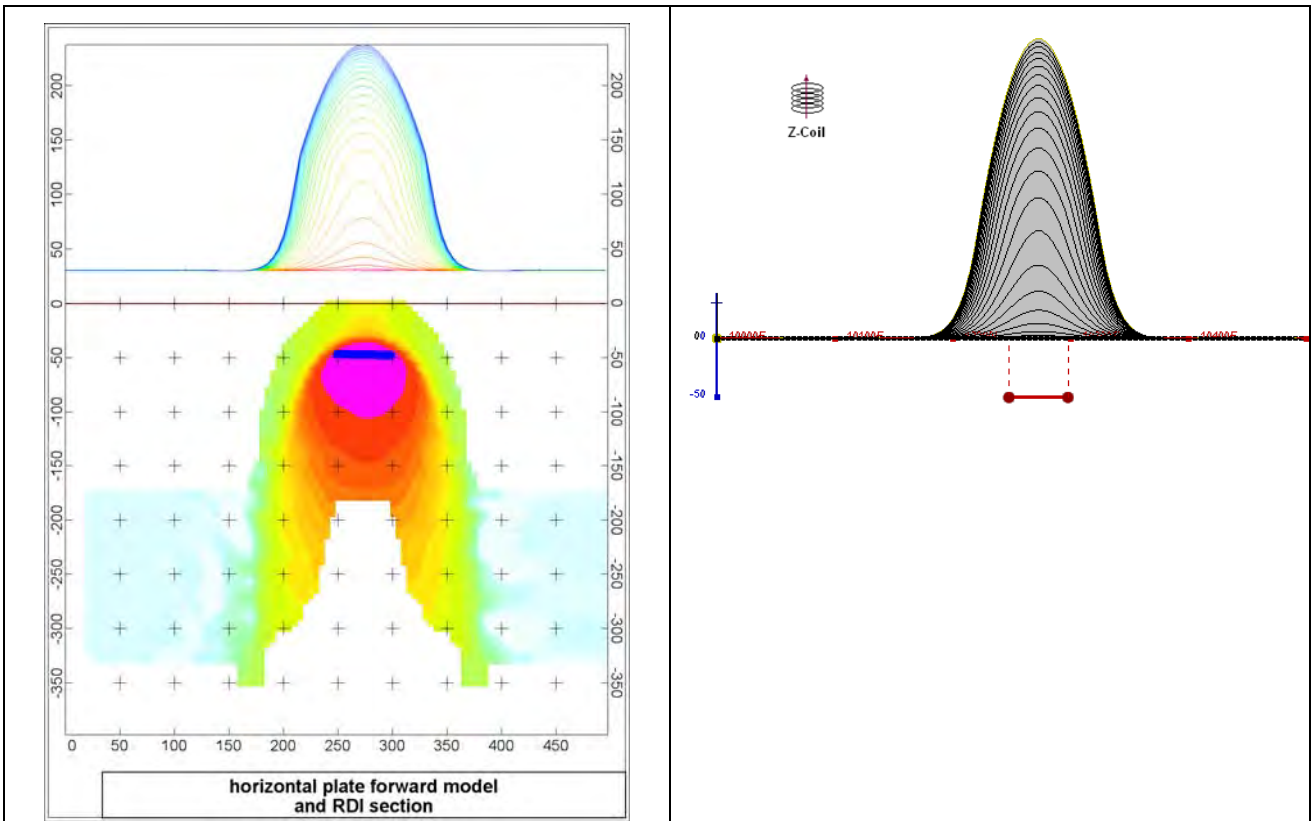


Figure F-5: Maxwell plate model and RDI from the calculated response for horizontal thin plate (depth 50 m, dim 50x100 m). 15-44 chan.

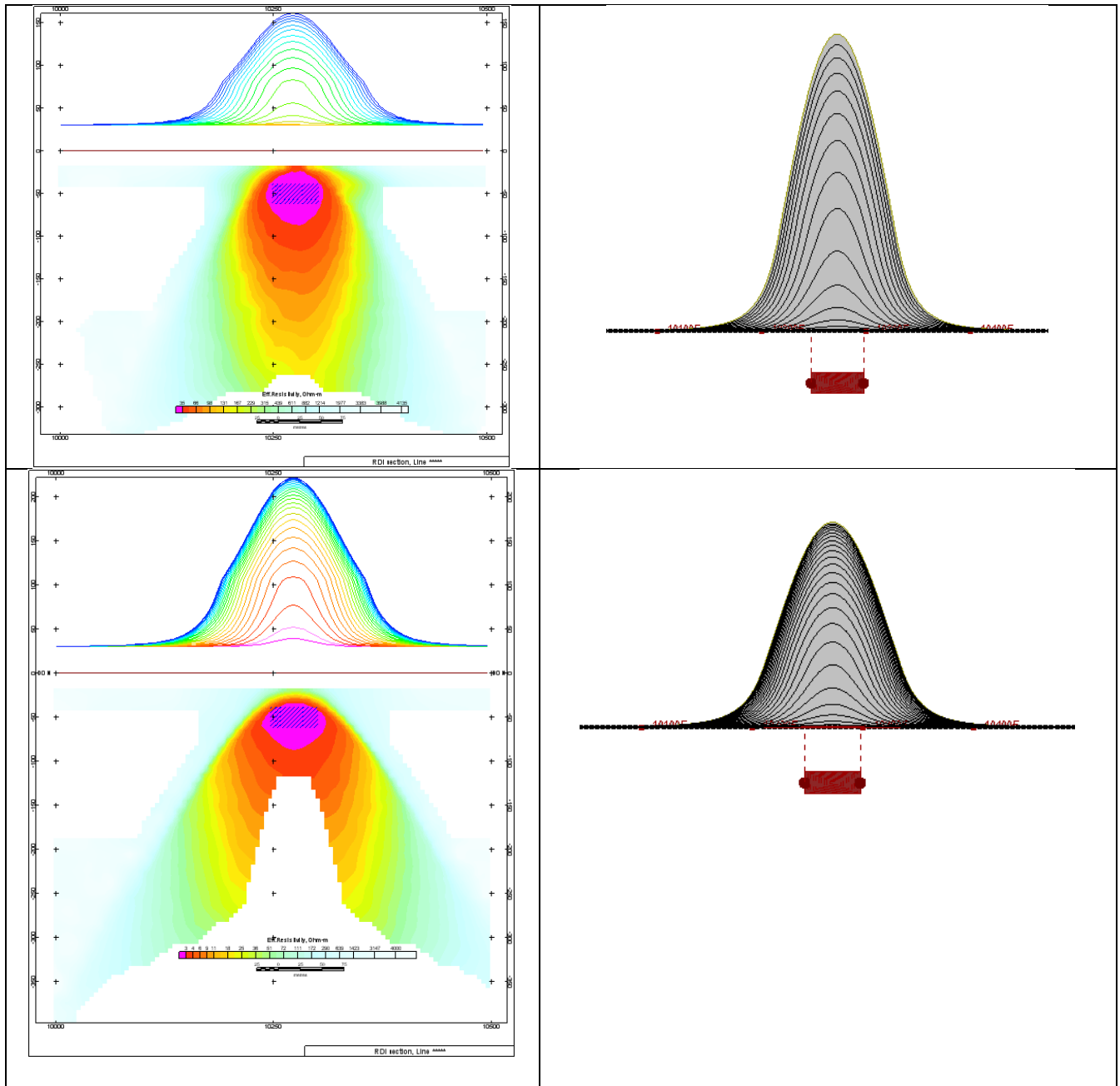


Figure F-6: Maxwell plate model and RDI from the calculated response for horizontal thick (20m) plate – less conductive (on the top), more conductive (below).

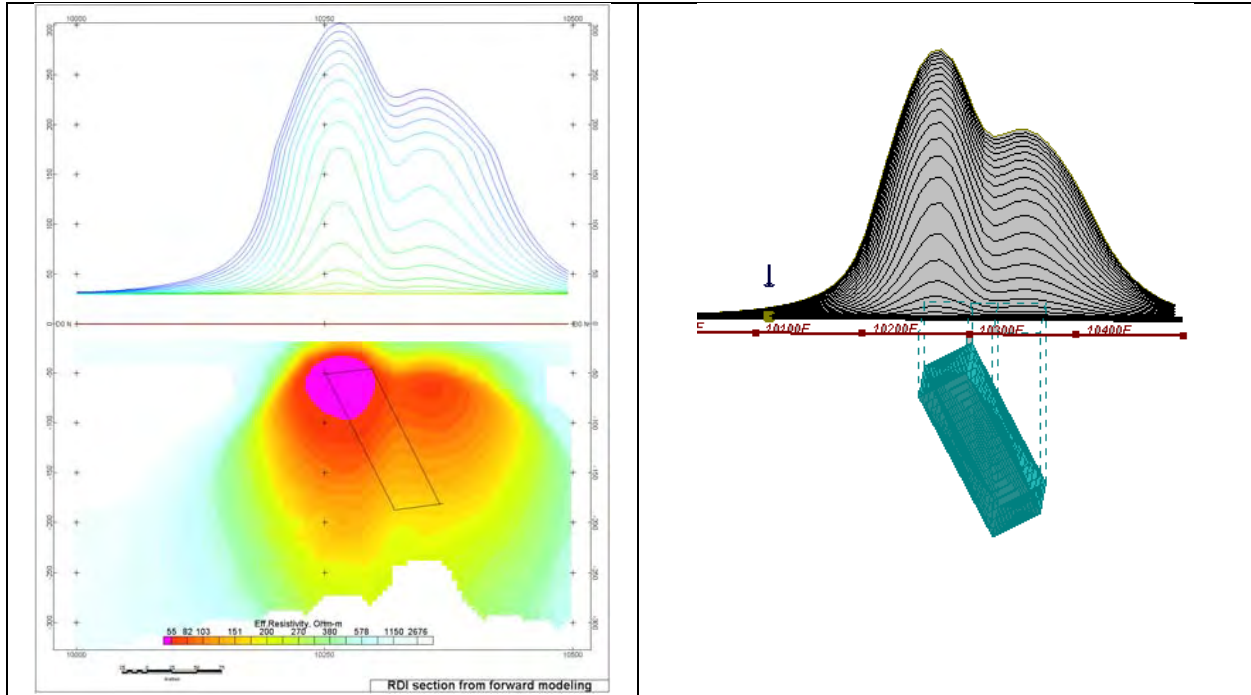


Figure F-7: Maxwell plate model and RDI from the calculated response for inclined thick (50m) plate. Depth extends 150 m, depth to the target 50 m.

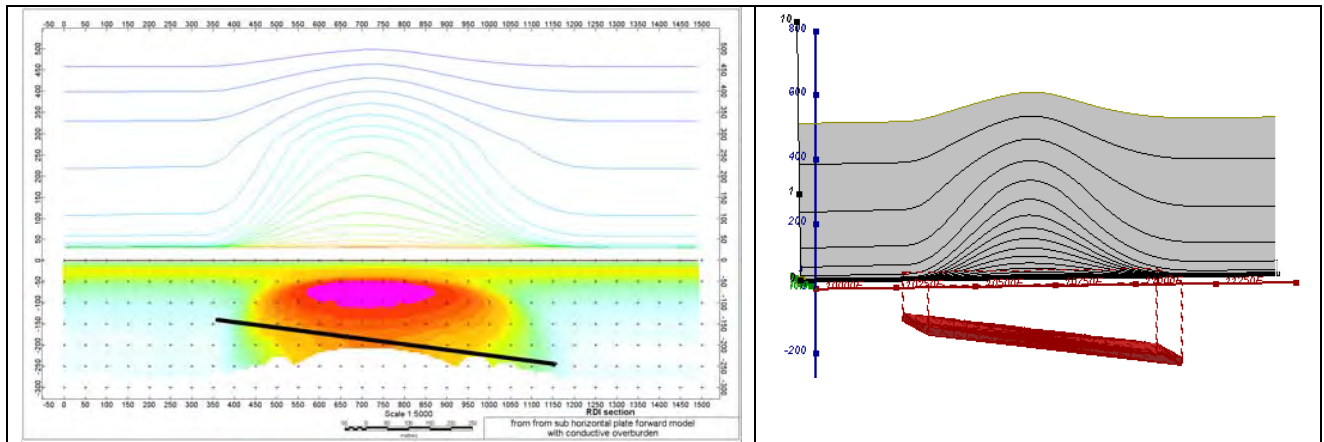


Figure F-8: Maxwell plate model and RDI from the calculated response for the long, wide and deep subhorizontal plate (depth 140 m, dim 25x500x800 m) with conductive overburden.

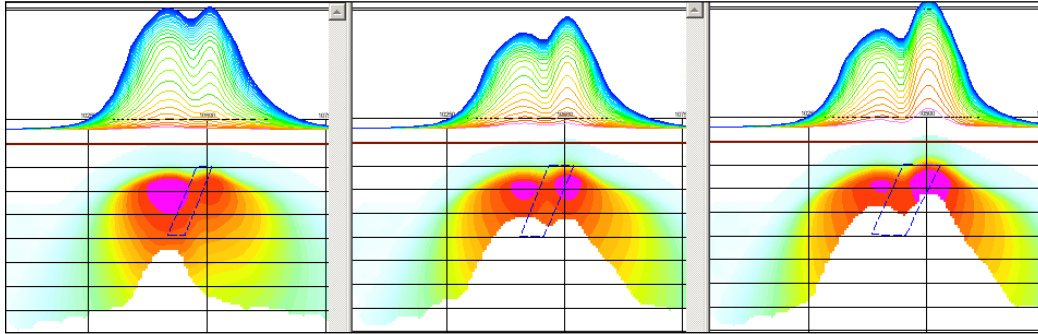


Figure F-9: Maxwell plate models and RDIs from the calculated response for “thick” dipping plates (35, 50, 75 m thickness), depth 50 m, conductivity 2.5 S/m.

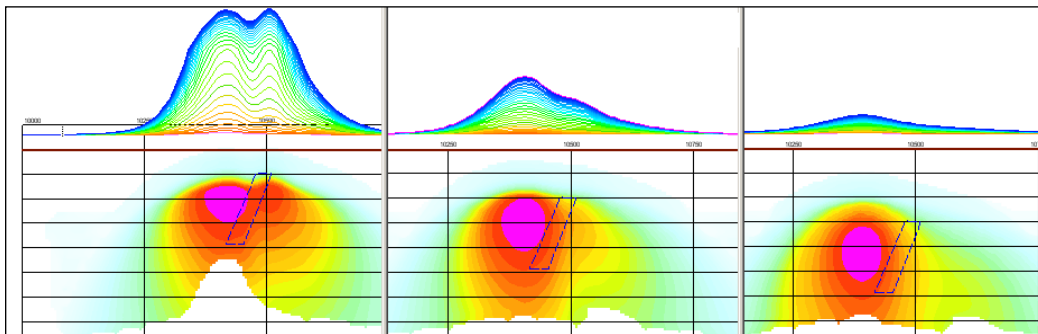


Figure F-10: Maxwell plate models and RDIs from the calculated response for “thick” (35 m thickness) dipping plate on different depth (50, 100, 150 m), conductivity 2.5 S/m.

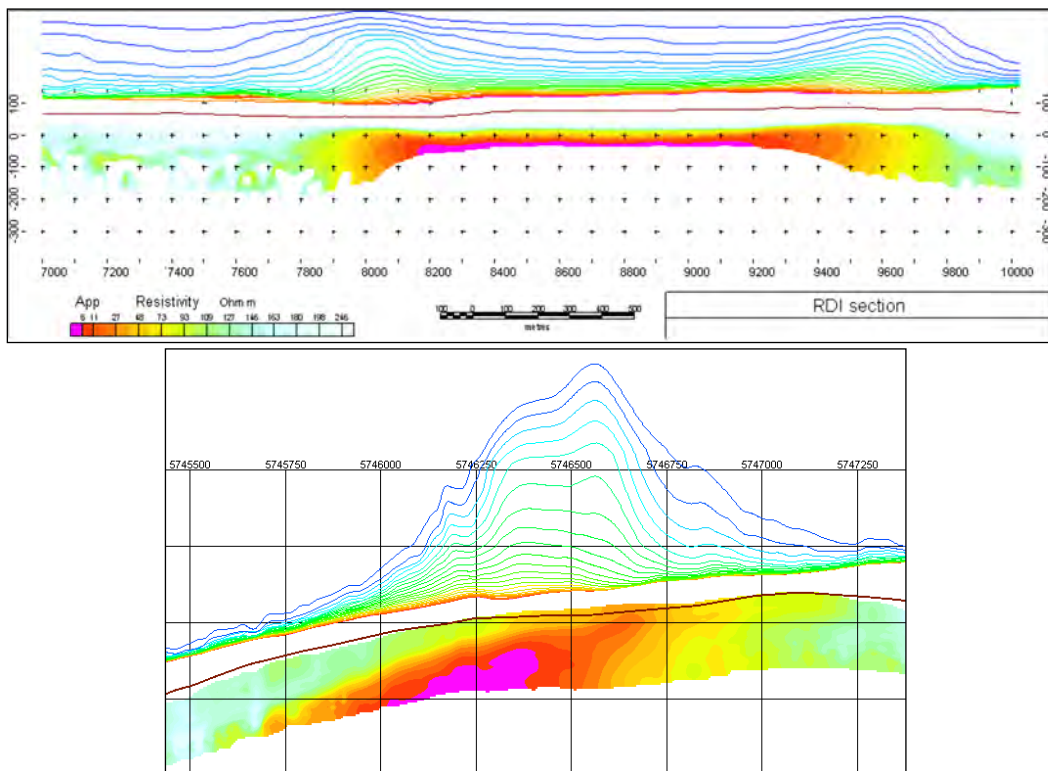
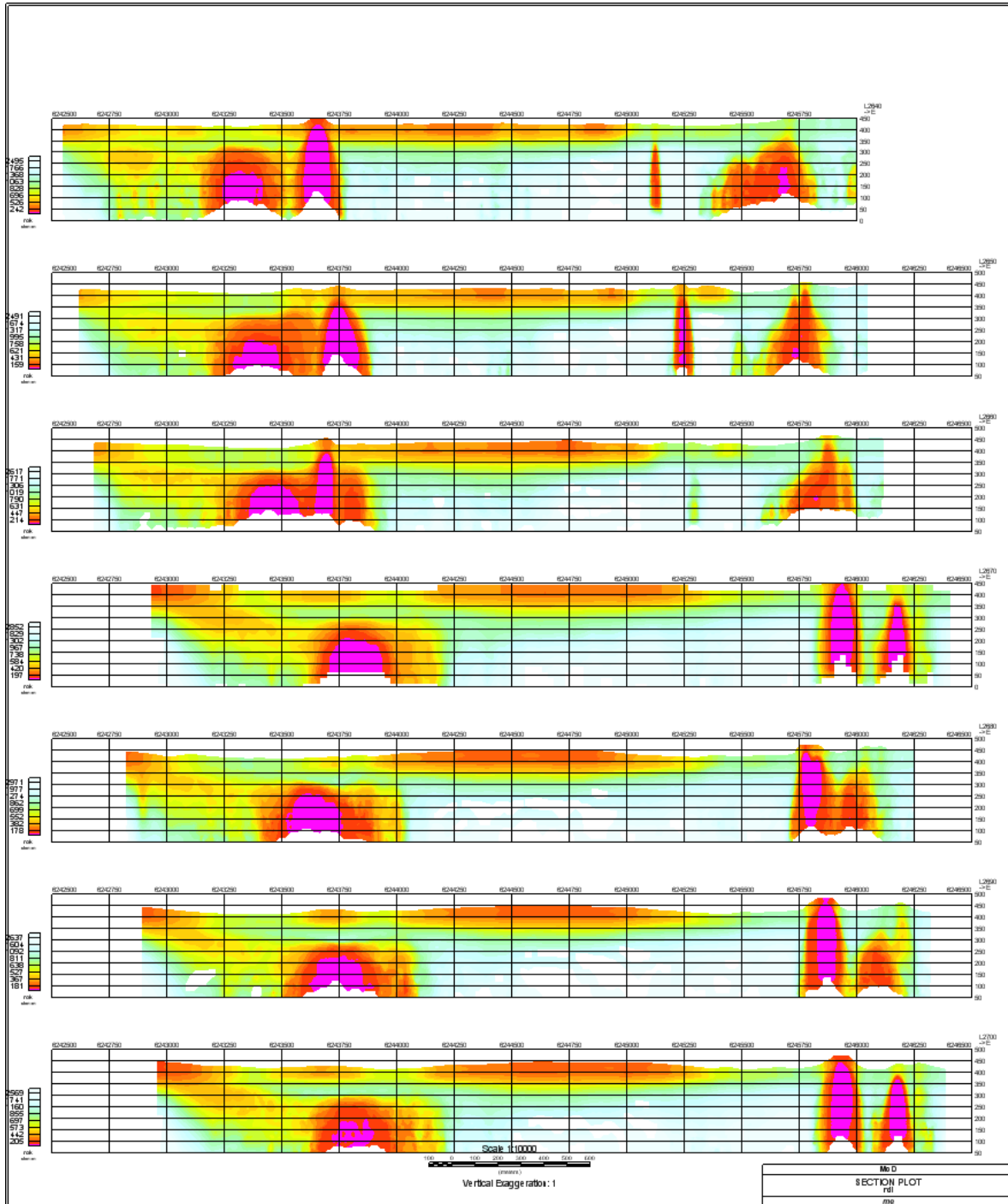


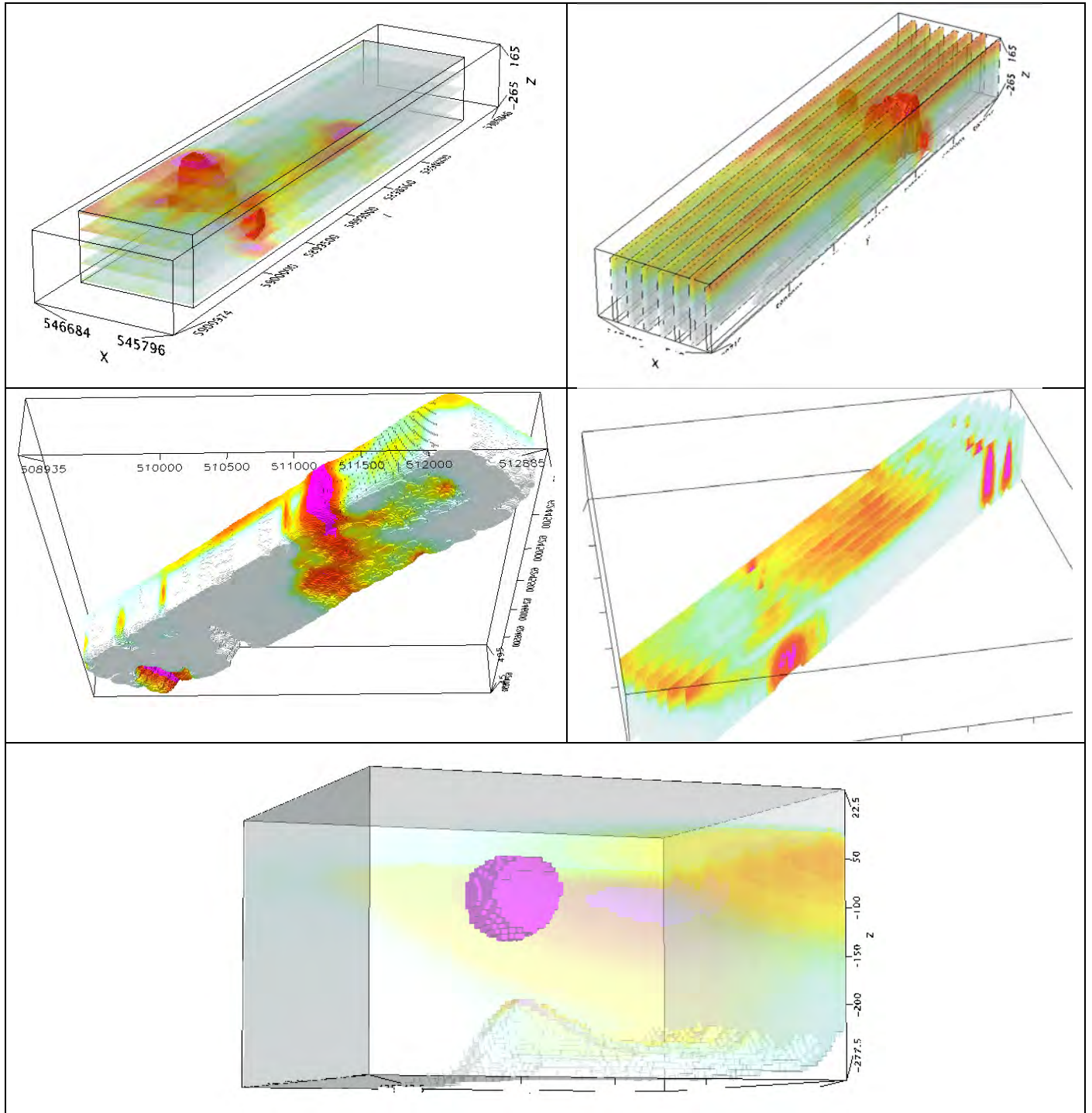
Figure F-11: RDI section for the real horizontal and slightly dipping conductive layers.

FORMS OF RDI PRESENTATION

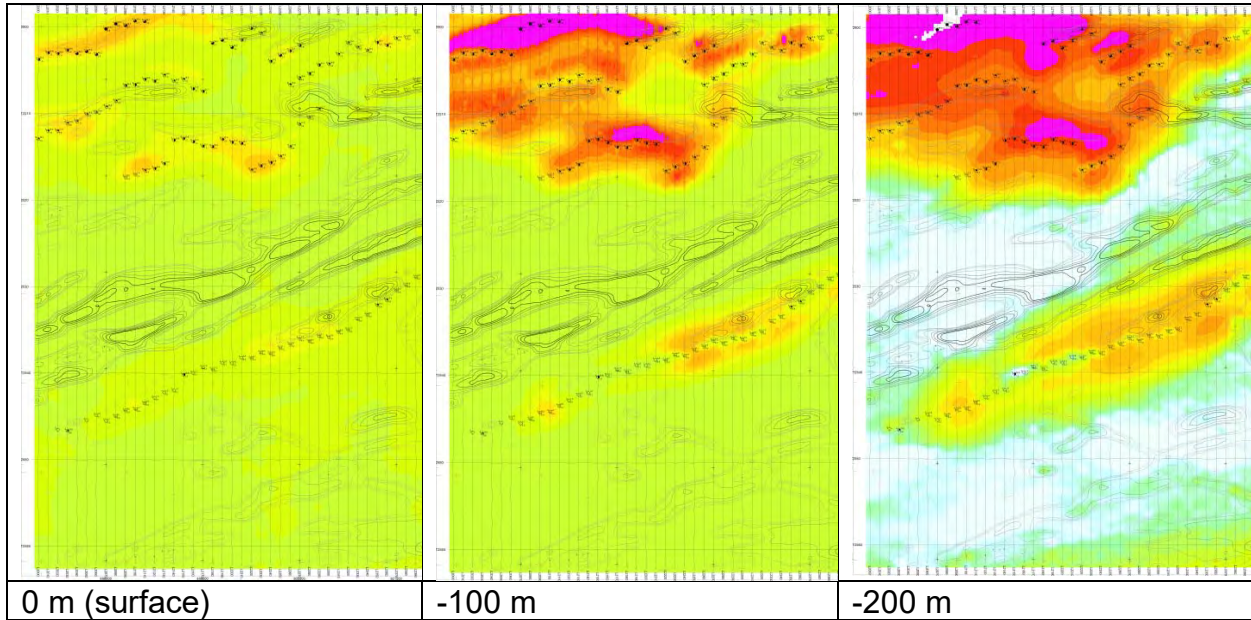
PRESENTATION OF SERIES OF LINES



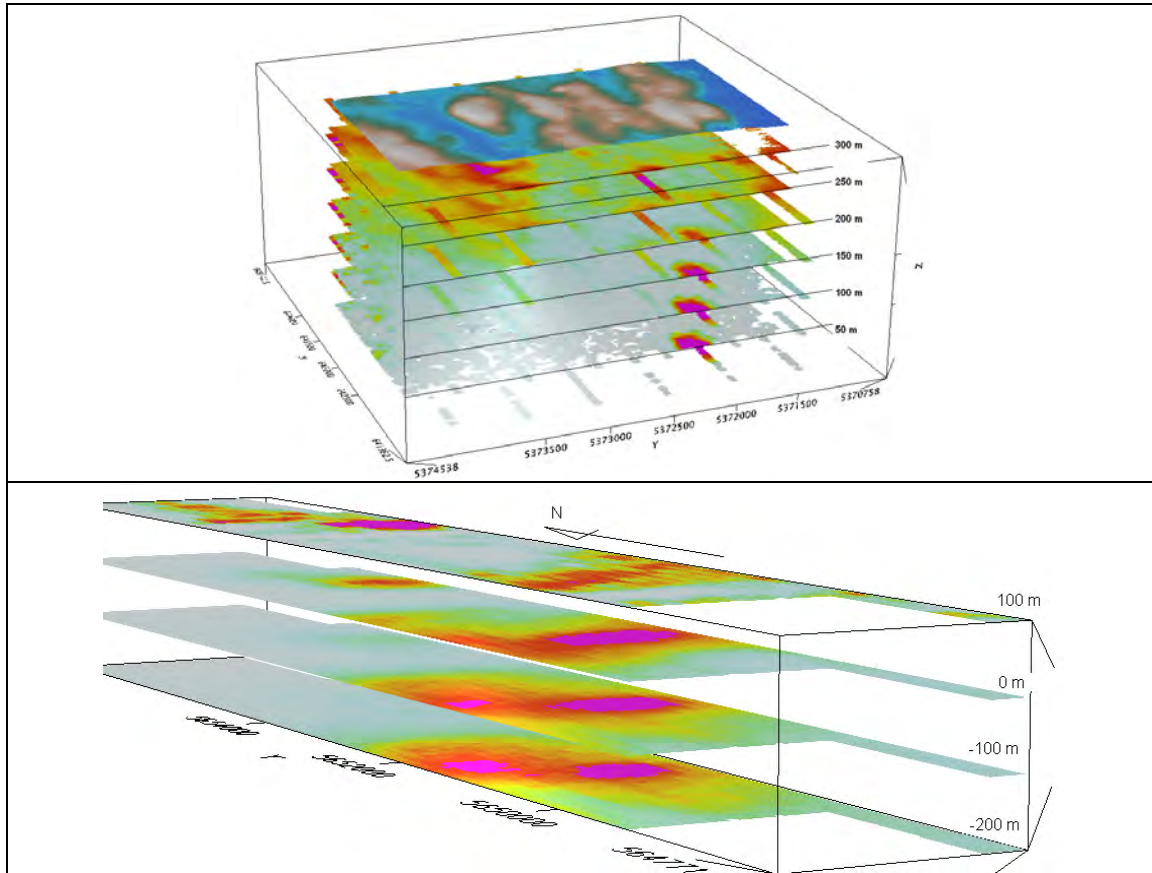
3D PRESENTATION OF RDIS



APPARENT RESISTIVITY DEPTH SLICESPLANS:

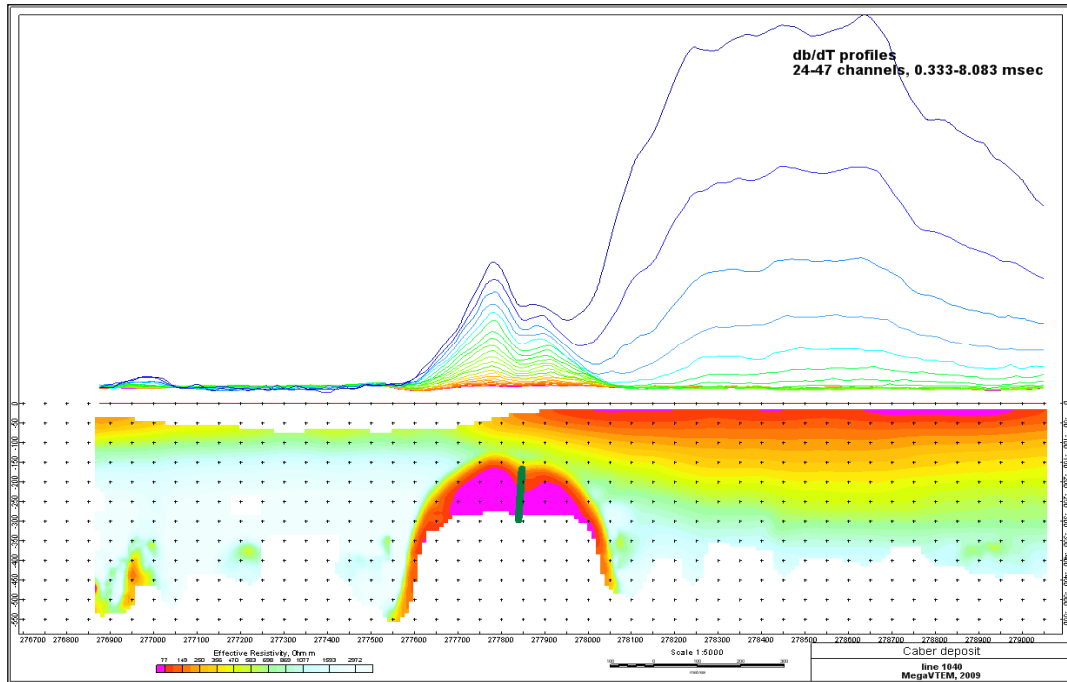


3D VIEWS OF APPARENT RESISTIVITY DEPTH SLICES:

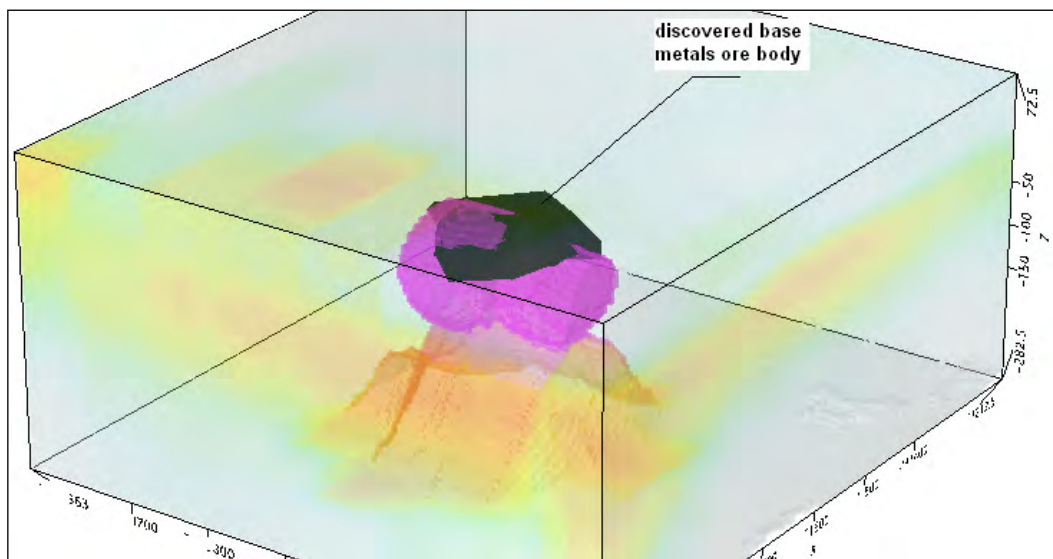


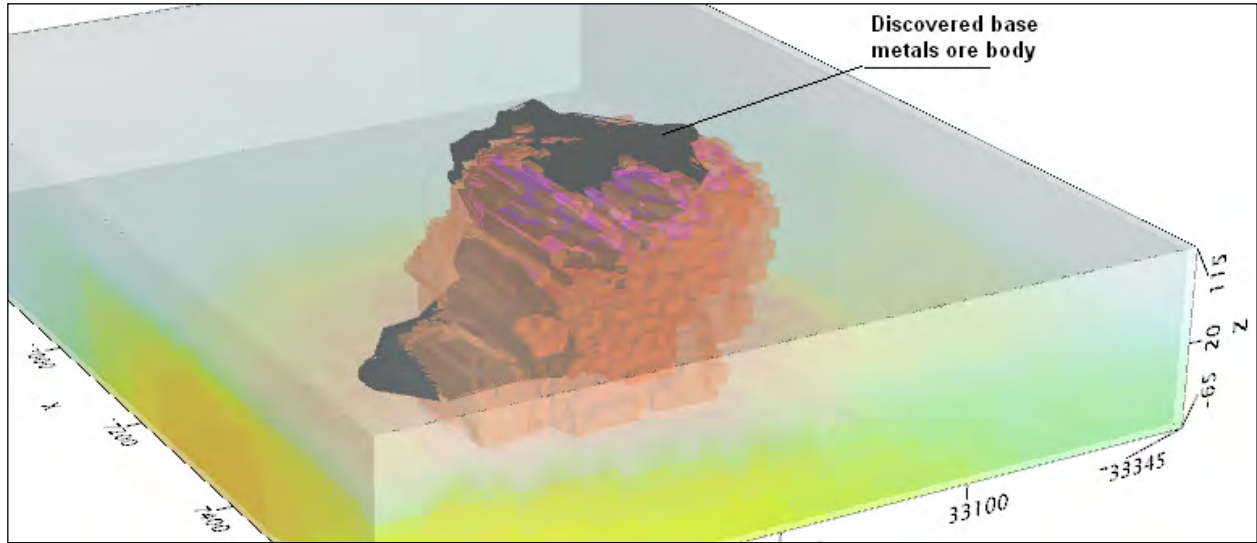
REAL BASE METAL TARGETS IN COMPARISON WITH RDIS:

RDI section of the line over Caber deposit ("thin" subvertical plate target and conductive overburden).



3D RDI VOXELS WITH BASE METALS ORE BODIES (MIDDLE EAST):





Geotech Ltd.
April 2011

APPENDIX G

RESISTIVITY DEPTH IMAGES (RDI)
Please see RDI Folder on DVD for the PDF's

APPENDIX 3

Cost Summary

<u>Work</u>	<u>Company</u>	<u>Invoice</u>	<u>Amount</u>
Survey	Geotech	996639	\$ 24,530.00
Survey	Geotech	996640	\$ 22,077.00
Survey	Geotech	996772	\$ 30,863.00
Interpretation/processing	ST PIERRE GEOCONSULTANT INC.	ALX2021-2	\$ 3,062.50
Interpretation/processing	ST PIERRE GEOCONSULTANT INC.	ALX2021-4	\$ 3,875.00
Interpretation/processing	ST PIERRE GEOCONSULTANT INC.	ALX2022-21	\$ 4,050.00
			\$ 88,457.50

APPENDIX 4

Certificate

I, Martin St-Pierre, of the City of Coquitlam, British Columbia, do certify that:

- 1) I am a graduate of the University of McGill, where in 1985 I received a B.Sc. of Solid Earth Geophysics degree;
- 2) I have practiced my profession continuously for 37 years since my graduation;
- 3) I am a Professional Geoscientist registered as a practicing member of the Association of Professional Geoscientists of Ontario;
- 3) The information presented herein is based on literature research, supervision and overall review of the work described herein;
- 4) I have no beneficial interest in the properties discussed in this report nor do I expect to receive any in the future.

A handwritten signature in black ink, appearing to read 'Martin St-Pierre', with a stylized flourish at the end.

Martin St-Pierre
PGO Registration Number: 3616
June 22, 2022